Electrical imaging surveys for environmental and engineering studies

A practical guide to 2-D and 3-D surveys

Dr. M.H.Loke

email : mhloke@pc.jaring.my
drmhloke@hotmail.com

Copyright and disclaimer notice

It is hoped that the information provided will prove useful for those carrying out 2-D and 3-D field surveys, but the author will not assume responsibility for any damage or loss caused by any errors in the information provided. If you find any errors, please inform me by email and I will make every effort to correct it in the next edition.

You can download the programs mentioned in the text (RES2DMOD, RES2DINV, RES3DMOD, RES3DINV) from the following Web sites

www.abem.se
www.agiusa.com
www.geometrics.com
www.geoelectrical.com

M.H.Loke
October 2000

Table of Contents

List of Figures

1 Introduction to resistivity surveys

1.1 Introduction

The purpose of electrical surveys is to determine the subsurface resistivity distribution by making measurements on the ground surface. From these measurements, the true resistivity of the subsurface can be estimated. The ground resistivity is related to various geological parameters such as the mineral and fluid content, porosity and degree of water saturation in the rock. Electrical resistivity surveys have been used for many decades in hydrogeological, mining and geotechnical investigations. More recently, it has been used for environmental surveys.

The resistivity measurements are normally made by injecting current into the ground through two current electrodes (C1 and C2 in Figure 1), and measuring the resulting voltage difference at two potential electrodes (P1 and P2). From the current (I) and voltage (V) values, an apparent resistivity (p_a) value is calculated.

$$p_a = \mathrm{k}\ \mathrm{V} / \mathrm{I}$$

where k is the geometric factor which depends on the arrangement of the four electrodes. Figure 2 shows the common arrays used in resistivity surveys together with their geometric factors. In a later section, we will examine the advantages and disadvantages of some of these arrays.

Resistivity meters normally give a resistance value, R = V/I, so in practice the apparent resistivity value is calculated by

$$p_a = \mathrm{k}\ \mathrm{R}$$

The calculated resistivity value is not the true resistivity of the subsurface, but an “apparent” value which is the resistivity of a homogeneous ground which will give the same resistance value for the same electrode arrangement. The relationship between the “apparent” resistivity and the “true” resistivity is a complex relationship. To determine the true subsurface resistivity, an inversion of the measured apparent resistivity values using a computer program must be carried out.

1.2 Traditional resistivity surveys

The resistivity method has its origin in the 1920’s due to the work of the Schlumberger brothers. For approximately the next 60 years, for quantitative interpretation, conventional sounding surveys (Koefoed 1979) were normally used. In this method, the centre point of the electrode array remains fixed, but the spacing between the electrodes is increased to obtain more information about the deeper sections of the subsurface.

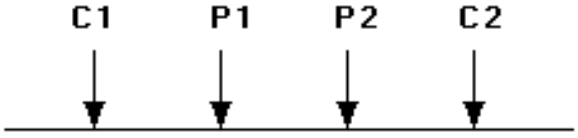

Figure 1. A conventional four electrode array to measure the subsurface resistivity.

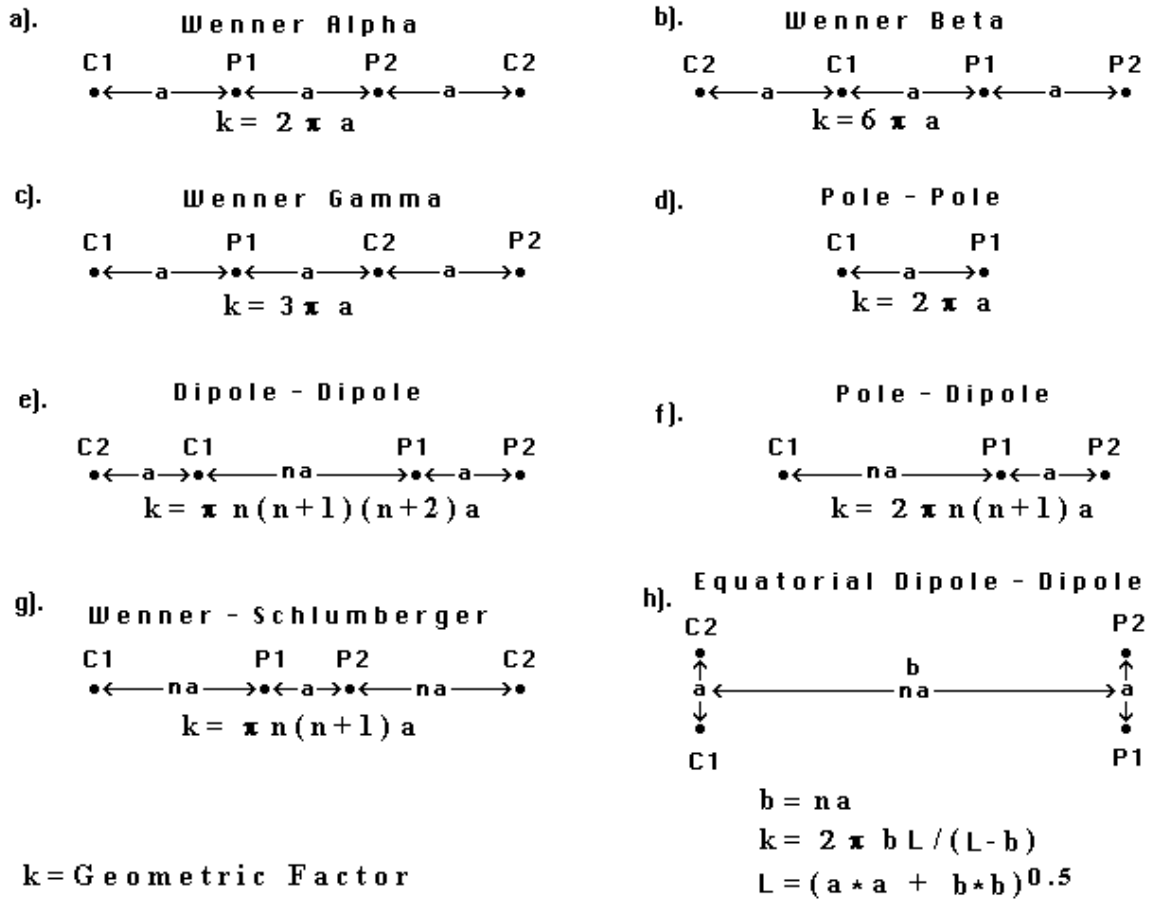

Figure 2. Common arrays used in resistivity surveys and their geometric factors.

The measured apparent resistivity values are normally plotted on a log-log graph paper. To interpret the data from such a survey, it is normally assumed that the subsurface consists of horizontal layers. In this case, the subsurface resistivity changes only with depth, but does not change in the horizontal direction. A one-dimensional model of the subsurface is used to interpret the measurements (Figure 3a). Figure 4 shows an example of the data from a sounding survey and a possible interpretation model. Despite this limitation, this method has given useful results for geological situations (such the water-table) where the one-dimensional model is approximately true. Another classical survey technique is the profiling method. In this case, the spacing between the electrodes remains fixed, but the entire array is moved along a straight line. This gives some information about lateral changes in the subsurface resistivity, but it cannot detect vertical changes in the resistivity. Interpretation of data from profiling surveys is mainly qualitative.

The most severe limitation of the resistivity sounding method is that horizontal (or lateral) changes in the subsurface resistivity are commonly found. The ideal situation shown in Figure 3a is rarely found in practice. Lateral changes in the subsurface resistivity will cause changes in the apparent resistivity values that might be, and frequently are, misinterpreted as changes with depth in the subsurface resistivity. In many engineering and environmental studies, the subsurface geology is very complex where the resistivity can change rapidly over short distances. The resistivity sounding method might not be sufficiently accurate for such situations.

Despite its obvious limitations, there are two main reasons why 1-D resistivity sounding surveys are common. The first reason was the lack of proper field equipment to

carry out the more data intensive 2-D and 3-D surveys. The second reason was the lack of practical computer interpretation tools to handle the more complex 2-D and 3-D models. However, 2-D and even 3-D electrical surveys are now practical commercial techniques with the relatively recent development of multi-electrode resistivity surveying instruments (Griffiths et al. 1990) and fast computer inversion software (Loke 1994).

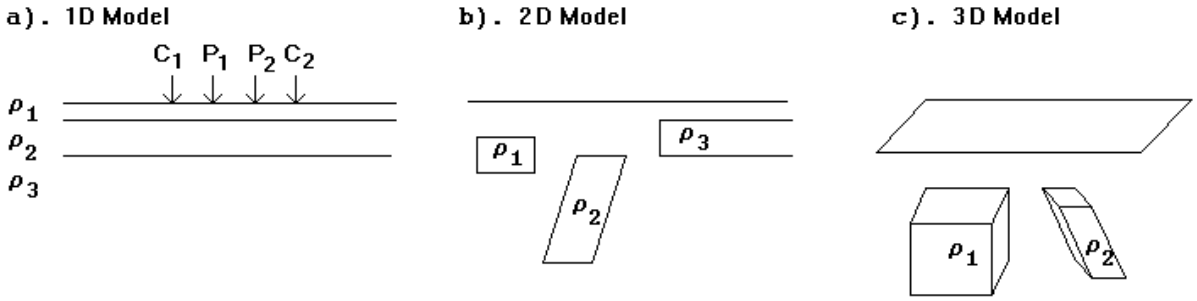

Figure 3. The three different models used in the interpretation of resistivity measurements.

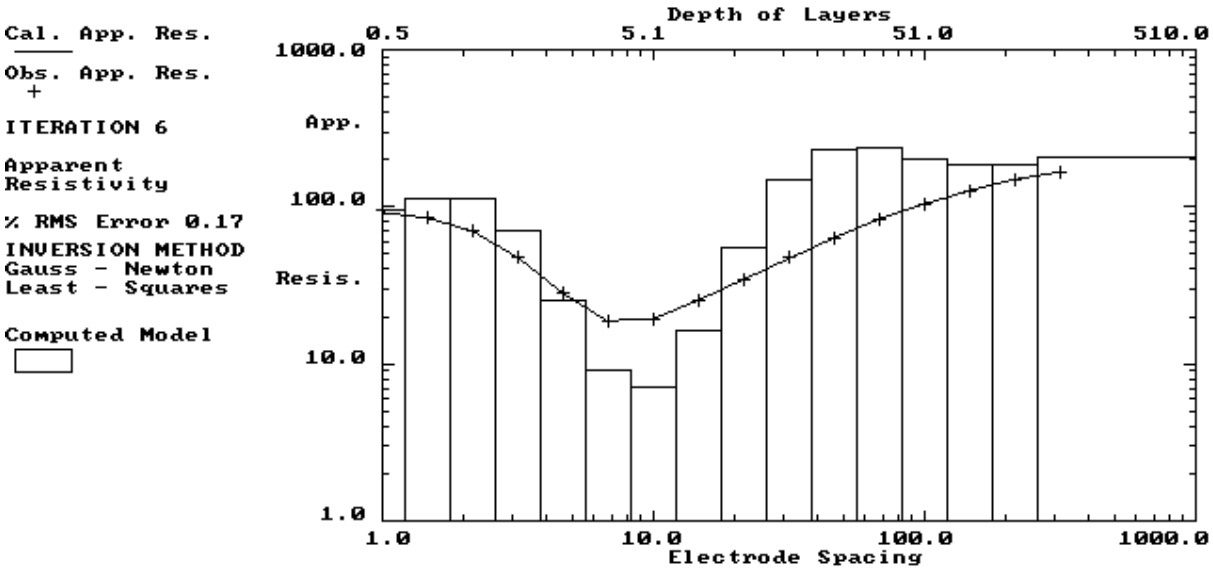

Figure 4. A typical 1-D model used in the interpretation of resistivity sounding data for the Wenner array.

1.3 The relationship between geology and resistivity

Before dealing with the 2-D and 3-D resistivity surveys, we will briefly look at the resistivity values of some common rocks, soils and other materials. Resistivity surveys give a picture of the subsurface resistivity distribution. To convert the resistivity picture into a geological picture, some knowledge of typical resistivity values for different types of subsurface materials and the geology of the area surveyed, is important.

Table 1 gives the resistivity values of common rocks, soil materials and chemicals (Keller and Frischknecht 1966, Daniels and Alberty 1966). Igneous and metamorphic rocks typically have high resistivity values. The resistivity of these rocks is greatly dependent on the degree of fracturing, and the percentage of the fractures filled with ground water. Sedimentary

rocks, which usually are more porous and have a higher water content, normally have lower resistivity values. Wet soils and fresh ground water have even lower resistivity values. Clayey soil normally has a lower resistivity value than sandy soil. However, note the overlap in the resistivity values of the different classes of rocks and soils. This is because the resistivity of a particular rock or soil sample depends on a number of factors such as the porosity, the degree of water saturation and the concentration of dissolved salts.

The resistivity of ground water varies from 10 to 100 ohm•m. depending on the concentration of dissolved salts. Note the low resistivity (about 0.2 ohm•m) of sea water due to the relatively high salt content. This makes the resistivity method an ideal technique for mapping the saline and fresh water interface in coastal areas.

The resistivity values of several industrial contaminants are also given in Table 1. Metals, such as iron, have extremely low resistivity values. Chemicals which are strong electrolytes, such as potassium chloride and sodium chloride, can greatly reduce the resistivity of ground water to less than 1 ohm•m even at fairly low concentrations. The effect of weak electrolytes, such as acetic acid, is comparatively smaller. Hydrocarbons, such as xylene, typically have very high resistivity values.

Resistivity values have a much larger range compared to other physical quantities mapped by other geophysical methods. The resistivity of rocks and soils in a survey area can vary by several orders of magnitude. In comparison, density values used by gravity surveys usually change by less than a factor of 2, and seismic velocities usually do not change by more than a factor of 10. This makes the resistivity and other electrical or electromagnetic based methods very versatile geophysical techniques.

Table 1. Resistivities of some common rocks, minerals and chemicals.

Material	Resistivity (Ω•m)	Conductivity (Siemen/m)
Igneous and Metamorphic Rocks		
Granite	$5x10^{3}$ - 10^{6}	10^{-6} - $2x10^{-4}$
Basalt	10^{3} - 10^{6}	10^{-6} - 10^{-3}
Slate	$6x10^{2}$ - $4x10^{7}$	$2.5x10^{-8}$ - $1.7x10^{-3}$
Marble	10^{2} - $2.5x10^{8}$	$4x10^{-9}$ - 10^{-2}
Quartzite	10^{2} - $2x10^{8}$	$5x10^{-9}$ - 10^{-2}
Sedimentary Rocks		
Sandstone	8 - $4x10^{3}$	$2.5x10^{-4}$ - 0.125
Shale	20 - $2x10^{3}$	$5x10^{-4}$ - 0.05
Limestone	50 - $4x10^{2}$	$2.5x10^{-3}$ - 0.02
Soils and waters		
Clay	1 - 100	0.01 - 1
Alluvium	10 - 800	$1.25\ x10^{-3}$ - 0.1
Groundwater (fresh)	10 - 100	0.01 - 0.1
Sea water	0.2	5
Chemicals		
Iron	$9.074x10^{-8}$	$1.102x10^{7}$
0.01 M Potassium chloride	0.708	1.413
0.01 M Sodium chloride	0.843	1.185
0.01 M acetic acid	6.13	0.163
Xylene	$6.998x10^{16}$	$1.429x10^{-17}$

2 2-D electrical imaging surveys

2.1 Introduction

We have seen the greatest limitation of the resistivity sounding method is that it does not take into account horizontal changes in the subsurface resistivity. A more accurate model of the subsurface is a two-dimensional (2-D) model where the resistivity changes in the vertical direction, as well as in the horizontal direction along the survey line. In this case, it is assumed that resistivity does not change in the direction that is perpendicular to the survey line. In many situations, particularly for surveys over elongated geological bodies, this is a reasonable assumption. In theory, a 3-D resistivity survey and interpretation model should be even more accurate. However, at the present time, 2-D surveys are the most practical economic compromise between obtaining very accurate results and keeping the survey costs down. Typical 1-D resistivity sounding surveys usually involve about 10 to 20 readings, while 2-D imaging surveys involve about 100 to 1000 measurements. In comparison, 3-D surveys usually involve several thousand measurements.

The cost of a typical 2-D survey could be several times the cost of a 1-D sounding survey, and is probably comparable with a seismic survey. In many geological situations, 2-D electrical imaging surveys can give useful results that are complementary to the information obtained by other geophysical method. For example, seismic methods can map undulating interfaces well, but will have difficulty (without using advanced data processing techniques) in mapping discrete bodies such as boulders, cavities and pollution plumes. Ground radar surveys can provide more detailed pictures but have very limited depth penetration in areas with conductive unconsolidated sediments, such as clayey soils. Two-dimensional electrical surveys should be used in conjunction with seismic or GPR surveys as they provide complementary information about the subsurface.

2.2 Field survey method - instrumentation and measurement procedure

One of the new developments in recent years is the use of 2-D electrical imaging/tomography surveys to map areas with moderately complex geology (Griffiths and Barker 1993). Such surveys are usually carried out using a large number of electrodes, 25 or more, connected to a multi-core cable. A laptop microcomputer together with an electronic switching unit is used to automatically select the relevant four electrodes for each measurement (Figure 5). At present, field techniques and equipment to carry out 2-D resistivity surveys are fairly well developed. The necessary field equipment is commercially available from a number of international companies. These systems typically costs from about US$15,000 upwards. Some institutions have even constructed “home-made” manually operated switching units at a nominal cost by using a seismic cable as the multi-core cable!

Figure 5 shows the typical setup for a 2-D survey with a number of electrodes along a straight line attached to a multi-core cable. Normally a constant spacing between adjacent electrodes is used. The multi-core cable is attached to an electronic switching unit which is connected to a laptop computer. The sequence of measurements to take, the type of array to use and other survey parameters (such the current to use) is normally entered into a text file which can be read by a computer program in a laptop computer. Different resistivity meters use different formats for the control file, so you will need to refer to the manual for your system. After reading the control file, the computer program then automatically selects the appropriate electrodes for each measurement. In a typical survey, most of the fieldwork is in laying out the cable and electrodes. After that, the measurements are taken automatically and stored in the computer. Most of the survey time is spent waiting for the resistivity meter to

complete the set of measurements!

To obtain a good 2-D picture of the subsurface, the coverage of the measurements must be 2-D as well. As an example, Figure 5 shows a possible sequence of measurements for the Wenner electrode array for a system with 20 electrodes. In this example, the spacing between adjacent electrodes is "**a**". The first step is to make all the possible measurements with the Wenner array with an electrode spacing of "**1a**". For the first measurement, electrodes number 1, 2, 3 and 4 are used. Notice that electrode 1 is used as the first current electrode C1, electrode 2 as the first potential electrode P1, electrode 3 as the second potential electrode P2 and electrode 4 as the second current electrode C2. For the second measurement, electrodes number 2, 3, 4 and 5 are used for C1, P1, P2 and C2 respectively. This is repeated down the line of electrodes until electrodes 17, 18, 19 and 20 are used for the last measurement with "**1a**" spacing. For a system with 20 electrodes, note that there are 17 (20 - 3) possible measurements with "**1a**" spacing for the Wenner array.

After completing the sequence of measurements with "**1a**" spacing, the next sequence of measurements with "**2a**" electrode spacing is made. First electrodes 1, 3, 5 and 7 are used for the first measurement. The electrodes are chosen so that the spacing between adjacent electrodes is "**2a**". For the second measurement, electrodes 2, 4, 6 and 8 are used. This process is repeated down the line until electrodes 14, 16, 18 and 20 are used for the last measurement with spacing "**2a**". For a system with 20 electrodes, note that there are 14 (20 - 2x3) possible measurements with "**2a"** spacing.

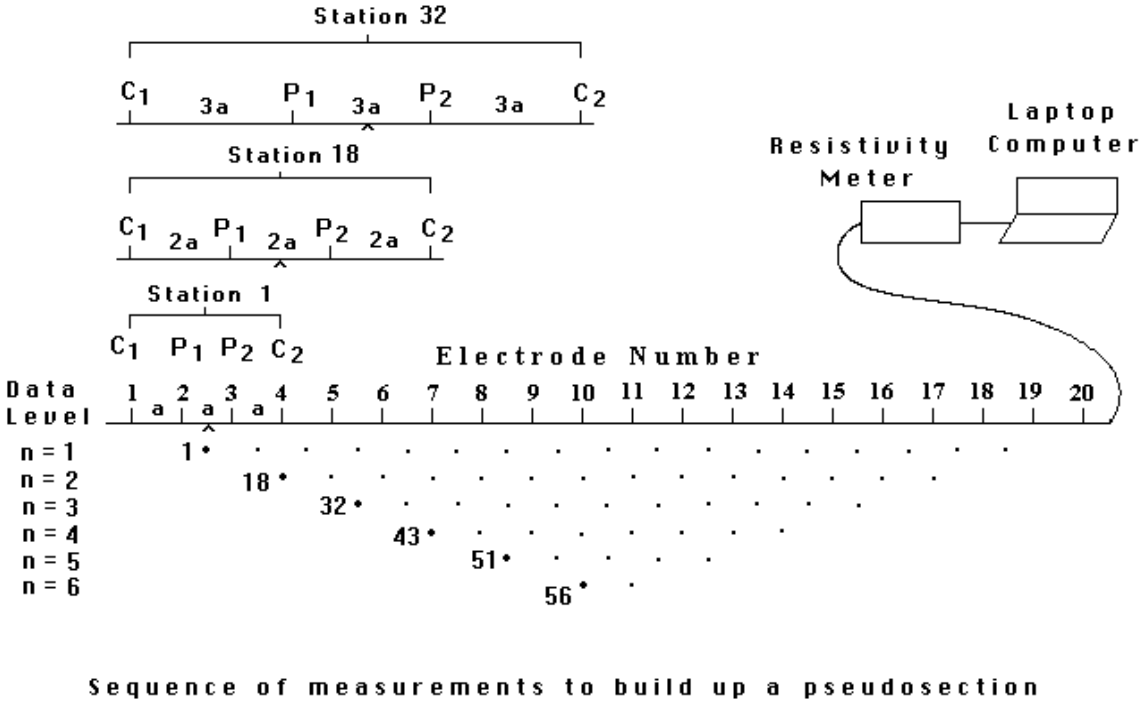

Figure 5. The arrangement of electrodes for a 2-D electrical survey and the sequence of measurements used to build up a pseudosection.

The same process is repeated for measurements with "**3a**", "**4a**", "**5a**" and "**6a**" spacings. To get the best results, the measurements in a field survey should be carried out in a systematic manner so that, as far as possible, all the possible measurements are made. This will affect the quality of the interpretation model obtained from the inversion of the apparent resistivity measurements (Dahlin and Loke 1998).

Note that as the electrode spacing increases, the number of measurements decreases. The number of measurements that can be obtained for each electrode spacing, for a given number of electrodes along the survey line, depends on the type of array used. The Wenner array gives the smallest number of possible measurements compared to the other common arrays that are used in 2-D surveys.

The survey procedure with the pole-pole array is similar to that used for the Wenner array. For a system with 20 electrodes, firstly 19 of measurements with a spacing of "**1a**" is made, followed by 18 measurements with "**2a**" spacing, followed by 17 measurements with "3**a**" spacing, and so on.

For the dipole-dipole, Wenner-Schlumberger and pole-dipole arrays (Figure 2), the survey procedure is slightly different. As an example, for the dipole-dipole array, the measurement usually starts with a spacing of "**1a**" between the C1-C2 (and also the P1-P2) electrodes. The first sequence of measurements is made with a value of 1 for the "**n**" factor (which is the ratio of the distance between the C1-P1 electrodes to the C1-C2 dipole spacing), followed by "**n**" equals to 2 while keeping the C1-C2 dipole pair spacing fixed at "**1a**". When "**n**" is equals to 2, the distance of the C1 electrode from the P1 electrode is twice the C1-C2 dipole pair spacing. For subsequent measurements, the "**n**" spacing factor is usually increased to a maximum value of about 6, after which accurate measurements of the potential are difficult due to very low potential values. To increase the depth of investigation, the spacing between the C1-C2 dipole pair is increased to "**2a**", and another series of measurements with different values of "**n**" is made. If necessary, this can be repeated with larger values of the spacing of the C1-C2 (and P1-P2) dipole pairs. A similar survey technique can be used for the Wenner-Schlumberger and pole-dipole arrays where different combinations of the "**a**" spacing and "**n**" factor can be used.

One technique used to extend horizontally the area covered by the survey, particularly for a system with a limited number of electrodes, is the roll-along method. After completing the sequence of measurements, the cable is moved past one end of the line by several unit electrode spacings. All the measurements which involve the electrodes on part of the cable which do not overlap the original end of the survey line are repeated (Figure 6).

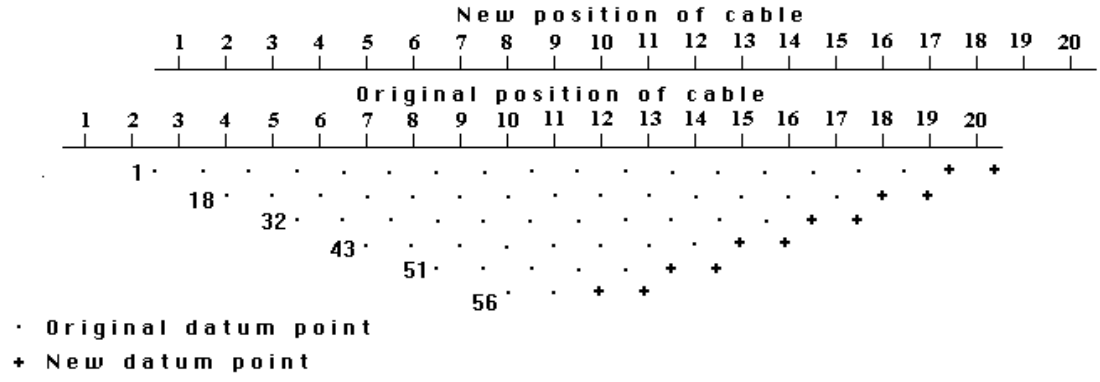

Figure 6. The use of the roll-along method to extend the area covered by a survey.

2.3 Pseudosection data plotting method

To plot the data from a 2-D imaging survey, the pseudosection contouring method is normally used. In this case, the horizontal location of the point is placed at the mid-point of the set of electrodes used to make that measurement. The vertical location of the plotting point is placed at a distance which is proportional to the separation between the electrodes. For IP surveys using the dipole-dipole array, one common method is to placed the plotting point at the intersection of two lines starting from the mid-point of the C1-C2 and P1-P2 dipole pairs, with a 45° angle to the horizontal. It is important to emphasise that this is merely a plotting convention, and it does not imply that the depth of investigation is given by the point of intersection of the two 45° angle lines (it certainly does not imply the current flow or isopotential lines have a 45° angle with the surface). Surprisingly, this is still a common misconception, particularly in North America!

Another method is to place the vertical position of the plotting point at the median depth of investigation (Edwards 1977), or pseudodepth, of the electrode array used. This pseudodepth value is based on the sensitivity values or Frechet derivative for a homogeneous half space. Since it appears to have some mathematical basis, this method that is used in plotting the pseudosections, particularly for field data sets, in the later part of these lecture notes. The pseudosection plot obtained by contouring the apparent resistivity values is a convenient means to display the data.

The pseudosection gives a very approximate picture of the true subsurface resistivity distribution. However the pseudosection gives a distorted picture of the subsurface because the shape of the contours depend on the type of array used as well as the true subsurface resistivity (Figure 7). The pseudosection is useful as a means to present the measured apparent resistivity values in a pictorial form, and as an initial guide for further quantitative interpretation. One common mistake made is to try to use the pseudosection as a final picture of the true subsurface resistivity. As Figure 7 shows, different arrays used to map the same region can give rise to very different contour shapes in the pseudosection plot. Figure 7 also gives you an idea of the data coverage that can be obtained with different arrays. Note that the pole-pole array gives the widest horizontal coverage, while the coverage obtained by the Wenner array decreases much more rapidly with increasing electrode spacing.

One useful practical application of the pseudosection plot is for picking out bad apparent resistivity measurements. Such bad measurements usually stand out as points with unusually high or low values.

2.4 Forward modeling program exercise

The free program, RES2DMOD.EXE, is a 2-D forward modeling program which calculates the apparent resistivity pseudosection for a user defined 2-D subsurface model. With this program, the user can choose the finite-difference (Dey and Morrison 1979a) or finite-element (Silvester and Ferrari 1990) method to calculate the apparent resistivity values. In the program, the subsurface is divided into a large number of small rectangular cells. This program is largely intended for teaching about the use of the 2-D electrical imaging method. The program might also assist the user in choosing the appropriate array for different geological situations or surveys. The arrays supported by this program are the Wenner (Alpha, Beta and Gamma configurations - the Alpha configuration is normally used for field surveys and usually just referred to as the “Wenner” array), Wenner-Schlumberger, pole-pole, inline dipole-dipole, pole-dipole and equatorial dipole-dipole (Edwards 1977). Each type of array has its advantages and disadvantages. This program will hopefully help you in choosing the "best" array for a particular survey area after carefully balancing factors such as the cost, depth of investigation, resolution and practicality.

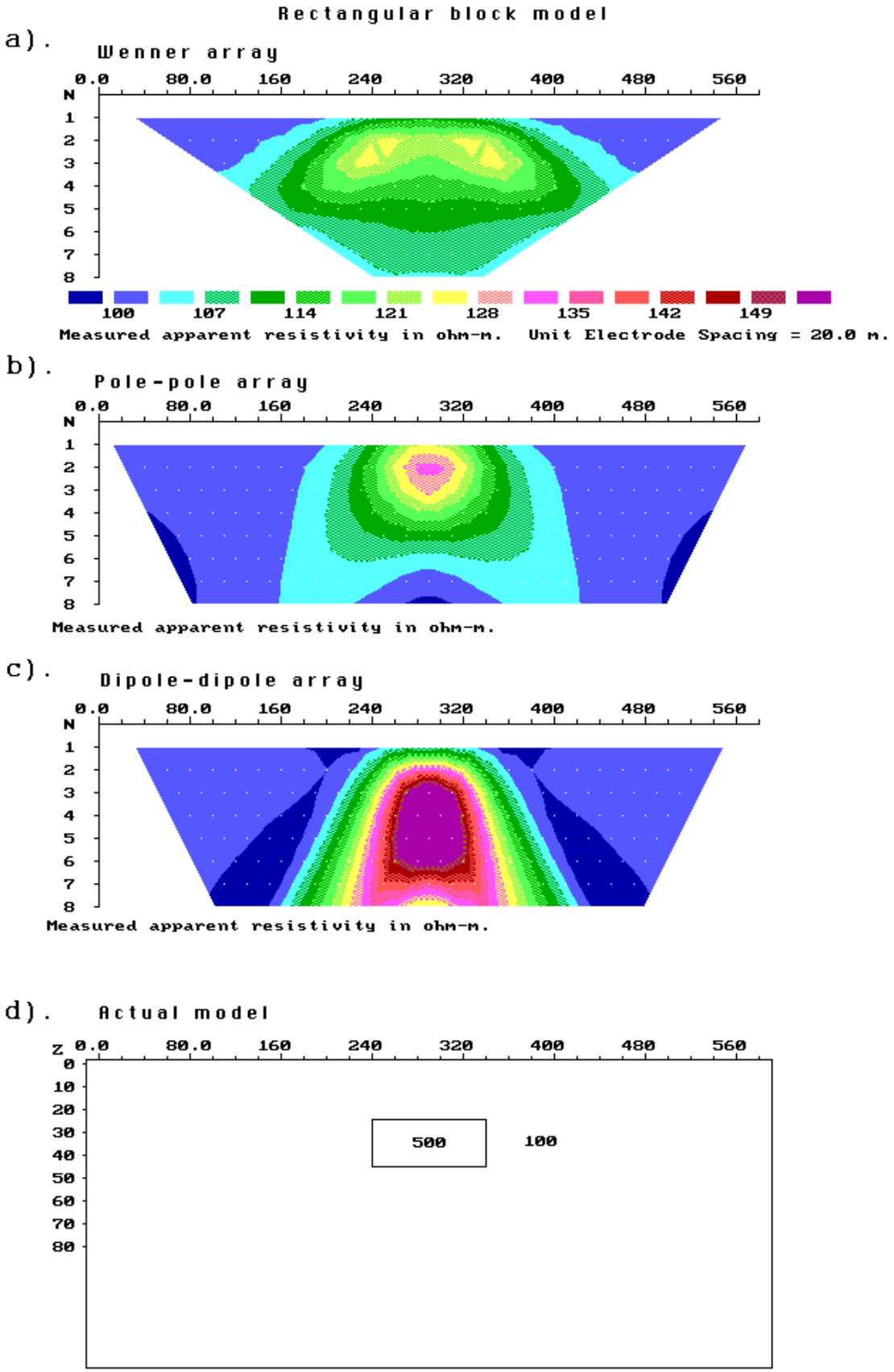

Figure 7. The apparent resistivity pseudosections from 2-D imaging surveys with different arrays over a rectangular block.

The program requires the resistivity model values to be typed in separately in a text file. The model data format, and other details about the use of this program, can be found in the electronic manual program MAN2DMOD.EXE. In this course, we will use several model files which are already present in the program package to take a look at the shapes of the pseudosections for different geological structures. By playing around with this program, you can get a feel of the effects of array type over the size and shape of the contours in the pseudosection.

This program and related files should be copied into the same subdirectory, for eg. C:\RES2DMOD. Go to this subdirectory, and type

RES2DMOD

to start up the program. First select the "File" option on the main menu bar by using the left and right arrow keys. Next select the "Read data file with forward model" suboption to read in one of the example input model files provided. As an example, read in the file BLOCKONE.MOD which has a simple model with a rectangular block. After reading in this file, select the "Edit/Display Model" option followed by the "Edit model" suboption to take a look at the model. Next select the "Model Computation" option to calculate the apparent resistivity values for this model. The calculations will probably only take a few seconds, after which you should go back to "Edit/Display Model" option. In this option, select the "Display model" suboption to see the apparent resistivity pseudosection for this model. To change the type of array, use the "Change Settings" suboption. Select another array, such as the pole-pole or dipole-dipole, and see what happens to the shape of the contours in the pseudosection.

A number of other example model files with an extension of .MOD are also provided. Try reading them and see the pseudosections that they give. The program also allows you to change the model interactively using the left and right mouse button. To change a single cell, click it with the left mouse button. Then move the cursor to one of the color boxes in the legend above the model, and click the resistivity value you want. Press the F1 key to get information about the keys used by the program to edit the model. Note that clicking the cells with the mouse buttons will only change the resistivity of the cells displayed on the screen, but will not change the resistivity of the buffer cells towards the left, right and bottom edges of the mesh. To change the resistivity of the buffer cells, you need to use the "[", "]" and "D" keys.

The program also allows you to save the apparent resistivity values in a format that can be read by the RES2DINV inversion program. This is useful in studying the model resolution that can be obtained over different structures using various arrays.

2.5 Advantages and disadvantages of the different arrays

The RES2DMOD.EXE program shows you that the shape of the contours in the pseudosection produced by the different arrays over the same structure can be very different. The arrays most commonly used for resistivity surveys were shown in Figure 2. The choice of the "best" array for a field survey depends on the type of structure to be mapped, the sensitivity of the resistivity meter and the background noise level. In practice, the arrays that are most commonly used for 2-D imaging surveys are the (a) Wenner, (b) dipole-dipole (c) Wenner-Schlumberger (d) pole-pole and (d) pole-dipole. Among the characteristics of an array that should be considered are (i) the sensitivity of the array to vertical and horizontal changes in the subsurface resistivity, (ii) the depth of investigation, (iii) the horizontal data coverage and (iv) the signal strength.

Figures 8a to 8c shows the contour pattern for the sensitivity function of the Wenner, Schlumberger and dipole-dipole arrays for a homogeneous earth model. The sensitivity

function basically tells us the degree to which a change in the resistivity of a section of the subsurface will influence the potential measured by the array. The higher the value of the sensitivity function, the greater is the influence of the subsurface region on the measurement. Note that for all the three arrays, the highest sensitivity values are found near the electrodes. At larger distances from the electrodes, the contour patterns are different for the different arrays. The difference in the contour pattern in the sensitivity function plot helps to explain the response of the different arrays to different types of structures.

Table 2 gives the median depth of investigation for the different arrays. The median depth of investigation gives an idea of the depth to which we can map with a particular array. The median depth values are determined by integrating the sensitivity function with depth. Please refer to the paper by Edwards (1977) listed in the Reference section for the details. In layman's terms, the upper section of the earth above the "median depth of investigation" has the same influence on the measured potential as the lower section. This tells us roughly how deep we can see with an array. This depth does not depend on the measured apparent resistivity or the resistivity of the homogeneous earth model. It should be noted that the depths are strictly only valid for a homogeneous earth model, but they are probably good enough for planning field surveys. If there are large resistivity contrasts near the surface, the actual depth of investigation could be somewhat different. For example, it has been observed that a large low resistivity body near the surface tends to create a “shadow zone” below it where it is more difficult to accurately determine the resistivity values.

To determine the maximum depth mapped by a particular survey, multiply the maximum “**a**” electrode spacing, or maximum array length “**L**“, by the appropriate depth factor given in Table 2. For example, if the maximum electrode “**a**” spacing used by the Wenner array is 100 metres (or maximum **L** 300 metres), then the maximum depth mapped is about 51 metres. For the dipole-dipole, pole-dipole and Wenner-Schlumberger arrays, another factor “**n**” must also be taken into consideration. For the arrays with four active electrodes (such as the dipole-dipole, Wenner and Wenner-Schlumberger arrays), it is probably easier to use the total array length “**L**”. As an example, if a dipole-dipole survey uses a maximum value of 10 metres for “**a**” and a corresponding maximum value of 6 for **n**, then the maximum “**L**” value is 80 metres. This gives a maximum depth of investigation of 80x0.216 or about 17 metres.

Table 2 also includes the geometric factor for the various arrays for an "**a**" spacing of 1.0 metre. The inverse of the geometric factor gives an indication of the voltage that would be measured between the P1 and P2 potential electrodes. The ratio of this potential compared to the Wenner alpha array is also given, for example a value of 0.01 means that the potential is 1% of the potential measured by the Wenner alpha array with the same "**a**" spacing.

2.5.1 Wenner array

This is a robust array that was popularized by the pioneering work carried by The University of Birmingham research group (Griffiths and Turnbull 1985; Griffiths, Turnbull and Olayinka 1990). Many of the early 2-D surveys were carried out with this array. In Figure 8a, the sensitivity plot for the Wenner array has almost horizontal contours beneath the centre of the array. Because of this property, the Wenner array is relatively sensitive to vertical changes in the subsurface resistivity below the centre of the array. However, it is less sensitive to horizontal changes in the subsurface resistivity. In general, the Wenner is good in resolving vertical changes (i.e. horizontal structures), but relatively poor in detecting horizontal changes (i.e. narrow vertical structures). In Table 2, we see that for the Wenner array, the median depth of investigation is approximately 0.5 times the “**a**” spacing used. Compared to other arrays, the Wenner array has a moderate depth of investigation. The signal

strength is inversely proportional to the geometric factor used to calculate the apparent resistivity value for the array (Figure 2). For the Wenner array, the geometric factor is **2πa**, which is smaller than the geometric factor for other arrays. Among the common arrays, the Wenner array has the strongest signal strength. This can be an important factor if the survey is carried in areas with high background noise. One disadvantage of this array for 2-D surveys is the relatively poor horizontal coverage as the electrode spacing is increased (Figure 7). This could be a problem if you use a system with a relatively small number of electrodes.

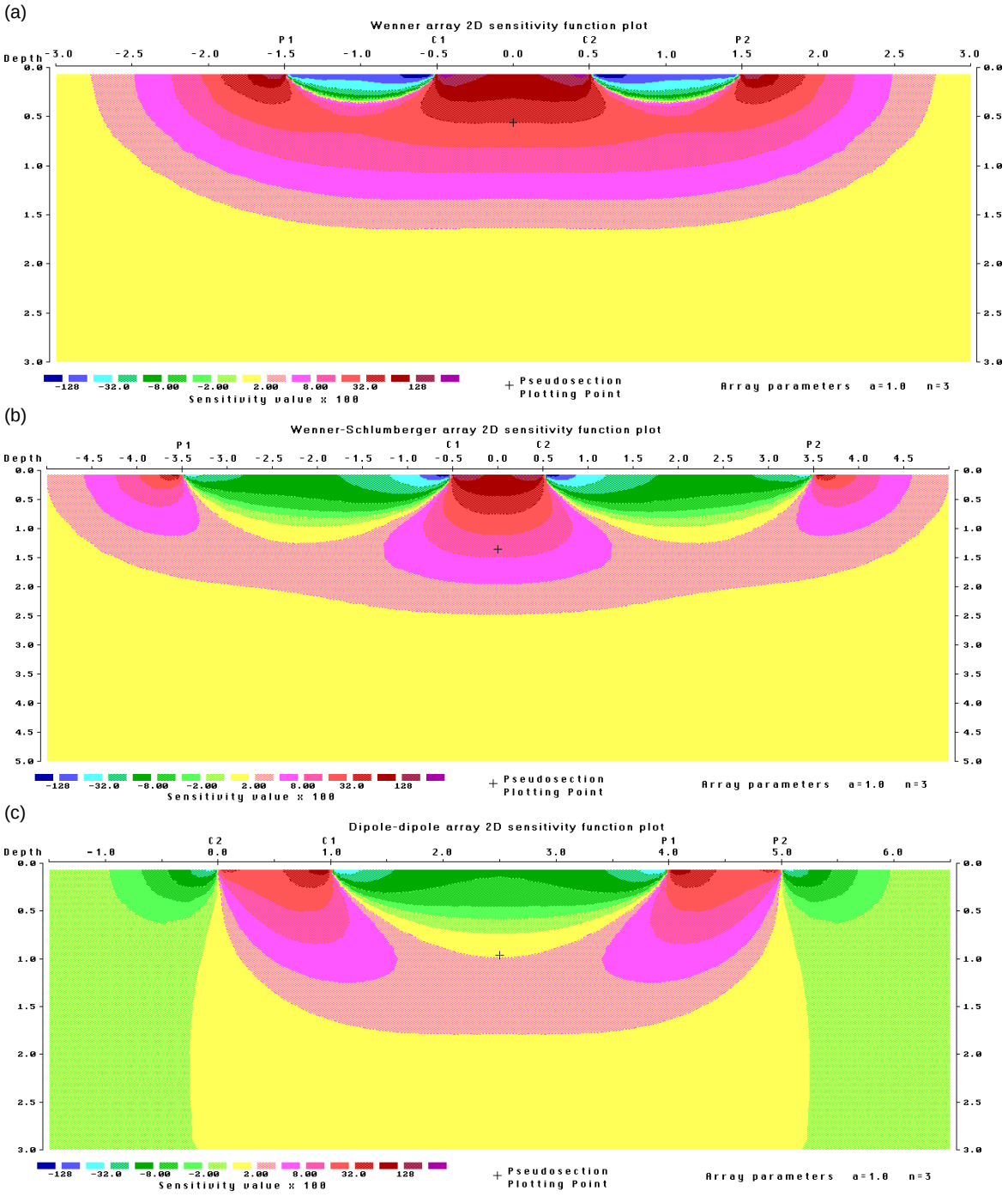

Figure 8. The sensitivity patterns for the (a) Wenner (b) Wenner-Schlumberger and (c) dipole-dipole arrays.

Table 2. The median depth of investigation (z_e) for the different arrays. **L** is the total length of the array. Note identical values of z_e/a for the Wenner-Schlumberger and pole-dipole arrays (after Edwards 1977). Please refer to Figure 2 for the arrangement of the electrodes for the different arrays. The geometric factor is for an "**a**" value of 1.0 metre.

Array type		z_e/a	z_e/L	Geometric Factor	Inverse Geometric Factor (Ratio)
Wenner Alpha		0.519	0.173	6.2832	0.15915 (1.0000)
Wenner Beta		0.416	0.139	18.850	0.05305 (0.3333)
Wenner Gamma		0.594	0.198	9.4248	0.10610 (0.6667)
Dipole-dipole	n = 1	0.416	0.139	18.850	0.05305 (0.3333)
	n = 2	0.697	0.174	75.398	0.01326 (0.0833)
	n = 3	0.962	0.192	188.50	0.00531 (0.0333)
	n = 4	1.220	0.203	376.99	0.00265 (0.0166)
	n = 5	1.476	0.211	659.73	0.00152 (0.0096)
	n = 6	1.730	0.216	1055.6	0.00095 (0.0060)
	n = 7	1.983	0.220	1583.4	0.00063 (0.0040)
	n = 8	2.236	0.224	2261.9	0.00044 (0.0028)
Equatorial dipole-dipole					
	n = 1	0.451	0.319	21.452	0.04662 (0.2929)
	n = 2	0.809	0.362	119.03	0.00840 (0.0528)
	n = 3	1.180	0.373	367.31	0.00272 (0.0171)
	n = 4	1.556	0.377	841.75	0.00119 (0.0075)
Wenner - Schlumberger					
	n = 1	0.519	0.173	6.2832	0.15915 (1.0000)
	n = 2	0.925	0.186	18.850	0.05305 (0.3333)
	n = 3	1.318	0.189	37.699	0.02653 (0.1667)
	n = 4	1.706	0.190	62.832	0.01592 (0.1000)
	n = 5	2.093	0.190	94.248	0.01061 (0.0667)
	n = 6	2.478	0.191	131.95	0.00758 (0.0476)
	n = 7	2.863	0.191	175.93	0.00568 (0.0357)
	n = 8	3.247	0.191	226.19	0.00442 (0.0278)
	n = 9	3.632	0.191	282.74	0.00354 (0.0222)
	n = 10	4.015	0.191	345.58	0.00289 (0.0182)
Pole-dipole	n = 1	0.519		12.566	0.07958 (0.5000)
	n = 2	0.925		37.699	0.02653 (0.1667)
	n = 3	1.318		75.398	0.01326 (0.0833)
	n = 4	1.706		125.66	0.00796 (0.0500)
	n = 5	2.093		188.50	0.00531 (0.0334)
	n = 6	2.478		263.89	0.00379 (0.0238)
	n = 7	2.863		351.86	0.00284 (0.0178)
	n = 8	3.247		452.39	0.00221 (0.0139)
Pole-Pole		0.867		6.28319	0.15915 (1.0000)

2.5.2 Dipole-dipole array

This array has been, and is still, widely used in resistivity/I.P. surveys because of the low E.M. coupling between the current and potential circuits. The arrangement of the electrodes is shown in Figure 2. The spacing between the current electrodes pair, C2-C1, is given as "**a**" which is the same as the distance between the potential electrodes pair P1-P2. This array has another factor marked as "**n**" in Figure 2. This is the ratio of the distance between the C1 and P1 electrodes to the C2-C1 (or P1-P2) dipole separation "**a**". For surveys with this array, the "**a**" spacing is initially kept fixed and the "**n**" factor is increased from 1 to 2 to 3 until up to about 6 in order to increase the depth of investigation. The sensitivity function plot in Figure 8c shows that the largest sensitivity values are located between the C2-C1 dipole pair, as well as between the P1-P2 pair. This means that this array is most sensitive to resistivity changes between the electrodes in each dipole pair. Note that the sensitivity contour pattern is almost vertical. Thus the dipole-dipole array is very sensitive to horizontal changes in resistivity, but relatively insensitive to vertical changes in the resistivity. That means that it is good in mapping vertical structures, such as dykes and cavities, but relatively poor in mapping horizontal structures such as sills or sedimentary layers. The median depth of investigation of this array also depends on the "**n**" factor, as well as the "**a**" factor (Table 2). In general, this array has a shallower depth of investigation compared to the Wenner array. However, for 2-D surveys, this array has a better horizontal data coverage than the Wenner (Figure 7).

One possible disadvantage of this array is the very small signal strength for large values of the "**n**" factor. The voltage is inversely proportional to the **cube** of the "**n**" factor. This means that for the same current, the voltage measured by the resistivity meter drops by about 200 times when "**n**" is increased from 1 to 6. One method to overcome this problem is to increase the "**a**" spacing between the C1-C2 (and P1-P2) dipole pair to reduce the drop in the potential when the overall length of the array is increased to increase the depth of investigation. Figure 9 shows two different arrangements for the dipole-dipole array with the same array length but with different "**a**" and "**n**" factors. The signal strength of the array with the smaller "**n**" factor (Figure 9b) is about 28 times stronger than the one with the larger "**n**" factor.

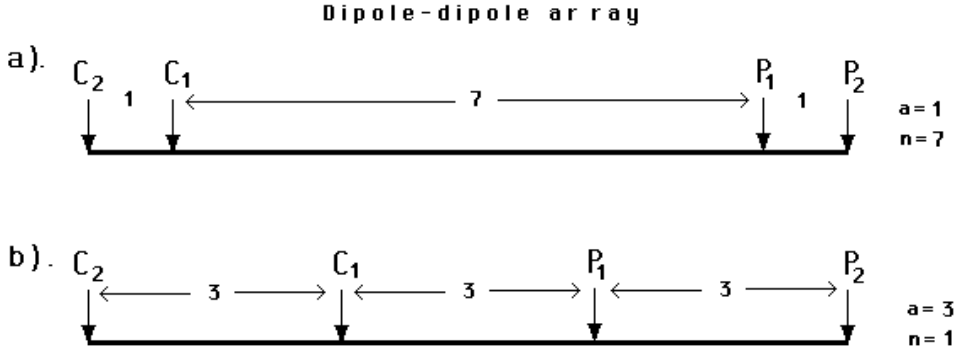

Figure 9. Two different arrangements for a dipole-dipole array measurement with the same array length but with different "**a**" and "**n**" factors resulting in very different signal strengths.

To use this array effectively, the resistivity meter should have comparatively high sensitivity and very good noise rejection circuitry, and there should be good contact between the electrodes and the ground in the survey. With the proper field equipment and survey techniques, this array has been successfully used in many areas to detect structures such as cavities where the good horizontal resolution of this array is a major advantage.

The plotting location of the corresponding datum point (based on the median depth of

investigation) used in drawing the apparent resistivity pseudosection is also shown in Figure 8c. Note that the pseudosection plotting point falls in an area with very low sensitivity values. For the dipole-dipole array, the regions with the high sensitivity values are concentrated below the C1-C2 electrodes pair and below the P1-P2 electrodes pair. In effect, the dipole-dipole array gives minimal information about the resistivity of the region surrounding the plotting point, and the distribution of the data points in the pseudosection plot does not reflect the subsurface area mapped by the apparent resistivity measurements. Note that if the datum point is plotted at the point of intersection of the two 45° angle lines drawn from the centres of the two dipoles, it would be located at a depth of 2.0 units (compared with 0.96 units given by the median depth of investigation method) where the sensitivity values are almost zero!

Loke and Barker (1996a) used an inversion model where the arrangement of the model blocks directly follows the arrangement of the pseudosection plotting points. This approach gives satisfactory results for the Wenner and Wenner-Schlumberger arrays where the pseudosection point falls in an area with high sensitivity values (Figures 8a and 8b). However, it is not suitable for arrays such as the dipole-dipole and pole-dipole where the pseudosection point falls in an area with very low sensitivity values. The RES2DINV program uses a more sophisticated method to generate the inversion model where the arrangement the model blocks is not tightly bound to the pseudosection.

2.5.3 Wenner-Schlumberger array

This is a new hybrid between the Wenner and Schlumberger arrays (Pazdirek and Blaha 1996) arising out of relatively recent work with electrical imaging surveys. The classical Schlumberger array is one of the most commonly used array for resistivity sounding surveys. A modified form of this array so that it can be used on a system with the electrodes arranged with a constant spacing is shown in Figure 10b. Note that the "**n**" factor for this array is the ratio of the distance between the C1-P1 (or P2-C2) electrodes to the spacing between the P1-P2 potential pair. The sensitivity pattern for the Schlumberger array (Figure 8b) is slightly different from the Wenner array with a slight vertical curvature below the centre of the array, and slightly lower sensitivity values in the regions between the C1 and P1 (and also C2 and P2) electrodes. There is a slightly greater concentration of high sensitivity values below the P1-P2 electrodes. This means that this array is moderately sensitive to both horizontal and vertical structures. In areas where both types of geological structures are expected, this array might be a good compromise between the Wenner and the dipole-dipole array. The median depth of investigation for this array is about 10% larger than that for the Wenner array for the same distance between the outer (C1 and C2) electrodes. The signal strength for this array is smaller than that for the Wenner array, but it is higher than the dipole-dipole array.

Note that the Wenner array is a special case of this array where the "**n**" factor is equals to 1. Figures 10c and 10d shows the pattern of the data points in the pseudosections for the Wenner and Wenner-Schlumberger arrays. The Wenner-Schlumberger array has a slightly better horizontal coverage compared with the Wenner array. For the Wenner array each deeper data level has 3 data points less than the previous data level, while for the Wenner-Schlumberger array there is a loss of 2 data points with each deeper data level. The horizontal data coverage is slightly wider than the Wenner array (Figures 10c and 10d), but narrower than that obtained with the dipole-dipole array.

2.5.4 Pole-pole array

This array is not as commonly used as the Wenner, dipole-dipole and Schlumberger arrays. In practice the ideal pole-pole array, with only one current and one potential electrode

(Figure 2), does not exist. To approximate the pole-pole array, the second current and potential electrodes (C2 and P2) must be placed at a distance which is more than 20 times the maximum separation between C1 and P1 electrodes used in the survey. The effect of the C2 (and similarly for the P2) electrode is approximately proportional to the ratio of the C1-P1 distance to the C2-P1 distance. If the effects of the C2 and P2 electrodes are not taken into account, the distance of these electrodes from the survey line must be at least 20 times the largest C1-P1 spacing used to ensure that the error is less than 5%. In surveys where the inter-

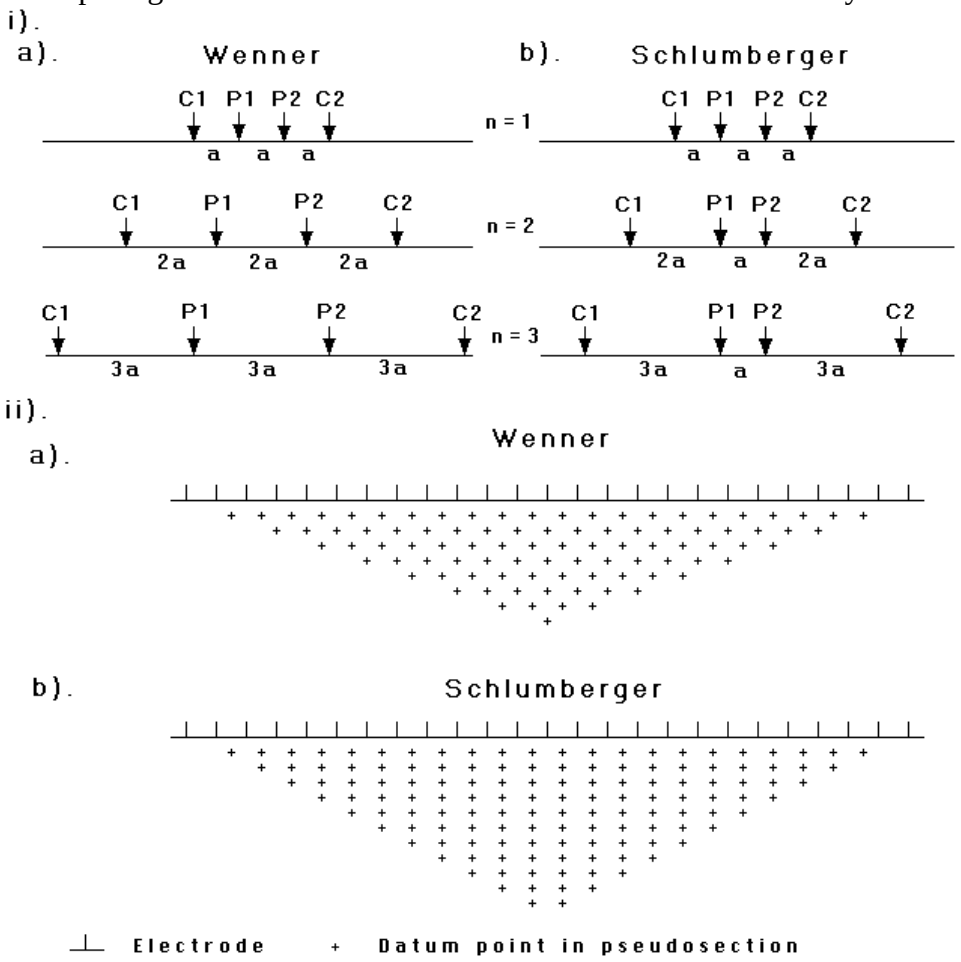

Figure 10. A comparison of the (i) electrode arrangement and (ii) pseudosection data pattern for the Wenner and Wenner-Schlumberger arrays.

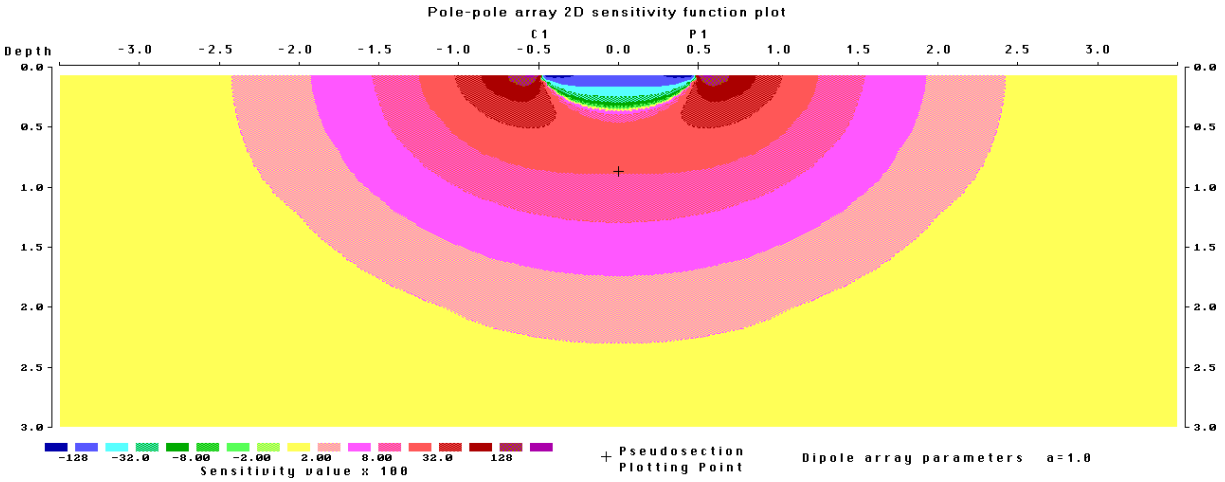

Figure 11. The sensitivity pattern for the pole-pole array.

electrode spacing along the survey line is more than a few metres, there might be practical problems in finding suitable locations for the C2 and P2 electrodes to satisfy this requirement. Another disadvantage of this array is that because of the large distance between the P1 and P2 electrodes, it is can pick up a large amount of telluric noise which can severely degrade the quality of the measurements. Thus this array is mainly used in surveys where relatively small electrode spacings (less than 10 metres) are used. It is popular in some applications such as archaeological surveys where small electrode spacings are used. It has also been used for 3-D surveys (Li and Oldenburg 1992).

This array has the widest horizontal coverage and the deepest depth of investigation. However, it has the poorest resolution, which is reflected by the comparatively large spacing between the contours in the sensitivity function plot (Figure 11).

2.5.5 Pole-dipole array

The pole-dipole array also has relatively good horizontal coverage, but it has a significantly higher signal strength compared with the dipole-dipole array and it is not as sensitive to telluric noise as the pole-pole array. Unlike the other common arrays, the pole-dipole array is an asymmetrical array (Figure 12a) and over symmetrical structures the apparent resistivity anomalies in the pseudosection are asymmetrical. In some situations, the asymmetry in the measured apparent resistivity values could influence the model obtained after inversion. One method to eliminate the effect of this asymmetry is to repeat the measurements with the electrodes arranged in the reverse manner (Figure 12b). By combining the measurements with the "forward" and "reverse" pole-dipole arrays, any bias in the model due to the asymmetrical nature of this array would be removed.

The pole-dipole array also requires a remote electrode, the C2 electrode, which must be placed sufficiently far from the survey line. For the pole-dipole array, the effect of the C2 electrode is approximately proportional to the *square* of ratio of the C1-P1 distance to the C2-P1 distance. Thus the pole-dipole array is less affected by the C2 remote electrode compared with the pole-pole array. If the distance of the C2 electrode is more than 5 times the largest C1-P1 distance used, the error caused by neglecting the effect of the C2 electrode is less than 5% (the exact error also depends on the location of the P2 electrode for the particular measurement and the subsurface resistivity distribution).

Due to its good horizontal coverage, this is an attractive array for multi-electrode resistivity meter systems with a relatively small number of nodes. The signal strength is lower compared with the Wenner and Wenner-Schlumberger arrays but higher than the dipole-dipole array. For IP surveys, the higher signal strength (compared with the dipole-dipole array) combined with the lower EM coupling (compared with the Wenner and Wenner-Schlumberger arrays) due to the separation of the circuitry of the current and potential electrodes makes this array an attractive alternative.

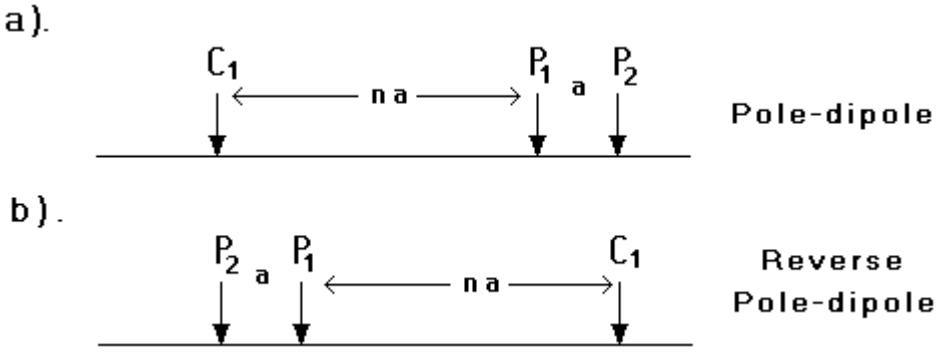

Figure 12. The forward and reverse pole-dipole arrays.

The signal strength for the pole-dipole array decreases with the *square* of the "**n**" factor. While this effect is not as severe as the dipole-dipole array, it is usually not advisable to use "**n**" values of greater than 8 to 10. Beyond this, the "**a**" spacing between the P1-P2 dipole pair should be increased to obtain a stronger signal strength.

2.5.6 High-resolution electrical surveys with overlapping data levels

In seismic reflection surveys, the common depth point method is frequently used to improve the quality of the signals from subsurface reflectors. A similar technique can be used to improve the data quality for resistivity/IP surveys, particularly in noisy areas. This is by using overlapping data levels with different combinations of "**a**" and "**n**" values for the Wenner-Schlumberger, dipole-dipole and pole-dipole arrays.

To simplify matters, let us consider the case for the Wenner-Schlumberger array with an inter-electrode spacing of 1 metre along the survey line. A high-resolution Wenner-Schlumberger survey will start with the "**a**" spacing (which is the distance between the P1-P2 potential dipole) equals to 1 metre and repeat the measurements with "**n**" values of 1, 2, 3 and 4. Next the "**a**" spacing is increased to 2 metres, and measurements with "**n**" equals to 1, 2, 3 and 4 are made. This process is repeated for all possible values of the "**a**" spacing. To be on the safe side, the data set should contain all the possible data points for the Wenner array. The number of data points produced by such a survey is more than twice that obtained with a normal Wenner array survey. Thus the price of better horizontal data coverage and resolution is an increase in the field survey time.

A Wenner array with "**a**" equals to 2 metres (Figure 10a) will have a total array length of 6 metres and a median depth of investigation of about 1.04 metres. In comparison, a measurement made with "**a**" equals to 1 metre and "**n**" equals to 2 using the Wenner-Schlumberger array will have a total array length of 5 metres and a slightly smaller depth of investigation of 0.93 metre (Figure 10b). While the depth of investigation of the two arrangements are similar, the section of the subsurface mapped by the two arrays will be slightly different due to the different sensitivity patterns (Figures 9a and 9b). So the two measurements will give slightly different information about the subsurface. A measurement with "**a**" equals to 1 metre and "**n**" equals to 3 (Figure 10b) will have a depth of investigation of 1.32 metres. If all the 3 combinations are used, the data set will have measurements with pseudodepths of 0.93, 1.02 and 1.32 metres. This results in a pseudosection with overlapping data levels.

A similar "high-resolution" survey technique can also be used with the dipole-dipole and pole-dipole arrays by combining measurements with different "**a**" and "**n**" values to give overlapping data levels. In particular, this technique might be useful for the dipole-dipole array since the signal strength decreases rapidly with increasing "**n**" values (section 2.5.2). A typical high-resolution dipole-dipole survey might use the following arrangement; start with a dipole of "**1a**" and "**n**" values of 1, 2, 3, 4, 5, 6; followed by a dipole of "**2a**" and "**n**" values of 1, 2, 3, 4, 5, 6; and if necessary another series of measurements with a dipole of "**3a**" and "**n**" values of 1, 2, 3, 4, 5, 6. Measurements with the higher "**n**" values of over 4 would have higher noise levels. However, by having such redundant measurements using the overlapping data levels, the effect of the more noisy data points will be reduced. A field example from an IP survey using this sort of arrangement is given in section 2.7.7.

In theory, it should be possible to combine measurements made with different arrays to take advantage of the different properties of the various arrays. Although this is not a common practice, it could conceivably give useful results in some situations. The RES2DINV program supports the use of such mixed data sets.

2.5.7 Summary

If your survey is in a noisy area and you need good vertical resolution and you have limited survey time, use the Wenner array. If good horizontal resolution and data coverage is important, and your resistivity meter is sufficiently sensitive and there is good ground contact, use the dipole-dipole array. If you are not sure, or you need both reasonably good horizontal and vertical resolution, use the Wenner-Schlumberger array with overlapping data levels. If you have a system with a limited number of electrodes, the pole-dipole array with measurements in both the forward and reverse directions might be a viable choice. For surveys with small electrode spacings and good horizontal coverage is required, the pole-pole array might be a suitable choice.

2.6 Computer interpretation

After the field survey, the resistance measurements are reduced to apparent resistivity values. Practically all commercial multi-electrode systems come with the computer software to carry out this conversion. In this section, we will look at the steps involved in converting the apparent resistivity values into a resistivity model section that can be used for geological interpretation.

2.6.1 Data input and format

To interpret the data from a 2-D imaging survey, a 2-D model for the subsurface which consists of a large number of rectangular blocks is usually used (Figure 15a). A computer program is then used to determine the resistivity of the blocks so that the calculated apparent resistivity values agree with the measured values from the field survey. The computer program RES2DINV.EXE will automatically subdivide the subsurface into a number of blocks, and it then uses a least-squares inversion scheme to determine the appropriate resistivity value for each block. The location of the electrodes and apparent resistivity values must be entered into a text file which can be read by the RES2DINV program. The program manual gives a detailed description of the data format used. As an example, part of an example data file LANDFILL.DAT, is shown below with some comments :-

Data in file	**Comments**
LANDFILL SURVEY	*; Name of survey line*
3.0	*; Smallest electrode spacing*
1	*; Array type (Wenner = 1, Dipole-dipole = 3, Schlumberger = 7)*
334	*; Total number of measurements*
1	*; Type of x-location for datum points (1 for mid-point).*
0	*; Flag for I.P. data (enter 0 for resistivity data only)*
4.50 3.0 84.9	*; The x-location, electrode spacing, apparent resistivity value*
7.50 3.0 62.8	*; The same information for other data points*
0.50 3.0 49.2	
13.50 3.0 41.3	
16.50 3.0 34.9	
19.50 3.0 31.6	
22.50 3.0 25.2	
25.50 3.0 27.0	
28.50 3.0 22.4	

.
.
0
0
0
0

As an exercise, read in the LANDFILL.DAT file using the "**F**ile" option on the main menu bar of the RES2DINV program. Next select the "**I**nversion" option, and then the "**L**east-squares inversion" suboption. The program will then automatically try to determine the resistivity values of the blocks in the subsurface model. If you have time, try to interpret various types of data from other surveys. The file RATHCHRO.DAT is an interesting example with surface topography.

The data format for the pole-dipole, dipole-dipole and Wenner-Schlumberger arrays are slightly different as an additional parameter, the "**n**" factor (see Figure 2), is involved. Please refer to Appendix A for details concerning the data format for these arrays.

The program can also accept combined resistivity/IP data, data from underwater surveys and cross-borehole surveys. Please refer to Appendices F, H and K of the RES2DINV manual for the data format.

2.6.2 Guidelines for data inversion

Many professionals carrying out resistivity imaging surveys will likely to be field engineers, geologists or geophysicists who might not familiar with geophysical inversion theory. The RES2DINV program is designed to operate, as far as possible, in an automatic and robust manner with minimal input from the user. It has a set of default parameters which guides the inversion process. In most cases the default parameters give reasonable results. This section describes some of the parameters the user can modify to fine-tune the inversion process. A very brief outline of the theory behind the inversion methods used, and the role of some of the inversion parameters, is given in Appendix C.

The problem of non-uniqueness is well known in the inversion of resistivity sounding and other geophysical data. For the same measured data set, there is wide range of models giving rise to the same calculated apparent resistivity values. To narrow down the range of possible models, normally some assumptions are made concerning the nature of the subsurface that can be incorporated into inversion subroutine.

In almost all surveys, something is known about the geology of the subsurface. In some cases it is known whether the subsurface bodies of interest have gradational boundaries, such as pollution plumes (Figure 20) or bedrock with a thick transitional weathered layer. In such cases, the conventional smoothness-constrained inversion method (deGroot-Hedlin. and Constable, 1990) gives a model which more closely corresponds with reality. This is the default method used by the RES2DINV program. In others, the subsurface might consist of discrete geological bodies that are internally almost homogeneous with sharp boundaries between different bodies. Examples are igneous intrusives in sedimentary rocks and massive ore bodies (Figure 22). For such cases, a robust model inversion constrain is more suitable. Figure 13 shows the results from the inversion of a synthetic data set using the standard least-squares smoothness-constrain and the robust inversion model constrain. It should be emphasised that like most synthetic examples, it is an extreme case designed to highlight the advantages of a particular method. In this case, the bodies are internally homogeneous with sharp boundaries. As such, it is not surprising that robust model inversion method gives

significantly better results. However, it does illustrate the advantages of using suitable inversion constrains.

Most field data sets probably lie between the two extremes of a smoothly varying resistivity and discrete geological bodies with sharp boundaries. If you have a sufficiently fast computer (Pentium II upwards), and a relatively small data set (2000 datum points or less), it might be a good idea to invert the data twice. Once with the standard smoothness-constrain and again with the robust model constrain. This will give two extremes in the range of possible models that can be obtained for the same data set. Features that are common to both models are more likely to be real.

Some geological bodies have a predominantly horizontal orientation (for example sedimentary layers and sills) while others might have a vertical orientation (such as dykes and faults). This information can be incorporated into the inversion process by setting the relative weights given to the horizontal and vertical flatness filters. If for example the structure has a predominantly vertical orientation, such as a dyke (Figure 17), the vertical flatness filter is given a greater weight than the horizontal filter.

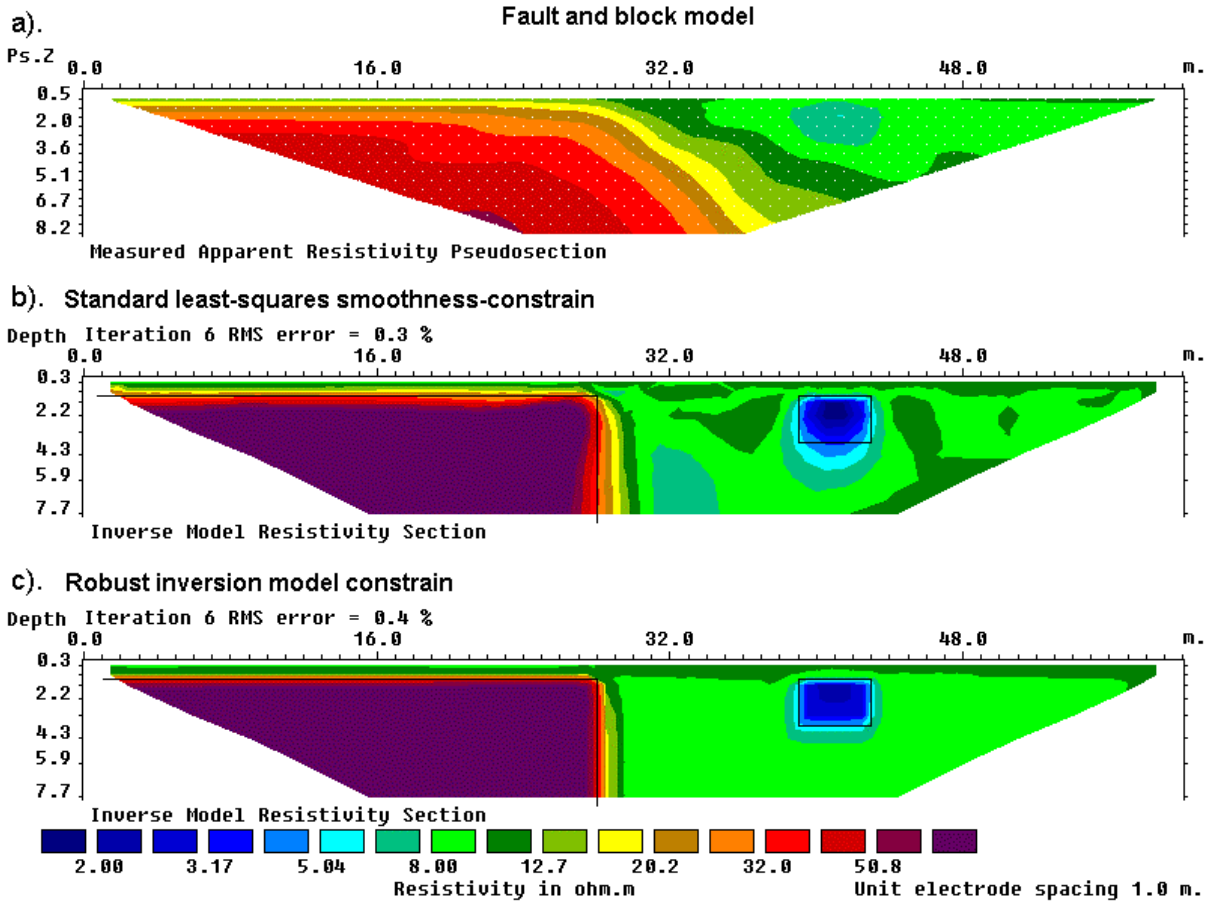

Figure 13. Example of inversion results using the smoothness-constrain and robust inversion model constrains. (a) Apparent resistivity pseudosection (Wenner array) for a synthetic test model with a faulted block (100 ohm.m) in the bottom-left side and a small rectangular block (2 ohm.m) on the right side with a surrounding medium of 10 ohm.m. The inversion models produced by (b) the conventional least-squares smoothness-constrained method and (c) the robust inversion method.

Another important factor is the quality of the field data. Good quality data usually show a smooth variation of apparent resistivity values in the pseudosection. To get a good model, the data must be of equally good quality. If the data is of poorer quality, with

unusually high or low apparent resistivity values, there are several things that could be done. The first step is to look at the apparent resistivity pseudosection. If there are spots with relatively low or high values, they are likely to be bad data points (Figure 14a). With the RES2DINV program, you can also plot the data in profile form that helps to highlight the bad datum points, and remove them from the data set manually. If the bad datum points are more widespread and random in nature, there are two program inversion parameters that you can modify. Firstly, increase the damping factors. A larger damping factor would tend to produce smoother models with less structure, and thus poorer resolution, but it would less sensitive to noisy data. The second setting is the robust data constrain option. The inversion subroutine normally tries to reduce the *square* of the difference between the measured and calculated apparent resistivity values. Data points with a larger difference between the measured and calculated apparent resistivity values are given a greater weight. This normally gives acceptable results if the noise is random in nature. However, in some cases, a few bad data points with unusually low or high apparent resistivity values (outliers) could distort the results. To reduce the effect of such bad datum points, the robust data constrain causes the program to reduce the *absolute* difference between measured and calculated apparent resistivity values. The bad data points are given the same weight as the other data points, and thus their effect on the inversion results is considerably reduced. Another method to remove bad data points after carrying out the inversion is described in Appendix C.

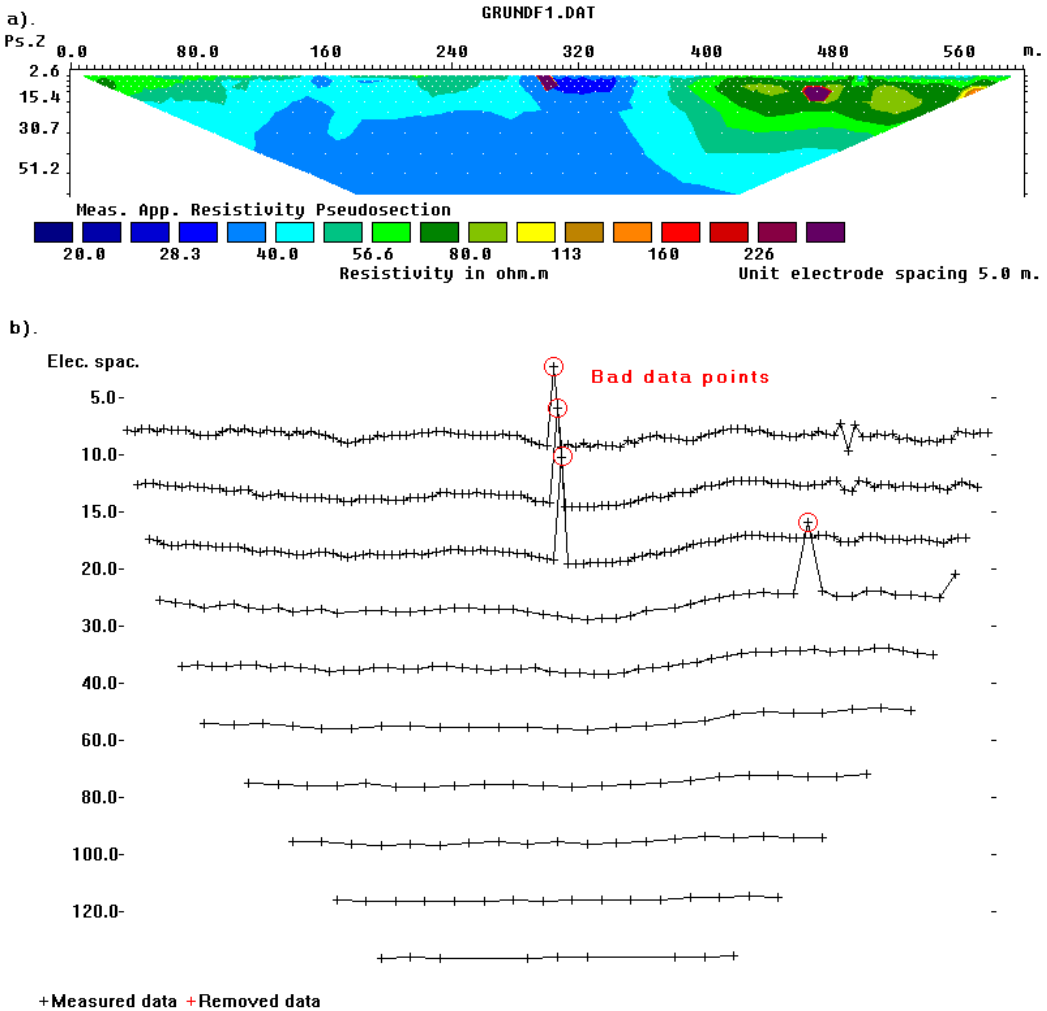

Figure 14. An example of a field data set with a few bad data points. The most obvious bad datum points are located below the 300 metres and 470 metres marks. (a) The apparent resistivity data in pseudosection form and in (b) profile form.

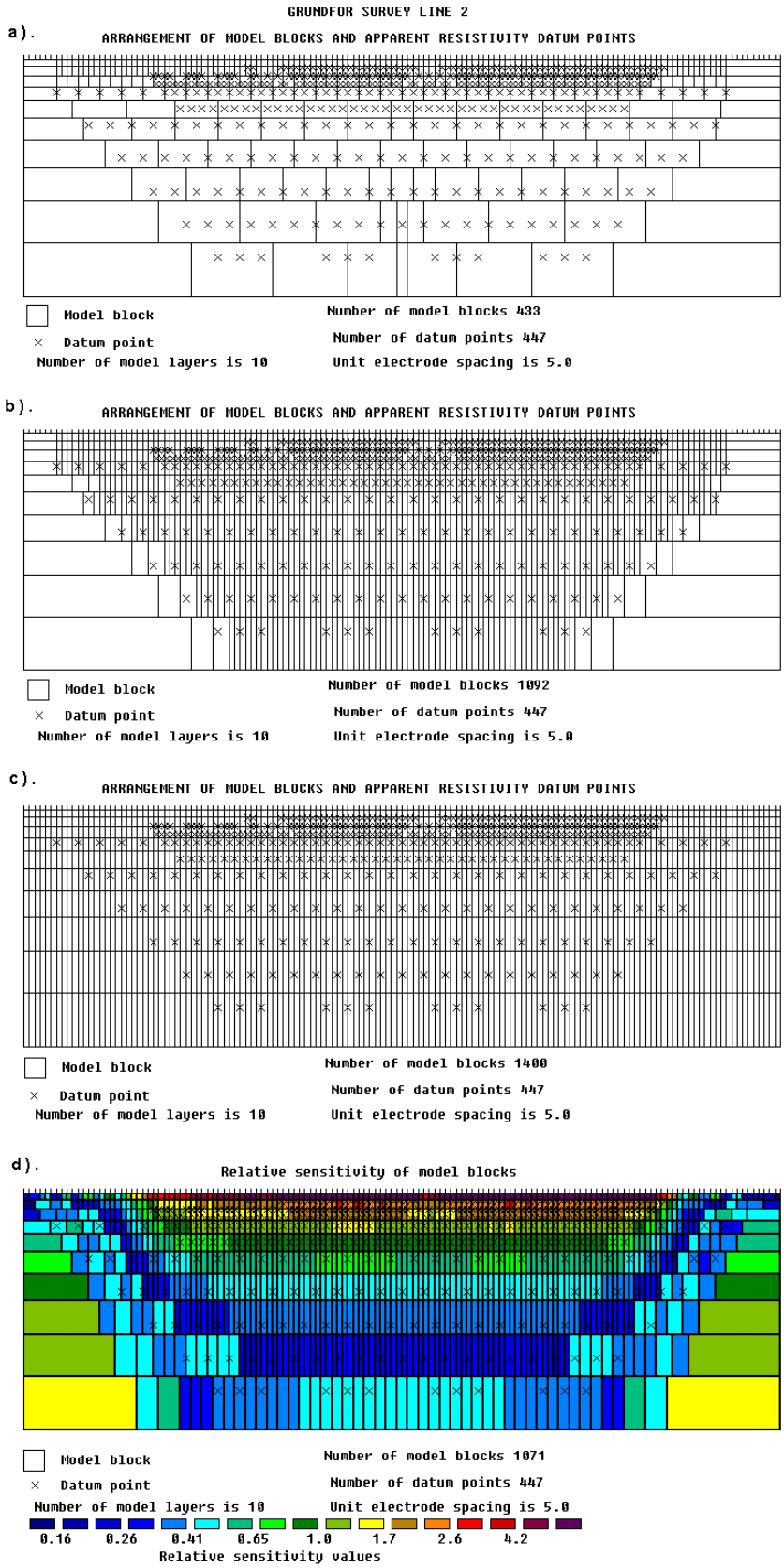

Figure 15. Subdivision of the subsurface into rectangular blocks to interpret the data from a 2-D imaging survey using different algorithms. Models obtained with (a) the default algorithm, (b) by allowing the number of model blocks to exceed the number of datum points, (c) a model which extends to the edges of the survey line and (d) using the sensitivity values for a homogeneous earth model.

Another factor that the user can control is the size and distribution of the rectangular blocks used by the inversion model (Figure 15). By default, the program uses a heuristic algorithm partly based on the position of the data points to generate the size and position of the model blocks. The depth to the deepest layer in the model is set to be about the same as the largest depth of investigation of the datum points, and the number of model blocks does not exceed the number of datum points. In general, this produces a model where the thickness of the layers increase with depth, and with thicker blocks at the sides and in the deeper layers (Figure 16a). For most cases, this gives an acceptable compromise. The distribution of the datum points in the pseudosection is used as a rough guide in allocating the model blocks, but the model section does not rigidly follow the pseudosection. To produce a model with more uniform widths, the user can select a model where the number of model blocks can exceed the number of datum points (Figure 16b). Another possible configuration with model blocks of uniform thickness right up to the edges of the survey line is shown in Figure 16c. This is probably an extreme case. As the number of model blocks increase, the computer time needed to carry out the inversion also increases. This can be an important consideration for very large data sets with several hundred electrodes. Figure 16d shows the block distribution generated by a more quantitative approach based the sensitivity values of the model blocks. This technique takes into account the information contained in the data set concerning the resistivity of the subsurface for a homogeneous earth model. It tries to ensure that the data sensitivity of any block does not become too small (in which case the data set does not have much information about the resistivity of the block).

The thickness of the layers can also be modified by the user. This can be used to extend the maximum depth of the model section beyond the depth of investigation of the data set. This is useful in cases where a significant structure lies just below the maximum depth of investigation of the data set.

2.7 Field examples

Here we will look at a number of examples from various parts of the world to give you an idea of the range of practical survey problems in which the electrical imaging method has been successfully used.

2.7.1 Agricultural pollution - Aarhus, Denmark

In many parts of Western Europe, which has large areas under cultivation, the contamination of water supplies due to fertilisers and pesticides used in agriculture has become a serious problem. A combined electromagnetic and resistivity survey was carried out the Department of Earth Sciences, University of Aarhus to map the lithology of the near-surface unconsolidated sediments and aquifers in the Grundfor area at about 20 km northwest of Aarhus in Denmark (Christensen and Sorensen 1994). In this case, the concentration of the agricultural pollutants is very low and does not have a significant effect of the resistivity of the subsurface materials. The main purpose of the geophysical surveys was to map the lithology of the near-surface soil materials.

Clayey soil is known to be relatively impermeable, but sandy soil which is relatively permeable can provide an infiltration path for the pollutants to enter the aquifers. Figure 16 shows the results from one of the resistivity surveys. The clayey soils, which have a relatively lower resistivity, can be easily distinguished from the sandy soils. The interpretation model from this survey was confirmed by a number of boreholes along the survey line.

2.7.2 Odarslov Dyke - Sweden

A dolerite dyke surrounded by shales causes a prominent high resistivity zone (Dahlin 1996) near the middle of the pseudosection in the upper part of Figure 17. This is a particularly difficult data set to invert as the width of the high resistivity dyke is smaller than the depth to the lower section of the dyke. Thus the lower part of the dyke is less well resolved due to the reduction of the resolution of the resistivity method with depth. In the model section, the dyke shows up as a near vertical high resistivity body. This data set has 701 datum points and 181 electrodes. While the Wenner array is probably not the best array to map such a vertical structure, the dyke is still clearly shown in the model section. This survey was conducted in Sweden by Dr. Torleif Dahlin of the Department of Engineering Geology, Lund University. In the inversion of this data set, the robust inversion (Claerbout and Muir 1973) option in RES2DINV was used which sharpens the boundary between the dyke and the surrounding country rocks in the resulting inversion model. This choice is suitable for this data set since the dyke probably has a sharp boundary with the surrounding rocks.

2.7.3 Underground Cave - Texas, U.S.A

This is an interesting example of a dipole-dipole survey to map caves within a limestone bedrock. This survey was carried out to map a previously known cave at the 4T Ranch north of Austin, Texas. This cave, which is filled with air, causes a prominent high resistivity anomaly near the centre of the pseudosection (Figure 18). The data was recorded with the Sting/Swift automatic multielectrode system manufactured by Advanced Geosciences, Inc. in Austin, Texas and the actual recording time was less than 40 minutes. In the course of this survey a new cave, subsequently named the Sting Cave, was discovered. This cave causes a high resistivity anomaly near the bottom left corner of the pseudosection. The inversion model gives the depth to the top of the Sting Cave at around 20 feet which agrees with the actual depth directly measured by an underground cave survey.

This is a relatively small data set with 172 data points and 28 electrodes. A complete inversion took about 98 seconds (1.6 minutes) on a 90 Mhz Pentium computer, while on a 266 Mhz Pentium II computer it took only 23 seconds!

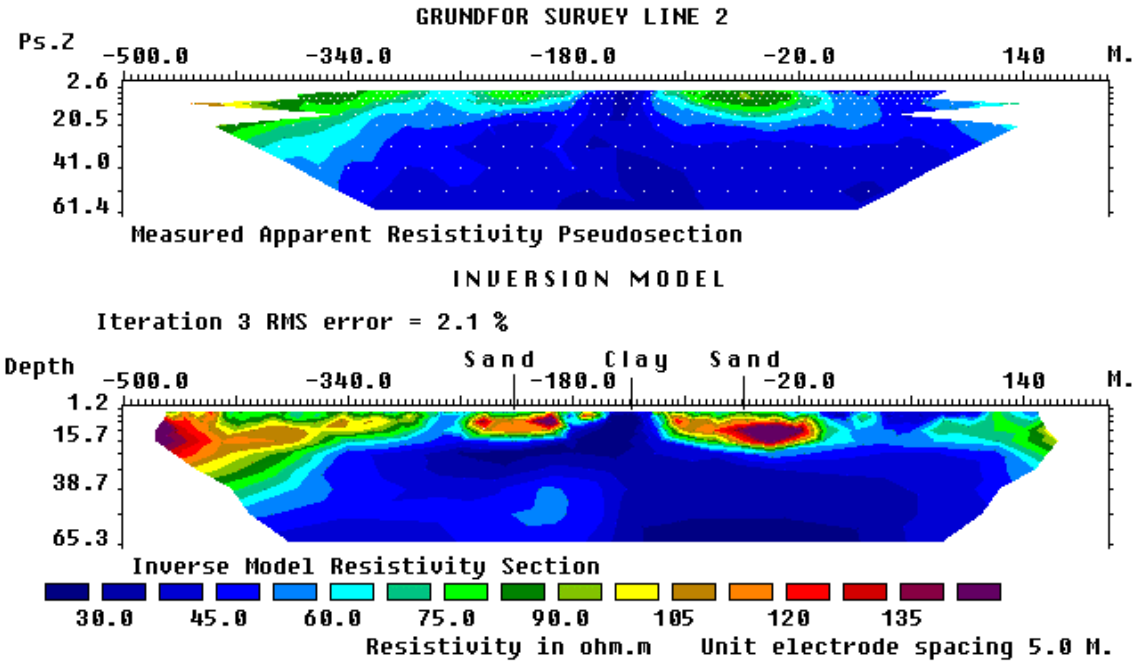

Figure 16. (a) The apparent resistivity pseudosection for the Grundfor Line 2 survey with (b) the interpretation model section.

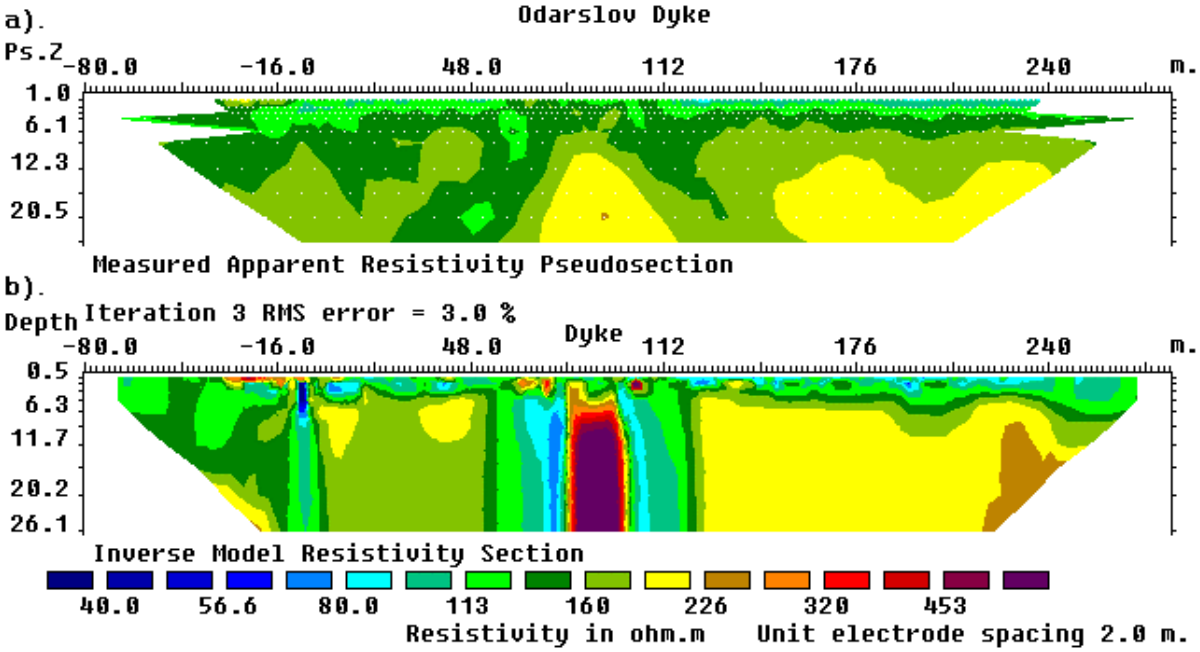

Figure 17. The observed apparent resistivity pseudosection for the Odarslov dyke survey together with an inversion model.

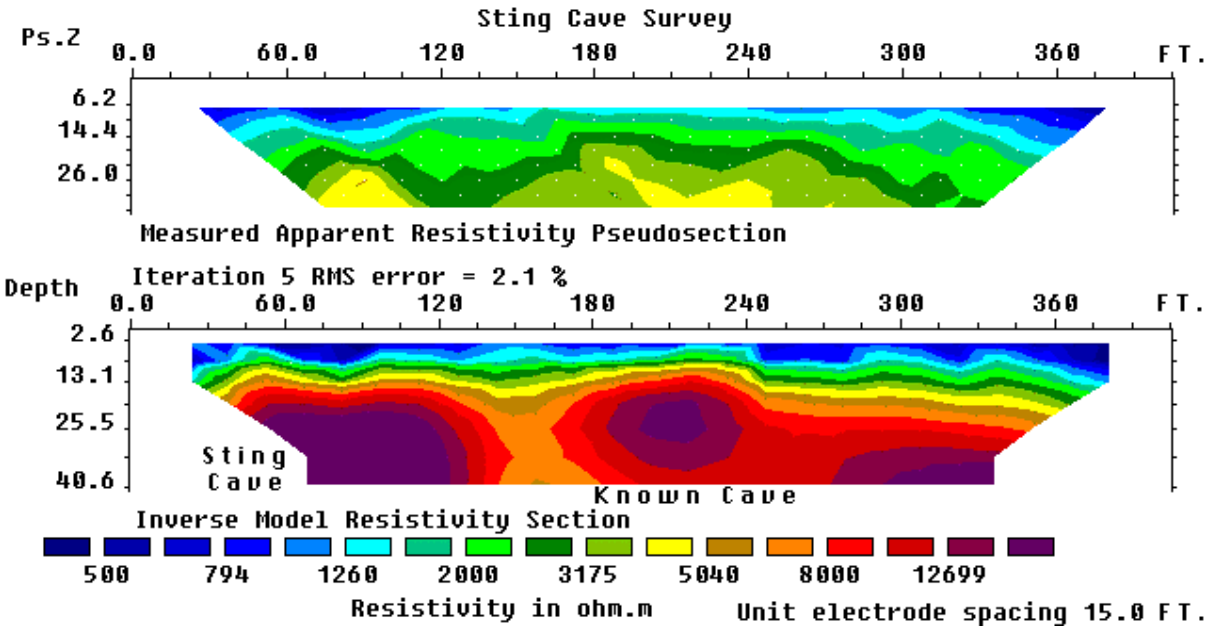

Figure 18. The observed apparent resistivity pseudosection for the Sting Cave survey together with an inversion model. The time taken to invert this data set on a 90 Mhz Pentium computer was 98 seconds (1.6 minutes), while on a 266 Mhz Pentium II it took 23 seconds.

2.7.4 Landslide - Cangkat Jering, Malaysia

A recent problem faced in Malaysia is landslides on hill slopes. The landslides are often triggered by water accumulation within part of the slope which leads to weakening of a section of the slope. Figure 19 shows the results from a survey conducted on the upper part of a slope where a landslide had occurred in the lower section. Weathering of the granitic bedrock produced a clayey sandy soil mixed with core boulders and other partially weathered material. The image obtained from this survey shows a prominent low resistivity zone below the centre of the survey line. This is probably caused by water accumulation in this region which reduces the resistivity to less than 600 Ohm•m. To stabilise the slope, it would be necessary to pump the excess water from this zone. Thus, it is important to accurately map the zone of ground water accumulation. This data set also shows an example with topography in the model section.

2.7.5 Old Tar Works - U.K.

A common environmental problem in industrial countries is derelict industrial land. Before such land can be rehabilitated, it is necessary to map old industrial materials (such as metals and concrete blocks) that are left buried in the ground. Another problem in such areas is chemical wastes that had been stored within the factory grounds. Due to the nature of such sites, the subsurface is often very complex and is a challenging target for most geophysical methods. The survey for this example was carried out on a derelict industrial site where leachate was known, from a small number of exploratory wells, to be moving from a surface waste lagoon into the underlying sandstones (Barker 1996). Eventually the leachate was seen seeping into a nearby stream. However, the extent of the subsurface contamination was not known.

An electrical imaging survey was carried out along an old railway bed between the lagoon and the stream. The metal railway lines had been removed except for short lengths embedded in asphalt below a large metal loading bay. In the apparent resistivity pseudosection (Figure 20a), the area with contaminated ground water shows up as a low resistivity zone to the right of the 140 metres mark. The metal loading bay causes a prominent inverted V shaped low resistivity anomaly at about the 90 metres mark. In the inversion model (Figure 20b), the computer program has managed to reconstruct the correct shape of the metal loading bay near the ground surface. There is an area of low resistivity at the right half of the section which agrees with what is known from wells about the occurrence of the contaminated ground water. The plume is clearly defined with a sharp boundary at 140 metres along the profile. The contaminated zone appears to extend to a depth of about 30 metres.

2.7.6 Holes in clay layer - U.S.A.

This survey was carried out for the purpose of mapping holes in a clay layer that underlies 8 to 20 feet of clean sand. The results from the electrical imaging survey were subsequently confirmed by boreholes.

The pseudosection from one line from this survey is shown in Figure 21a. The data in the pseudosection was built up using data from horizontally overlapping survey lines. One interesting feature of this survey is that it demonstrates the misleading nature of the pseudosection, particularly for the dipole-dipole array. In the inversion model, a high resistivity anomaly is detected below the 200 ft. mark, which is probably a hole in the lower clay layer (Figure 21b). This feature falls in an area in the pseudosection where there is an apparent gap in the data. However, a plot of the sensitivity value of the blocks used in the inversion model shows that the model blocks in the area of the high resistivity body have higher sensitivity values (i.e. more reliable model resistivity values) than adjacent areas at the

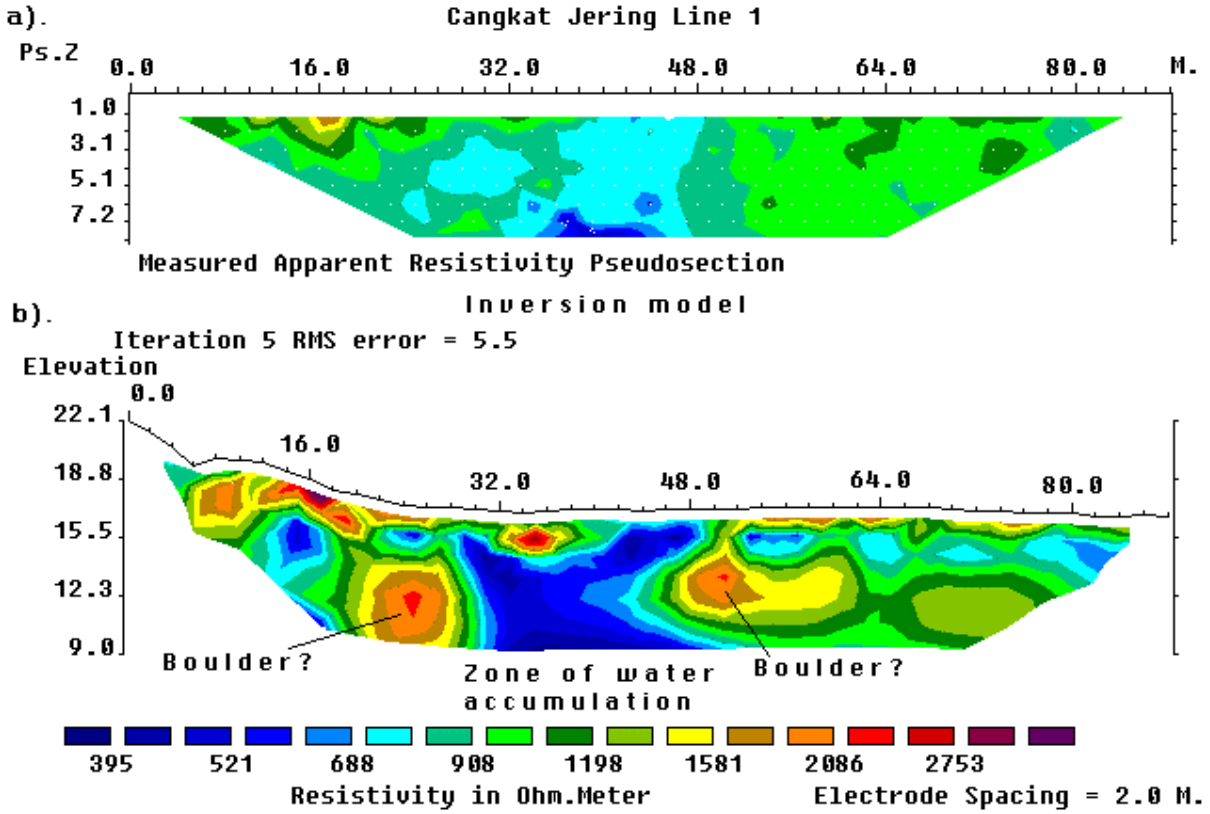

Figure 19. (a) The apparent resistivity pseudosection for a survey across a landslide in Cangkat Jering and (b) the interpretation model for the subsurface.

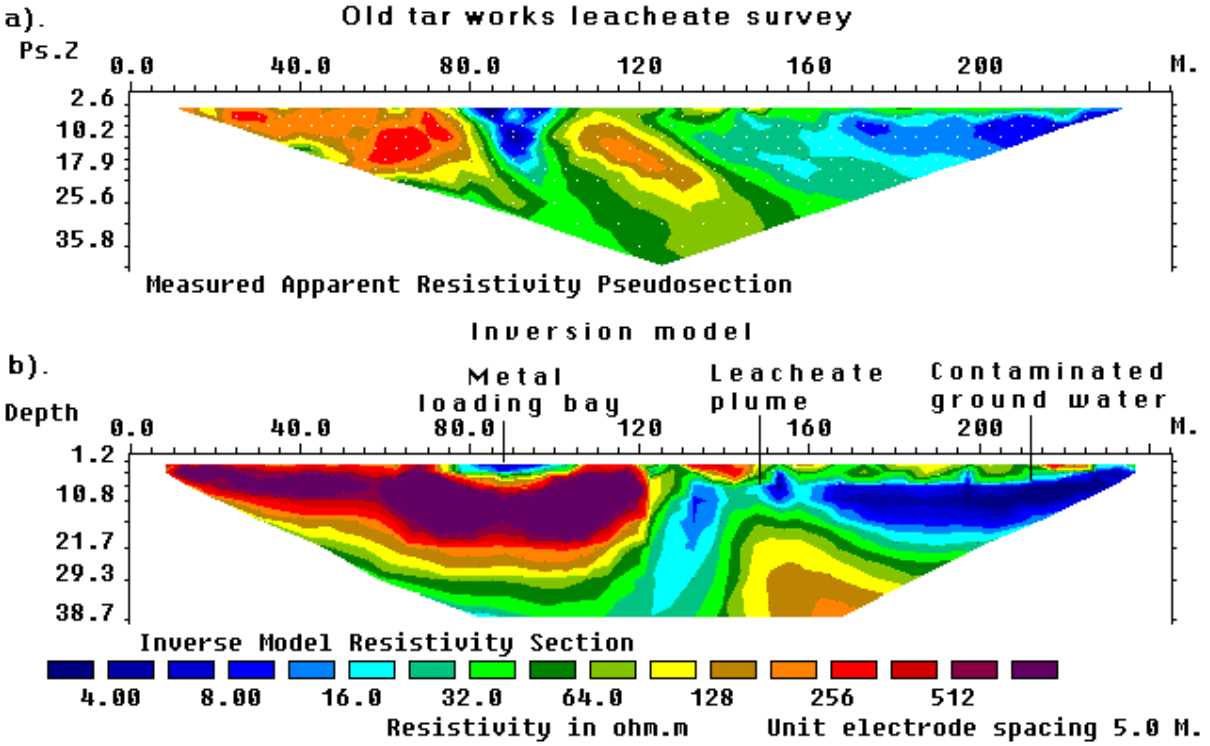

Figure 20. (a) The apparent resistivity pseudosection from a survey over a derelict industrial site, and the (b) computer model for the subsurface.

same depth with more data points in the pseudosection plot (Figure 21c). This phenomena is basically due to the shape of the contours in the sensitivity function of the dipole-dipole array (Figure 8c). This example illustrates the danger of only using the distribution of the datum points in the pseudosection to constrain the position of the model blocks (Loke and Barker, 1996a). If the model blocks are placed only at the location of the datum points, the high resistivity body will be missing from the inversion model, and an important subsurface feature would not be detected!

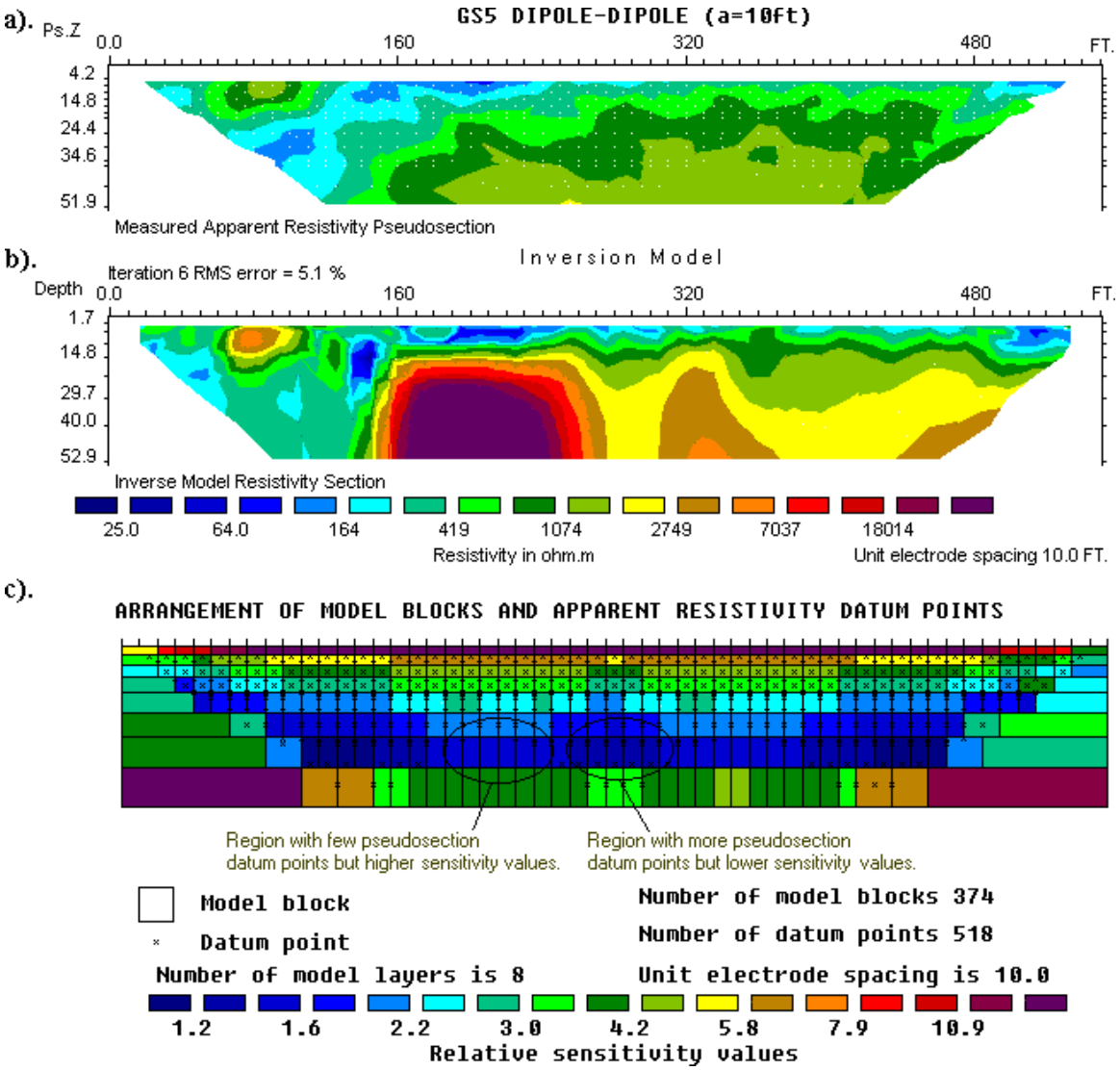

Figure 21. (a) Apparent resistivity pseudosection for the survey to map holes in the lower clay layer. (b) Inversion model and (c) sensitivity values of the model blocks used by the inversion program.

2.7.7 Magusi River Ore Body - Canada

This is an example of a combined resistivity and induced polarization (I.P.) survey. This survey was conducted over the Magusi River ore body where dipole spacings (the "**a**" factor in Figure 2) of 30.5 meters (100 feet), 61.0 meters (200 feet) and 91.4 meters (300 feet) were used (Edwards 1977). For each dipole length, measurements were made with values of 1 to 4 for the dipole separation factor "**n**". The I.P. measurements were given as metal factor values. The resulting resistivity and I.P. pseudosections have a very complex distribution of

the data points due to the overlapping data levels (Figure 22a). The original metal factor values given by Edwards (1977) were divided by two to conform with the more modern definition of this parameter (Witherly and Vyselaar 1990). The ore body shows up as a low resistivity body of less than 10 Ohm•m with high metal factor values of more than 350 near the middle of the survey line in the model sections (Figures 22b and 22d). The robust inversion option was also used for this data set since the metal sulphide ore body has a sharp and distinct resistivity/I.P. contrast with the igneous/metamorphic country rocks.

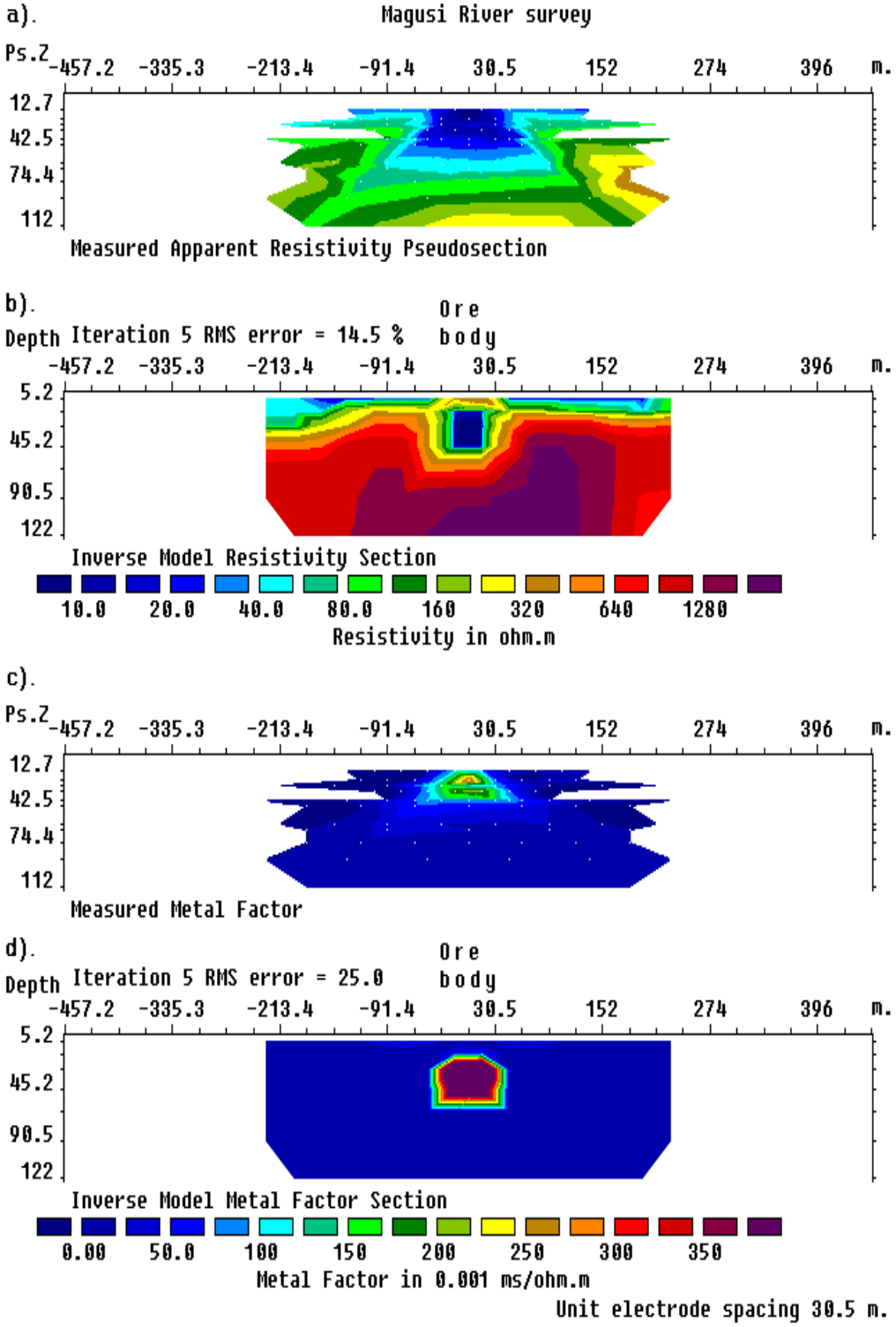

Figure 22. Magusi River ore body. (a) Apparent resistivity pseudosection, (b) resistivity model section, (c) apparent metal factor pseudosection and (d) metal factor model section.

2.7.8 Marine bottom resistivity survey - U.S.A.

Contrary to popular belief, it is actually possible to carry out resistivity surveys underwater, even in marine environments. Figure 23a shows the apparent resistivity pseudosection from a survey along the seabed between Fisher Island and the mainland in Miami, Florida (Lagmanson 1998). The seabed consists of mud with a thickness of up to about 3 metres followed by sand (up to 2 metres thick) overlying a sandstone and limestone bedrock which also contains cavities. Due to the low resistivity of the seawater, the electric potentials measured were extremely small, even with the Wenner-Schlumberger array. To get accurate readings under such adverse conditions, a very sensitive resistivity meter system was used (Lagmanson 1998). The subsurface model after inversion is shown in Figure 23c. Note the seabed topography, and the very low resistivity mud and sand upper layers overlying the higher resistivity bedrock.

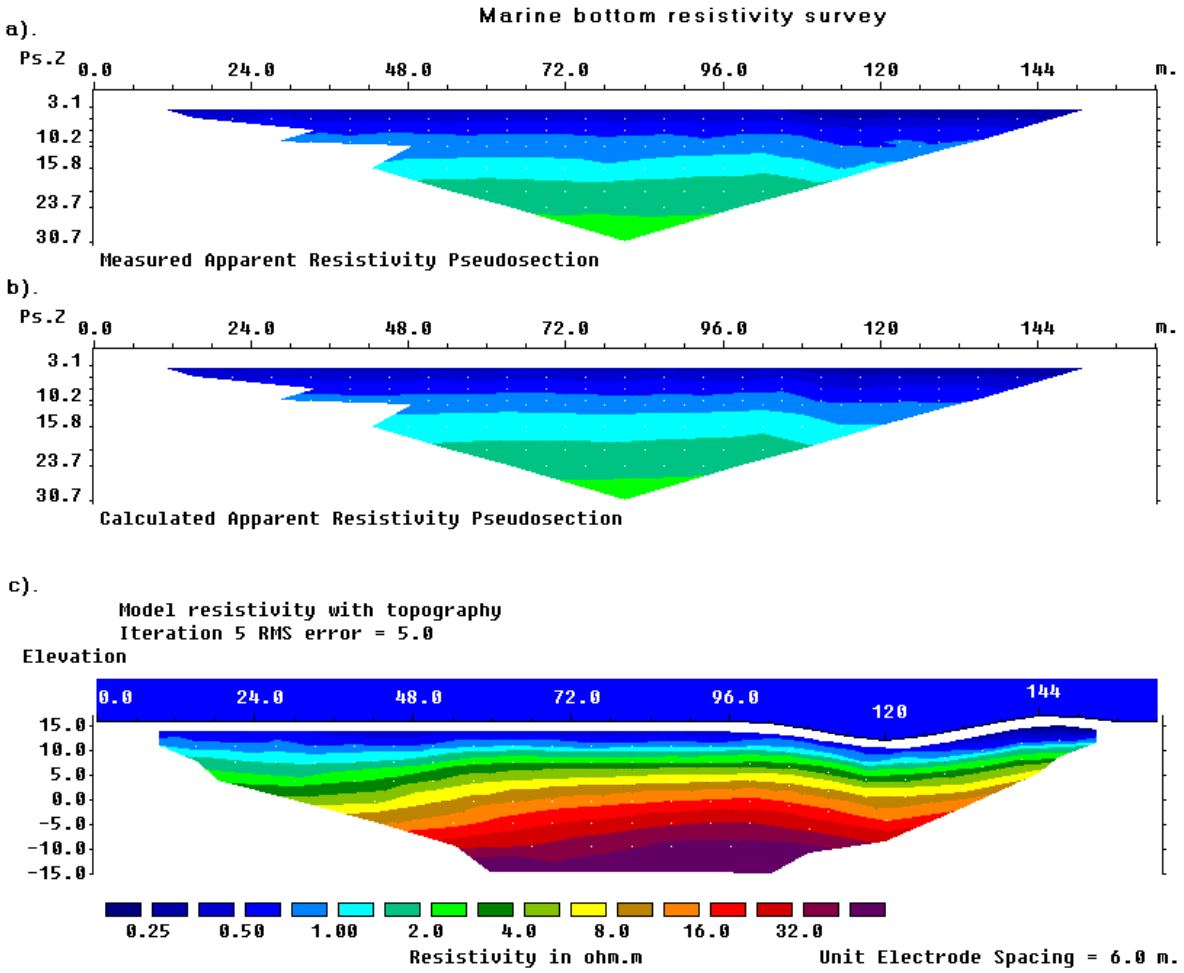

Figure 23. (a) The measured apparent resistivity pseudosection, (b) the calculated apparent resistivity pseudosection for the (c) model section from an underwater marine survey.

2.7.9 Time-lapse water infiltration survey - U.K.

Resistivity imaging surveys have not only been carried out in space, but also in time! In some studies, the change of the subsurface resistivity with time has important applications. Such studies include the flow of water through the vadose (unsaturated) zone, changes in the water table due to water extraction (Barker and Moore 1998), flow of chemical pollutants and leakage from dams (Johansson and Dahlin 1996).

A simple, but very interesting, experiment to map the flow of water from the ground surface downwards through the unsaturated zone and into the water table was described by Barker and Moore (1998). In this section, only some of the highlights of this experiment are described as an illustration of a time-lapse survey. This experiment was carried out in the Birmingham (England) area where forty thousand litres of water was poured on the ground surface using a garden hose over a period of 10 hours. Measurements were made before and during the irrigation of the ground surface, and after that for a period of about two weeks. Figure 24 (a and b) shows the results of a survey carried out at the beginning of the experiment before the irrigation started. The inversion model (Figure 24b) shows that the subsurface, that consists of sand and gravel, is highly inhomogeneous. The water was poured out near the 24 metres mark on this line, and Figure 24c shows the inversion model for the data set collected after 10 hours of continuous irrigation. While the model resistivity values in the vicinity of the 24 metres mark are generally lower than the initial data set model in Figure 24b, the subsurface distribution of the water is not very clear from a direct comparison of the inversion models alone.

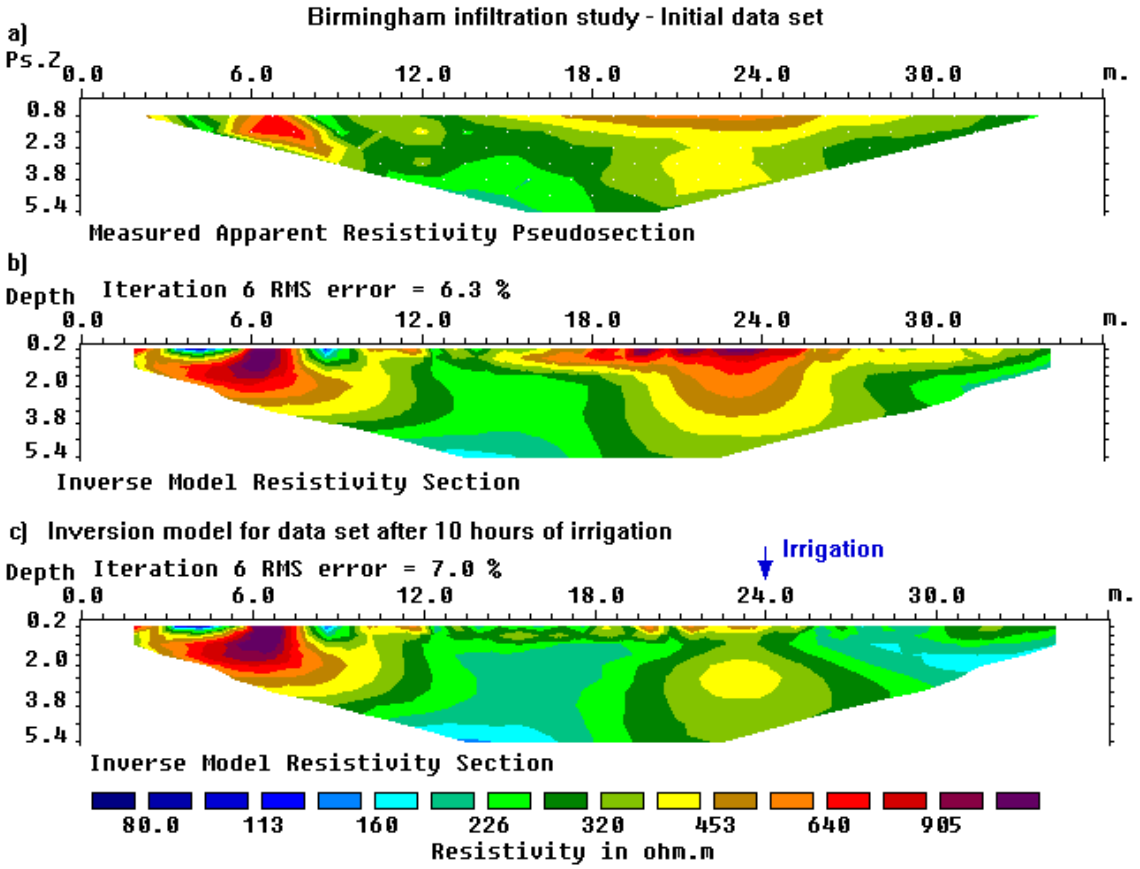

Figure 24. (a) The apparent resistivity and (b) inversion model sections from the survey conducted at the beginning of the Birmingham infiltration study. This shows the results from the initial data set that forms the base model in the joint inversion with the later time data sets. As a comparison, the model obtained from the inversion of the data set collected after 10 hours of irrigation is shown in (c).

The water distribution is more easily determined by plotting the percentage change in the subsurface resistivity of the inversion models for the data sets taken at different times (Figure 25) when compared with the initial data set model. The inversion of the data sets was carried using a joint inversion technique where the model obtained from the initial data set was used to constrain the inversion of the later time data sets (Loke 1999). The data set

collected at 5 hours after the pumping began shows a reduction in the resistivity (of up to over 50 percent) near the ground surface in the vicinity of the 24 metres mark. The near-surface low resistivity zone reaches its maximum amplitude after about 10 hours when the pumping was stopped (Figure 25b). Twelve hours after the pumping was stopped, the low resistivity plume has spread downwards and slightly outwards due to infiltration of the water through the unsaturated zone. There is a decrease in the maximum percentage reduction in the resistivity values near the surface due to migration of the water from the near surface zone. This effect of the spreading of the plume becomes increasingly more pronounced after 24 hours (Figure 25d) and 36 hours (Figure 25e) due to further migration of the water. Note that the bottom boundary of the zone with approximately 20 percent reduction in the resistivity values tends to flatten out at a depth of about 3 metres (Figure 25e) where the plume from the surface meets the water table.

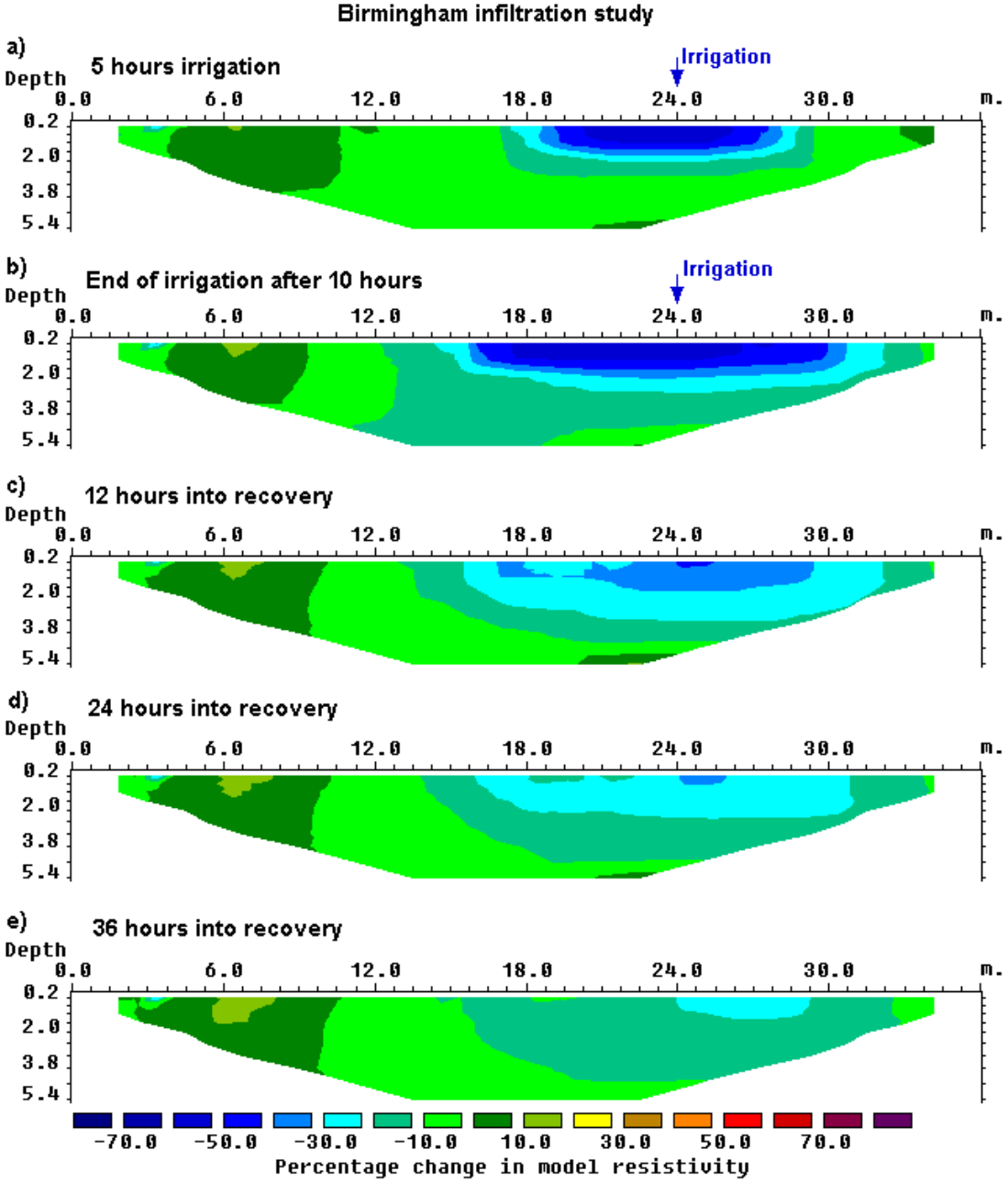

Figure 25. Sections showing the change in the subsurface resistivity values with time obtained from the inversion of the data sets collected during the irrigation and recovery phases of the study.

2.7.10 Cross-borehole survey - U.K.

Cross-borehole resistivity/I.P. tomography surveys which can give a much higher resolution than surface surveys have also been carried out. Figure 26 shows the inversion results from an interesting cross-borehole survey. This data set is one from a number which were collected by a survey to study the flow of fluids through the UK Chalk aquifer in east Yorkshire by using a saline tracer (Slater et al 1997). The dipole-dipole type of array was used in this survey. There is a low resistivity zone near the surface where the saline solution was irrigated onto the ground, and also prominent low resistivity zones below a depth of 7 metres due to the saline tracer which had flowed downwards. The inversion of this data set took about 15 minutes on a 200 Mhz Pentium Pro computer.

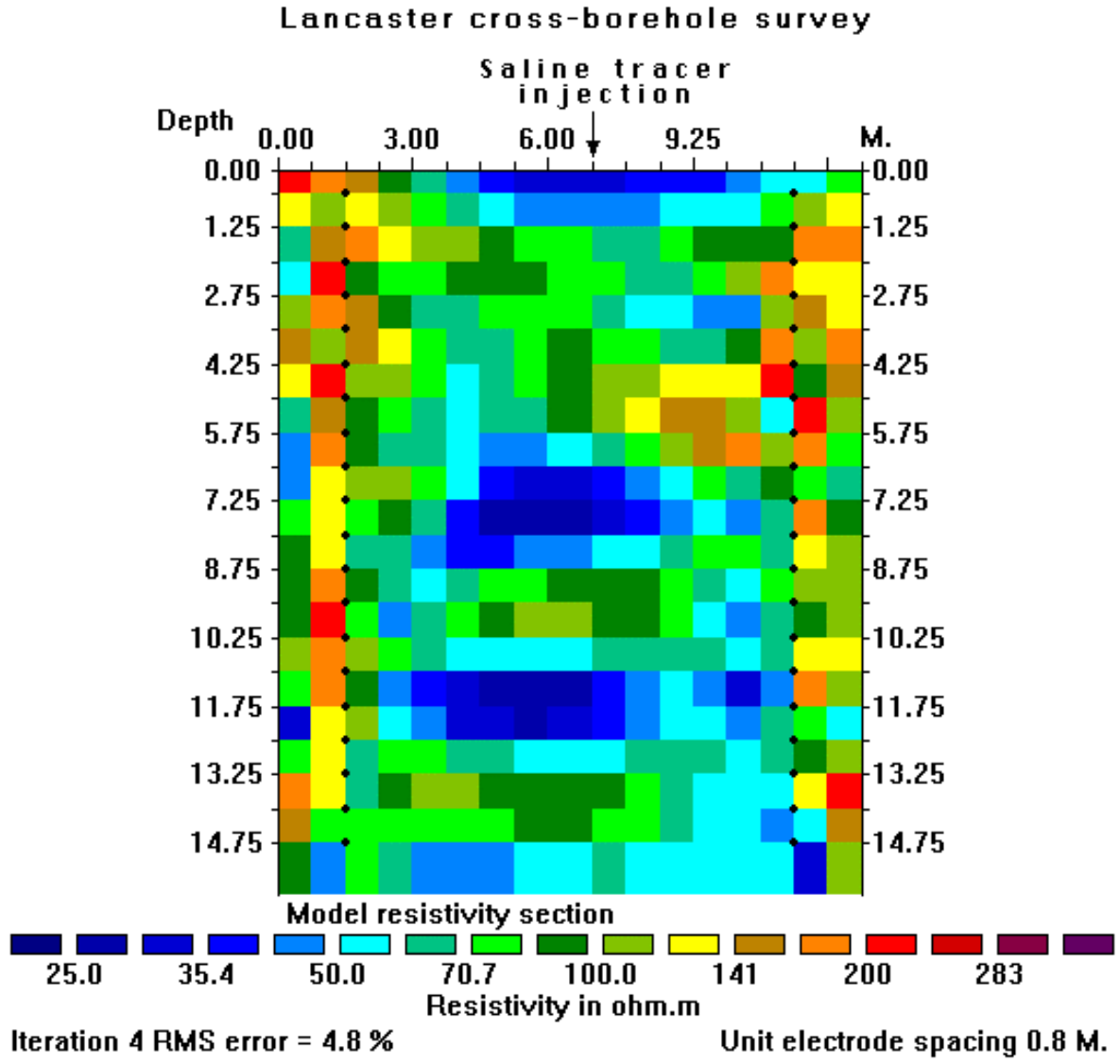

Figure 26. Model obtained from the inversion of data from a cross-borehole survey to map the flow of a saline tracer in between two boreholes. Note the low resistivity values near the surface where the tracer was injected, as well as the low resistivity zones below a depth of 7 metres. The locations of the borehole electrodes are shown by small black dots.

2.7.11 Wenner Gamma array survey - Nigeria

Technically, the “normal” Wenner array is the Wenner Alpha array (Figure 2a). As with any four electrodes array, there are two other possible variations that are usually referred to as the Beta and Gamma configurations (Carpenter and Habberjam 1956). The Wenner Beta array (Figure 2b) is in fact a special case of the dipole-dipole array. The Wenner Gamma array (Figure 2c) has a relatively unusual arrangement where the current and potential electrodes are interleaved. Compared to the Wenner Alpha and Beta (dipole-dipole) arrays, the Wenner Gamma array is much less frequently used in field surveys. However, in some situations, there might be some advantage in using this array. The depth of investigation is significantly deeper than the Wenner Alpha array (0.59a compared to 0.52a, see Table 2), but the voltage measured between the potential electrodes is only about 33% less than the Alpha array. In comparison, the voltage that would be measured by the Wenner Beta array is one-third that of the Alpha array which could be a serious disadvantage in noisy environments.

Figure 27a shows the Wenner Gamma array pseudosection from a groundwater survey in the Bauchi area of Nigeria (Acworth 1981). In this region, groundwater is frequently found in the weathered layer above the crystalline bedrock. The weathered layer is thicker in areas with fractures in the bedrock, and thus such fractures are good targets for groundwater. In this area, the surveys were carried out with the Wenner Alpha, Beta and Gamma arrays, together with electromagnetic profiling measurements using a Geonics EM34-3 system (Acworth 1999). Here, only the result from the Wenner Gamma array data set is shown as an example.

To emphasize the boundary between the soil layer and the bedrock, the robust inversion option was used (section 2.6.2). The inversion model in shown in Figure 27b. The thickness of the lower resistivity weathered layer is generally about 10 to 20 metres. There is a narrow vertical low resistivity zone with a width of less than 20 metres below the 190 metres mark which is probably a fracture zone in the bedrock. A borehole well that was placed at the 175 metres mark which lies just at the edge of the fracture zone. It had yields that were somewhat lower than expected (Acworth 1999). In such a situation, the 2D resistivity model would be useful to pinpoint the exact location of the centre of the fracture zone to improve the yield from the borehole. The placement of the well was largely based on resistivity and EM profiling data, and many years before 2D resistivity inversion software and fast microcomputers were widely available.

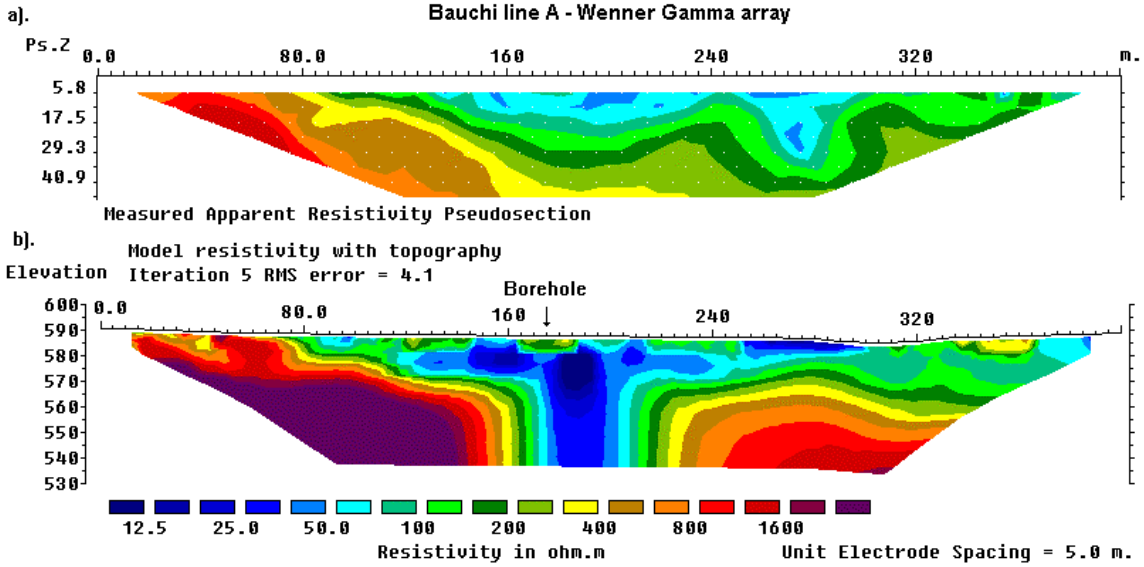

Figure 27. Bauchi Wenner Gamma array survey. (a). Apparent resistivity pseudosection. (b) The inversion model with topography. Note the location of the borehole at the 175 metres mark.

As a final note, it is possible to invert data collected with the Wenner Alpha, Beta and Gamma arrays along the same line simultaneously with the RES2DINV program as a single data set. This can be done by using the "non-conventional array" option in the program where the positions of all the four electrodes in an array are explicitly specified. This might be an interesting method to combine the advantages of the different variations of the Wenner array.

2.7.12 Mobile underwater survey - Belgium

This example is one of the most unusual data sets that I have come across, and a worthy challenge for any resistivity imaging inversion software. It is not only the longest in physical length and number of electrode positions, but also uses an unusual highly asymmetrical non-conventional electrode arrangement collected by an underwater mobile surveying system. Mobile surveying systems have an advantage of faster surveying speed, but on land they suffer from the problem of poor ground contact or low signal strength. Mobile land surveying systems consists of two main types, a pulled array type of system with a direct contact between the electrodes and the ground (Bernstone and Dahlin, 1999) and an electrostatic type of system with no direct ground contact (Panissod et. al, 1998). The type that requires direct contact can only be used on open ground where reasonably good contact can be obtained with the soil. The electrostatic type does not require direct ground contact and thus can be used in many areas where normal resistivity surveying systems cannot be used (for example in built-up areas) but has the problem of a more limited depth of penetration due to the limited amount of current induced. An underwater environment provides an almost ideal situation for a direct contact type of mobile system since there is no problem in obtaining good electrode contact!

Figure 28a shows the data from the first two kilometres of an eight kilometres survey line along a river. This survey was carried out by Sage Engineering of Belgium. The purpose of the survey was to map the near surface lithology of the riverbed where there were plans to lay a cable. The particular data subset in Figure 28a is slightly more than 2 kilometres long has an electrode position at almost every metre. It has a total of 1994 electrode positions and 1760 data points, whereas the inversion model used has 5312 blocks. On a 550 Mhz Pentium III computer, it took slightly over 14 hours to process this data set!

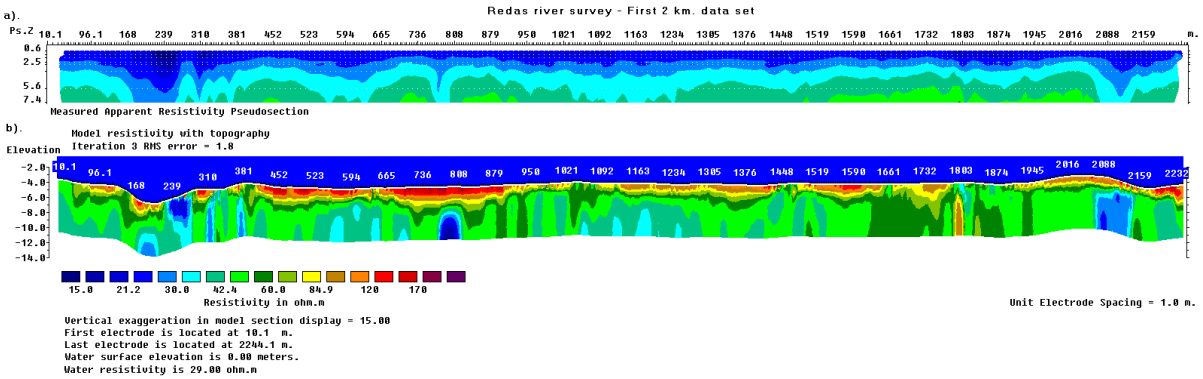

Figure 28. (a) The apparent resistivity pseudosection for the first two kilometres of an underwater survey along a riverbed by Sage Engineering, Belgium. (b) The inversion model after three iterations.

In the inversion model (Figure 28b), most of the riverbed materials have a resistivity of less than 120 ohm.m. There are several areas where the near-surface materials have significantly higher resistivities of over 150 ohm.m. Unfortunately, geological information in this area is rather limited. In the high resistivity areas, the divers faced problems in obtaining

sediment samples. The lower resistivity materials are possibly more coherent sediments (possibly sand with silt/clay), whereas the higher resistivity areas might be coarser and less coherent materials.

Shallow seismic reflection surveys are frequently used in rivers/lakes/marine environments for engineering site surveys. A mobile resistivity survey might be a useful addition in some situations, such as in seismically opaque areas. In theory, both surveys can be carried out simultaneously to reduce costs.

Besides these examples, 2-D imaging surveys have been carried for many other purposes such as detecting leakage of pollutants from landfill sites, areas with undulating limestone bedrock, mapping of the overburden thickness over bedrock, leakage of water from dams, and the saline water intrusion in coastal aquifers. The resistivity imaging method has also been used in underwater surveys in lakes and dams.

3 3-D Electrical Imaging Surveys

3.1 Introduction to 3-D surveys

Since all geological structures are 3-D in nature, a fully 3-D resistivity survey using a 3-D interpretation model (Figure 3c) should in theory give the most accurate results. At the present time 3-D surveys is a subject of active research. However it has not reached the level where, like 2-D surveys, it is routinely used. The main reason is that the survey cost is comparatively higher for a 3-D survey of an area which is sufficiently large. There are two current developments that should make 3-D surveys a more cost-effective option in the near future. One is the development of multi-channel resistivity meters which enables more than one reading to be taken at a single time. This is important to reduce the survey time. The second development is faster microcomputers to enable the inversion of very large data sets (with more than 8,000 data points and survey grids of greater than 30 by 30) to be completed within a reasonable time.

3.2 Array types for 3-D surveys

The pole-pole, pole-dipole and dipole-dipole arrays are frequently used for 3-D surveys. This is because other arrays have a poorer data coverage near the edges of the survey grid. The advantages and disadvantages of the pole-pole, pole-dipole and dipole-dipole arrays which were discussed in section 2.5 with regards to 2-D surveys are also valid for 3-D surveys.

3.2.1 Pole-pole array

Figure 29 shows one possible arrangement of the electrodes for a 3-D survey using a 25 electrodes system. For convenience the electrodes are usually arranged in a square grid with the same unit electrode spacing in the *x* and *y* directions. To map slightly elongated bodies, a rectangular grid with different numbers of electrodes and spacings in the *x* and *y* directions could be used. The pole-pole electrode configuration is commonly used for 3-D surveys, such as the E-SCAN method (Li and Oldenburg 1992). The maximum number of independent measurements, n_{max}, that can be made with n_e electrodes is given by

$$n_{max} = n_e (n_e - 1) / 2$$

In this case, each electrode is in turn used as a current electrode and the potential at all the other electrodes are measured. Note that because of reciprocity, it is only necessary to measure the potentials at the electrodes with a higher index number than the current electrode in Figure 30a. For a 5 by 5 electrodes grid, there are 300 possible measurements. For 7 by 7 and 10 by 10 electrodes grids, a survey to measure the complete data set would have 1176 and 4500 datum points respectively. For commercial surveys, grids of less than 10 by 10 are probably not practical as the area covered would be too small.

It is can be very time-consuming (at least several hours) to make such a large number of measurements, particularly with typical single-channel resistivity meters commonly used for 2-D surveys. To reduce the number of measurements required without seriously degrading the quality of the model obtained, an alternative measurement sequence shown in Figure 30b has been tested. In this proposed "cross-diagonal survey" method, the potential measurements are only made at the electrodes along the x-direction, the y-direction and the 45 degrees diagonal lines passing through the current electrode. The number of datum points with this arrangement for a 7 by 7 grid is reduced to 476 which is about one-third of that required by a complete data set survey (Loke and Barker 1996b).

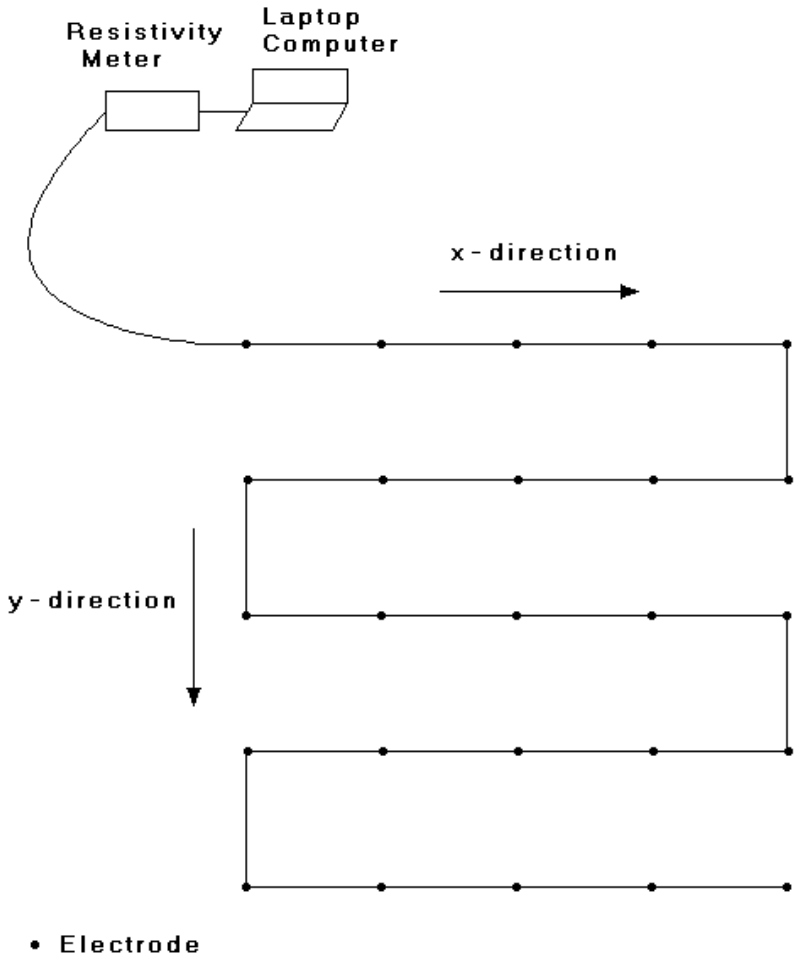

Figure 29. The arrangement of the electrodes for a 3-D survey.

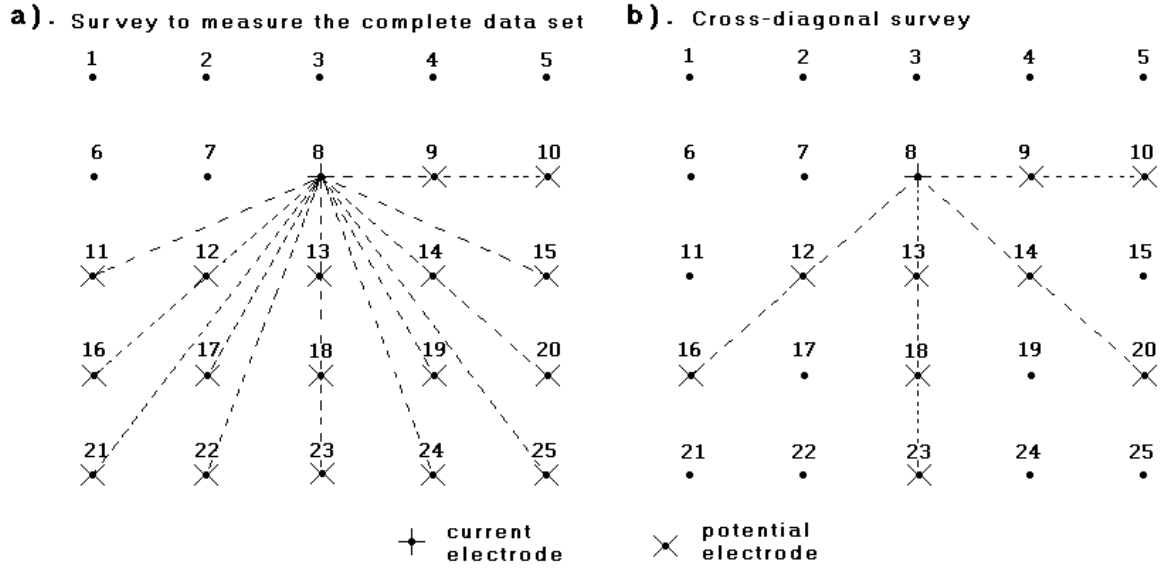

Figure 30. The location of potential electrodes corresponding to a single current electrode in the arrangement used by (a) a survey to measure the complete data set and (b) a cross-diagonal survey.

The pole-pole array has two main disadvantages. Firstly it has a much poorer resolution compared to other arrays. Subsurface structures tend to be smeared out in the final inversion model. The second disadvantage, particularly for large electrode spacings, is that the second current and potential electrodes must be placed at a sufficiently large distance from the survey grid. Both disadvantages were discussed in detail in Section 2.5.4.

3.2.2 Pole-dipole array

This array is an attractive alternative to the pole-pole array for surveys with medium and large survey grids (12 by 12 and above). It has a better resolving power than the pole-pole array (Sasaki 1992), and is less susceptible to telluric noise since both potential electrodes are kept within the survey grid. Compared to the dipole-dipole array, it has a significantly stronger signal strength. Although it has one "remote" electrode (the C2 electrode), the effect of this electrode on the measurements is much smaller compared to the pole-pole array (section 2.5.5). As the pole-dipole array is an asymmetrical array, measurements should be made with the "forward" and "reverse" arrangements of the electrodes (Figure 12). To overcome the problem of low signal strength for large values of the "**n**" factor (exceeding 8 to 10), the "**a**" spacing between the P1-P2 dipole pair should be increased to get a deeper depth of investigation with a smaller "**n**" factor. The use of redundant measurements with overlapping data levels to increase the data density can in some cases help to improve the resolution of the resulting inversion model (section 2.5.6).

3.2.3 Dipole-dipole array

This array can is recommended only for grids which are larger than 12 by 12 due to the poorer horizontal data coverage at the sides. The main problem that is likely to be faced with this array is the comparatively low signal strength. Similar to 2-D surveys, this problem can be overcome by increasing the "**a**" spacing between the P1-P2 dipole to get a deeper depth of investigation as the distance between the C1-C2 and P1-P2 dipoles is increased. Also, the use of overlapping data levels is recommended (section 2.5.6). In many cases, 3-D data sets for the pole-dipole and dipole-dipole arrays are constructed from a number of parallel 2-D survey lines (section 3.3).

3.2.4 Summary

For relatively small grids of less than 12 by 12 electrodes, the pole-pole array has a substantially larger number of possible independent measurements compared to other arrays. The loss of data points near the sides of the grid is kept to a minimum, and it provides a better horizontal data coverage compared to other arrays. This is an attractive array for small survey grids with relatively small spacings (less than 5 metres) between the electrodes. However, it has the disadvantage of requiring two "remote" electrodes which must be placed at a sufficiently large distance from the survey grid. Due to the large distance between the two potential electrodes, this array is more sensitive to telluric noise. The pole-dipole array is an attractive option for medium size grids. It has a higher resolution than the pole-pole array, it requires only one remote electrode and is much less sensitive to telluric noise. For surveys with large grids, particularly when there is no convenient location for a remote electrode, the dipole-dipole array can be used. For both the pole-dipole and dipole-dipole arrays, measurements with overlapping data levels using different "**a**" and "**n**" combinations should be used to improve the quality of the results.

The electrodes for 3-D surveys are normally arranged in a rectangular grid with a constant spacing between the electrodes (Figure 29). However, the RES3DINV resistivity and IP inversion program can also handle grids with a non-uniform spacing between the rows or

columns of electrodes.

3.3 3-D roll-along techniques

Most commercial 3-D surveys will probably involve grids of at least 16 by 16 in order to cover a reasonably large area. A 16 by 16 grid will require 256 electrodes which is more than that available on many multi-electrode resistivity meter systems. One method to survey such large grids with a limited number of electrodes is to extend the roll-along technique used in 2-D surveys to 3-D surveys (Dahlin and Bernstone 1997). Figure 30 shows an example of a survey using a multi-electrode resistivity-meter system with 50 electrodes to survey a 10 by 10 grid. Initially the electrodes are arranged in a 10 by 5 grid with the longer lines orientated in the x-direction (Figure 31a). Measurements are made primary in the x-direction, with some possible measurements in the diagonal directions. Next the entire grid is moved in the y-direction so that the 10 by 5 grid now covers the second half of the 10 by 10 grid area. The 10 by 5 grid of electrodes is next orientated in the y-direction (Figure 31b).

The example data file PIPE3D.DAT was obtained from a survey using such a roll-along technique. It was carried out with a resistivity-meter system with only 25 electrodes, with the electrodes arranged in an 8 by 3 grid. The long axis of this grid was orientated perpendicularly to two known subsurface pipes. The measurements were made using three such 8 by 3 subgrids so that the entire survey covers an 8 by 9 grid. For each 8 by 3 subgrid, all the possible measurements (including a limited number in the y-direction) for the pole-pole array were made. In this survey, the second set of measurements in the y-direction (as in Figure 31b) was not carried out to reduce the survey time, and also because the pipes have an almost two-dimensional structure.

For practical reasons, the number of field measurements in some surveys might be even less than the cross-diagonal technique. Another common approach is to just make the measurements in the *x*- and *y*- directions only, without the diagonal measurements. This is particularly common if the survey is made with a system with a limited number of independent electrodes, but a relatively large grid is needed.

In some cases, measurements are made only in one direction. The 3-D data set consists of a number of parallel 2-D lines. The data from each 2-D survey line is initially inverted independently to give 2-D cross-sections. Finally, the whole data set is combined into a 3-D data set and is inverted with RES3DINV to give a 3-D picture. While the quality of the 3-D model is expected to be poorer than that produced with a complete 3-D survey, such a “poor man’s” 3-D data set could reveal major resistivity variations across the survey lines. Until multi-channel resistivity instruments are widely used, this might be the most cost-effective solution to extract some 3-D information from 2-D surveys.

3.4 3-D forward modeling program

In the interpretation of data from 2-D resistivity imaging surveys, it is assumed that the subsurface geology does not change significantly in the direction that is perpendicular to the survey line. In areas with very complex geology, there are could be significant variations in the subsurface resistivity in this direction (i.e. the geology is 3-D), which could cause distortions in the lower sections of the 2-D model obtained. Measurements made with the larger electrode spacings are not only affected by the deeper sections of the subsurface, they are also affected by structures at a larger horizontal distance from the survey line. This effect is most pronounced when the survey line is placed near a steep contact with the line parallel to the contact.

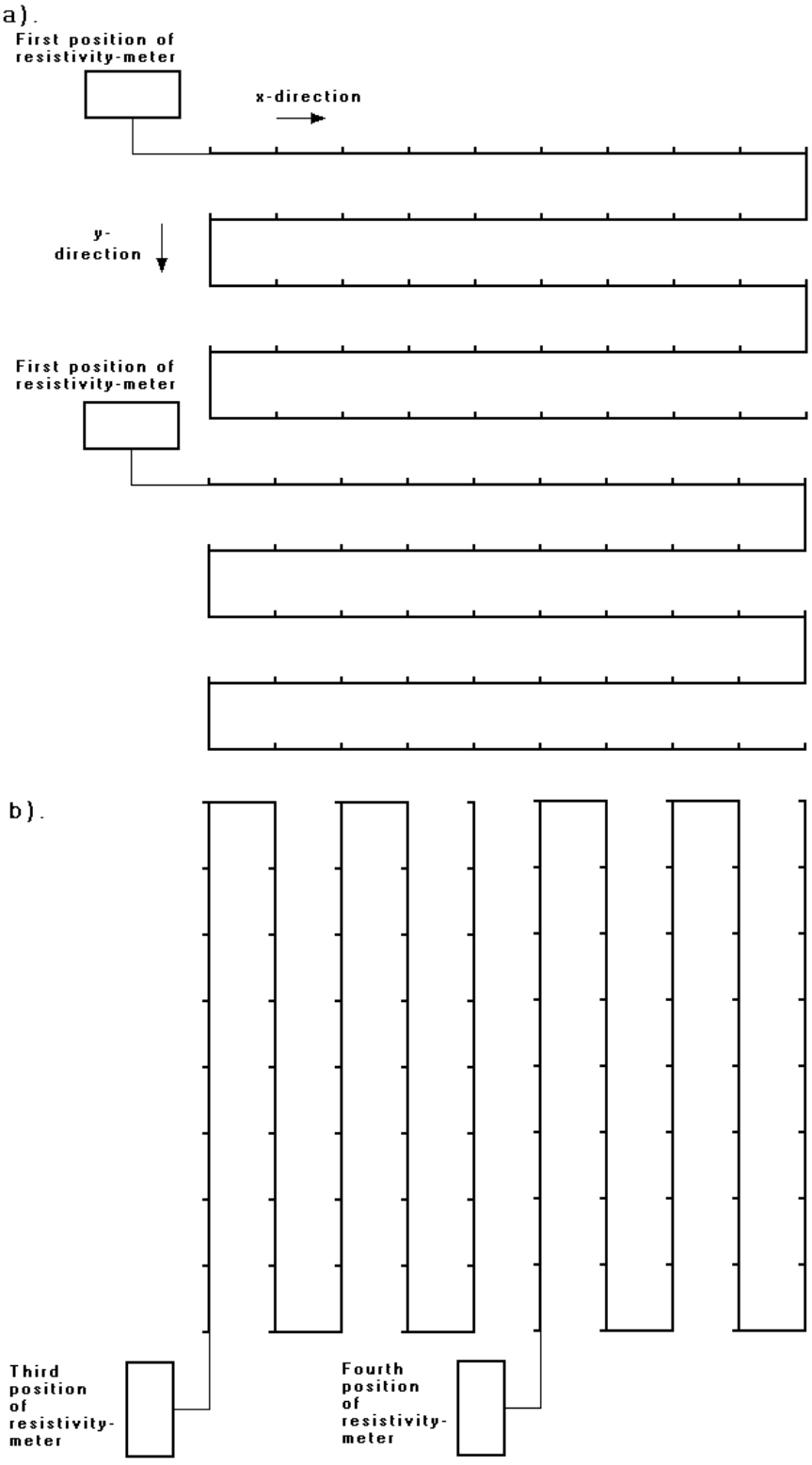

Figure 31. Using the roll-along method to survey a 10 by 10 grid with a resistivity-meter system with 50 electrodes. (a) Surveys using a 10 by 5 grid with the lines orientated in the x-direction. (b) Surveys with the lines orientated in the y-direction.

The free 3-D resistivity forward modeling program, RES3DMOD.EXE, enables you to calculate the apparent resistivity values for a survey with a rectangular grid of electrodes over a 3-D structure. This is a Windows based program that can be used from within Windows 3.1 or Windows 95/98/NT. To take a look the operation of the program, use the "File" option followed by "Read model data" to read in the file BLOCK11X.MOD, which has a 11 by 11 survey grid. After that, click the "Edit/Display" option. To modify the 3-D model, click the "Edit resistivity model" option. In this option, you can change the resistivity of the 3-D cells in the mesh used by the finite-difference method (Dey and Morrison 1979b) to calculate the apparent resistivity values. To quit from the "Edit" mode, press the Q or the Esc key. To calculate the apparent resistivity values, click the "Calculate" option. To take a look at the apparent resistivity pseudosections, click the "Display apparent resistivity" option. You can choose to display the apparent resistivity values in the form of horizontal pseudosections, or as vertical pseudosections as used in 2-D surveys. Displaying the vertical pseudosections will give you an idea of the effect of a 3-D structure on the measurements in a 2-D survey. A discussion of the sensitivity of different arrays to 3-D effects was given in the paper by Dahlin and Loke (1997). In general, it was found that for the models and arrays tested, the dipole-dipole array was the most sensitive to 3-D effects while the Wenner array was the least sensitive.

The RES3DMOD program also has an option to save the apparent resistivity values into a format that can be accepted by the RES3DINV inversion program. As an exercise, save the apparent resistivity values as a RES3DINV data file for one of the models, and later carry out an inversion of this synthetic data set.

Figure 32a shows an example of a 3-D model with a 15 by 15 survey grid (i.e. 255 electrodes). The model, which consists of four rectangular blocks embedded in a medium with a resistivity of 50 ohm.m, is shown in the form of horizontal slices through the earth. The apparent resistivity values for the pole-pole array (with the electrodes aligned in the x-direction) is shown in the form of horizontal pseudosections in Figure 32b. Note the low resistivity block with a resistivity of 10 ohm.m near the centre of the grid that extends from a depth of 1.0 to 3.2 metres. For measurements with the shorter electrode spacings of less than 4 metres this block causes a low resistivity anomaly. However, for electrode spacings of greater than 6 metres, this low resistivity block causes a high resistivity anomaly! This is an example of "anomaly inversion" which is caused by the near-surface zone of negative sensitivity values between the C1 and P1 electrodes (Figure 11).

3.5 Data inversion

One model used to interpret the 3-D data set is shown in Figure 33a. The subsurface is divided into several layers and each layer is further subdivided into a number of rectangular blocks. A 3-D resistivity inversion program, RES3DINV, is used to interpret the data from 3-D surveys. This program attempts to determine the resistivity of the blocks in the inversion model that will most closely reproduce the measured apparent resistivity values from the field survey. Within the RES3DINV program, the thickness of the layers can be modified by the user. Two other alternative models which can be used with the RES3DINV program are shown in Figures 33b and 33c. The second inversion model subdivides the top few layers vertically as well as horizontally by half. Another alternative is to subdivide the top few layers by half only in the horizontal directions (Figure 33c). Since the resolution of the resistivity method decreases rapidly with depth, it has been found that subdividing the blocks is only beneficial for the top two layers only. In many cases, subdividing the top layer only is enough. By subdividing the blocks, the number of model parameters and thus the computer time required to invert the data set can increase dramatically.

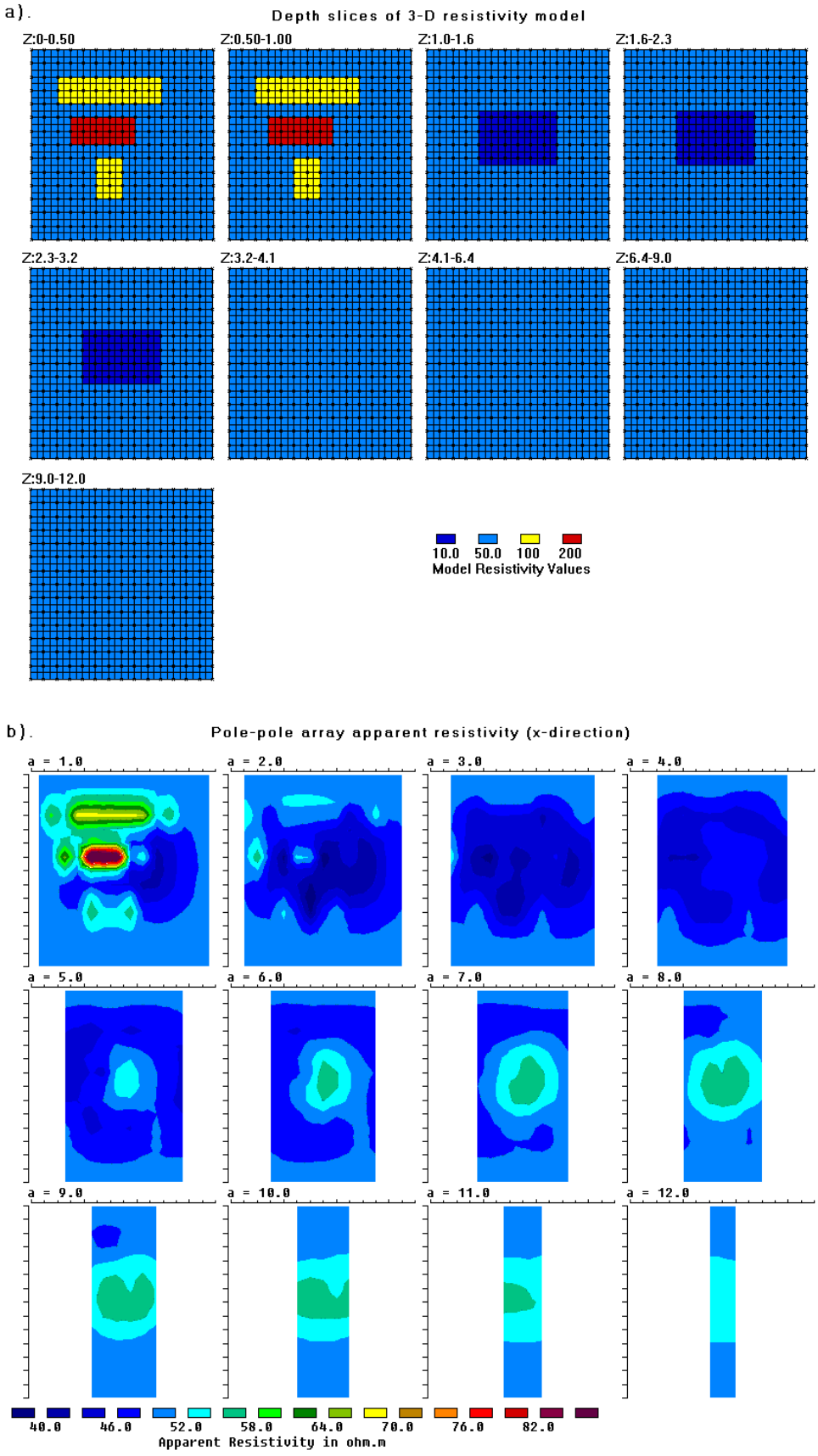

Figure 32. (a) 3-D model with 4 rectangular blocks and a 15 by 15 survey grid. (b) Horizontal apparent resistivity psudosections for the pole-pole array with the electrodes aligned in the x-direction.

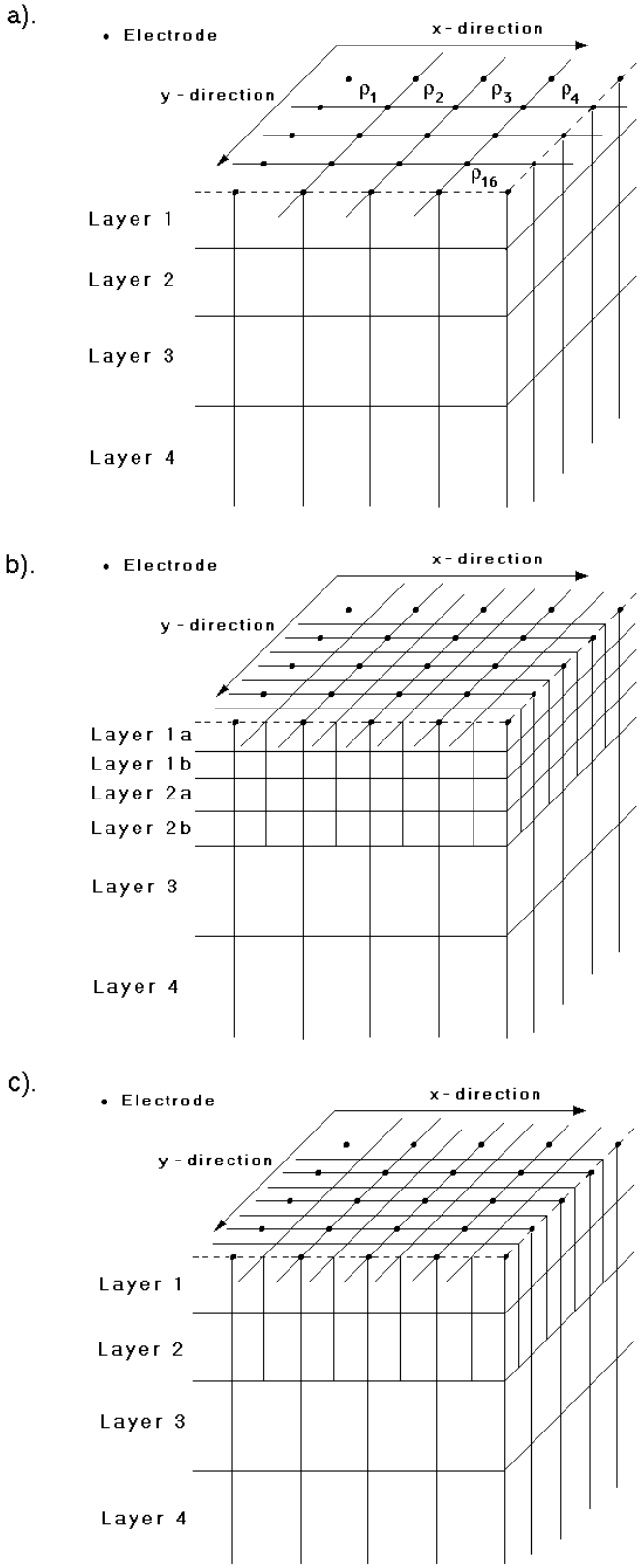

Figure 33. The models used in 3-D inversion. (a) Standard model where the widths of the rectangular blocks are equal to the unit electrode spacings in the x- and y-directions. (b) A model where the top few layers are divided by half, both vertically and horizontally, to provide better resolution. (c) A model where the model blocks are divided in the horizontal directions but not in the vertical direction.

Please refer to the instruction manual for the RES3DINV program for the data format. An online version of the manual is available by clicking the “Help” option on the Main Menu bar of the RES3DINV program. The set of files that comes with the RES3DINV program package has a number of field and synthetic data files. You can carry out an inversion of some of these files to get a feel of how the program works.

3.6 Examples of 3-D field surveys

In this section, we will take a look at the results from a few 3-D field surveys over areas with complex geology.

3.6.1 Birmingham field test survey - U.K.

This field test was carried out using a multi-electrode system with 50 electrodes commonly used for 2-D resistivity surveys. The electrodes are arranged in a 7 by 7 square grid with a unit spacing of 0.5 metre between adjacent electrodes (Figure 34). The two remote electrodes were placed at more than 25 metres from the grid to reduce their effects on the measured apparent resistivity values. To reduce the survey time, the cross-diagonal survey technique was used. The subsurface is known to be highly inhomogenous consisting of sands and gravels. Figure 35a shows the horizontal sections of the model obtained at the 6th iteration. The two high resistivity zones in the upper left quadrant and the lower right corner of Layer 2 are probably gravel beds. The two low resistivity linear features at the lower edge of Layer 1 are due to roots from a large sycamore tree just outside the survey area. The vertical extent of the gravel bed is more clearly shown in the vertical cross-sections across the model (Figure 35b). The inverse model shows that the subsurface resistivity distribution in this area is highly inhomogenous and can change rapidly within a short distance. In such a situation a simpler 2-D resistivity model (and certainly a 1-D model from conventional sounding surveys) would probably not be sufficiently accurate.

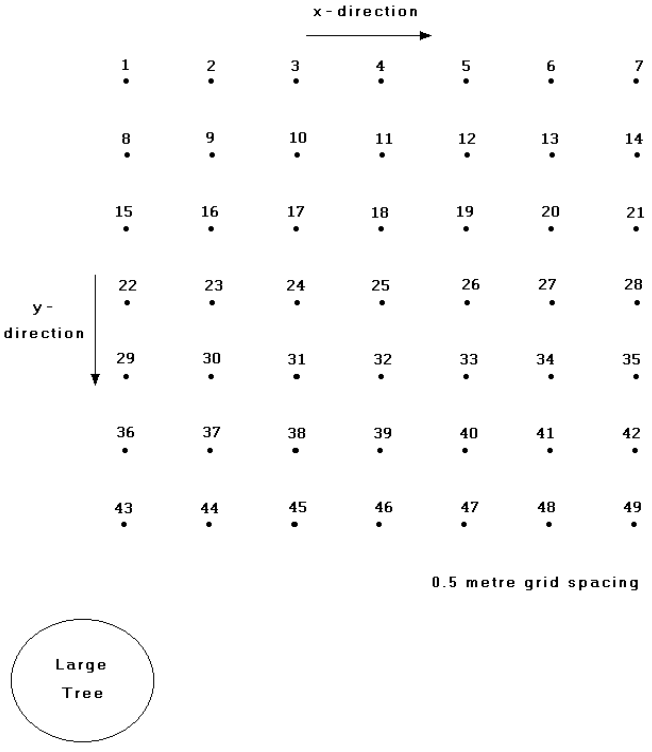

Figure 34. Arrangement of electrodes in the Birmingham 3-D field survey.

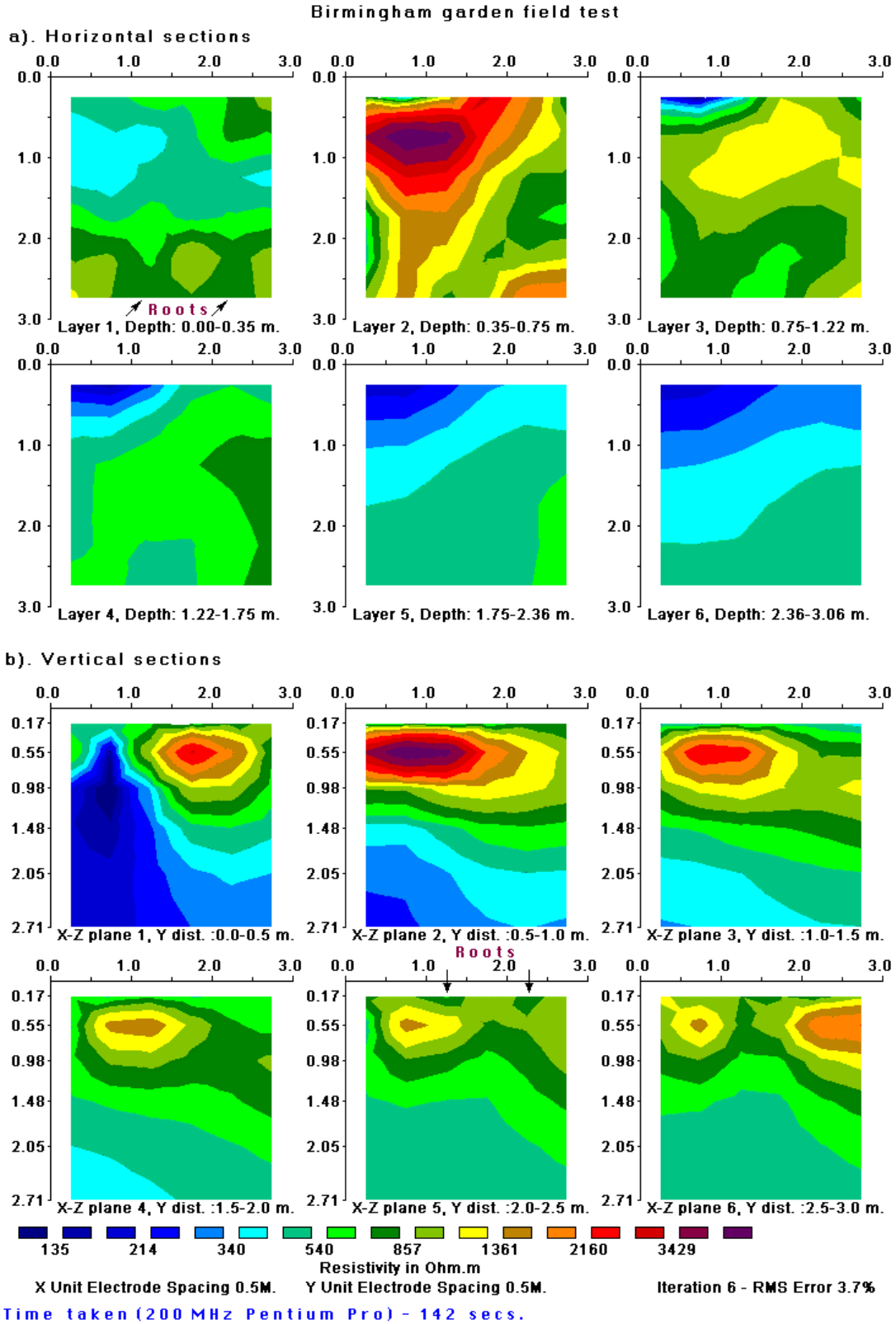

Figure 35. Horizontal and vertical cross-sections of the model obtained from the inversion of the Birmingham field survey data set. The location of observed tree roots on the ground surface are also shown.

3.6.2 Septic tank survey - Texas

This field survey was carried out using an 8 by 7 grid of electrodes over a buried septic tank. A Sting/Swift multi-electrode resistivity meter system (Lagmansson pers. comm.) was used for this survey. The distance between adjacent electrodes in the grid was 1 metre. All the possible measurements with the pole-pole array were made which gave a total of 1470 datum points. For the inversion of this data set, the model blocks in the top 2 layers are subdivided into smaller blocks. The results are shown in the form of horizontal slices through the subsurface (Figure 36). The septic tank appears as a large high resistivity area in the bottom left quadrant of survey area in Layers 2, 3 and 4. The topmost layer (Layer 1a in Figure 36) has a few areas with relatively large resistivity variations over short distances. In comparison, Layer 2b that extends from a depth of 1.1 to 1.5 metres shows more gradual lateral variations in the model resistivity values. In general, the deeper the layer, the smoother the lateral variations in the model resistivity values. This is probably partly caused by the decrease of the resolution of the resistivity surveying method with depth.

3.6.3 Sludge deposit - Sweden

This survey covers a relatively large 21 by 17 grid by using a 3-D roll-along method (Dahlin and Bernstone 1997). To reduce the survey time, a number of parallel multi-electrode cables were used. This survey was carried out at Lernacken in Southern Sweden over a closed sludge deposit. Seven parallel multi-electrode cables were used to cover a 21 by 17 grid with a 5 metres spacing between adjacent electrodes. There were a total number of 3840 data points in this data set.

In this survey, the cables were initially laid out in the x-direction, and measurements were made in the x-direction. After each set of measurements, the cables were shifted step by step in the y-direction until the end of the grid. In surveys with large grids, such as in this example, it is common to limit the maximum spacing for the measurements. The maximum spacing is chosen so that the survey will map structures to the maximum depth of interest (section 2.5). In this case, the maximum spacing was 40 metres compared to the total length of 100 metres along a line in the x-direction.

The model obtained from the inversion of this data set is shown in Figure 37. The former sludge ponds containing highly contaminated ground water show up as low resistivity zones in the top two layers (Dahlin and Bernstone 1997). This was confirmed by chemical analysis of samples. The low resistivity areas in the bottom two layers are due to saline water from a nearby sea. On a 200 Mhz Pentium Pro computer, it took slightly over 4 hours to invert this data set. On newer computers with operating frequencies of 550 Mhz or higher, the inversion time should be significantly shorter.

Other field applications include archaeological surveys and gold prospecting. A characteristic feature of 3-D surveys is the large number of electrodes and measurements. To carry out such surveys effectively, the multi-electrode system should have at least 64 (and preferably 100 or more) electrodes. This is an area where a multi-channel resistivity meter system would be useful. For fast computer inversion, the minimum requirement is a Pentium II system with at least 64 megabytes RAM and a 2 gigabyte hard-disk.

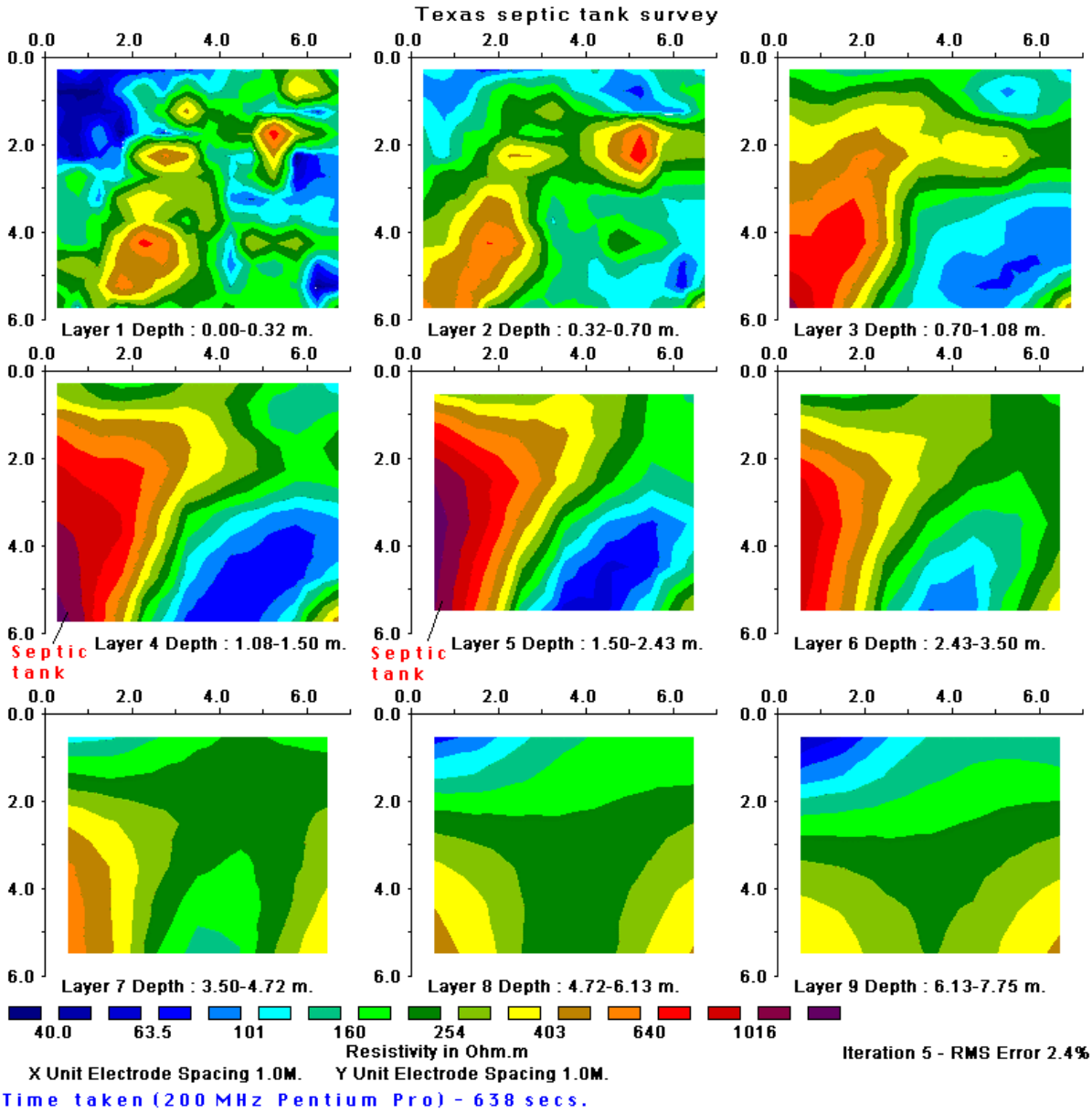

Figure 36. The model obtained from the inversion of the septic tank field survey data set. The model is shown in the form of horizontal slices through the earth.

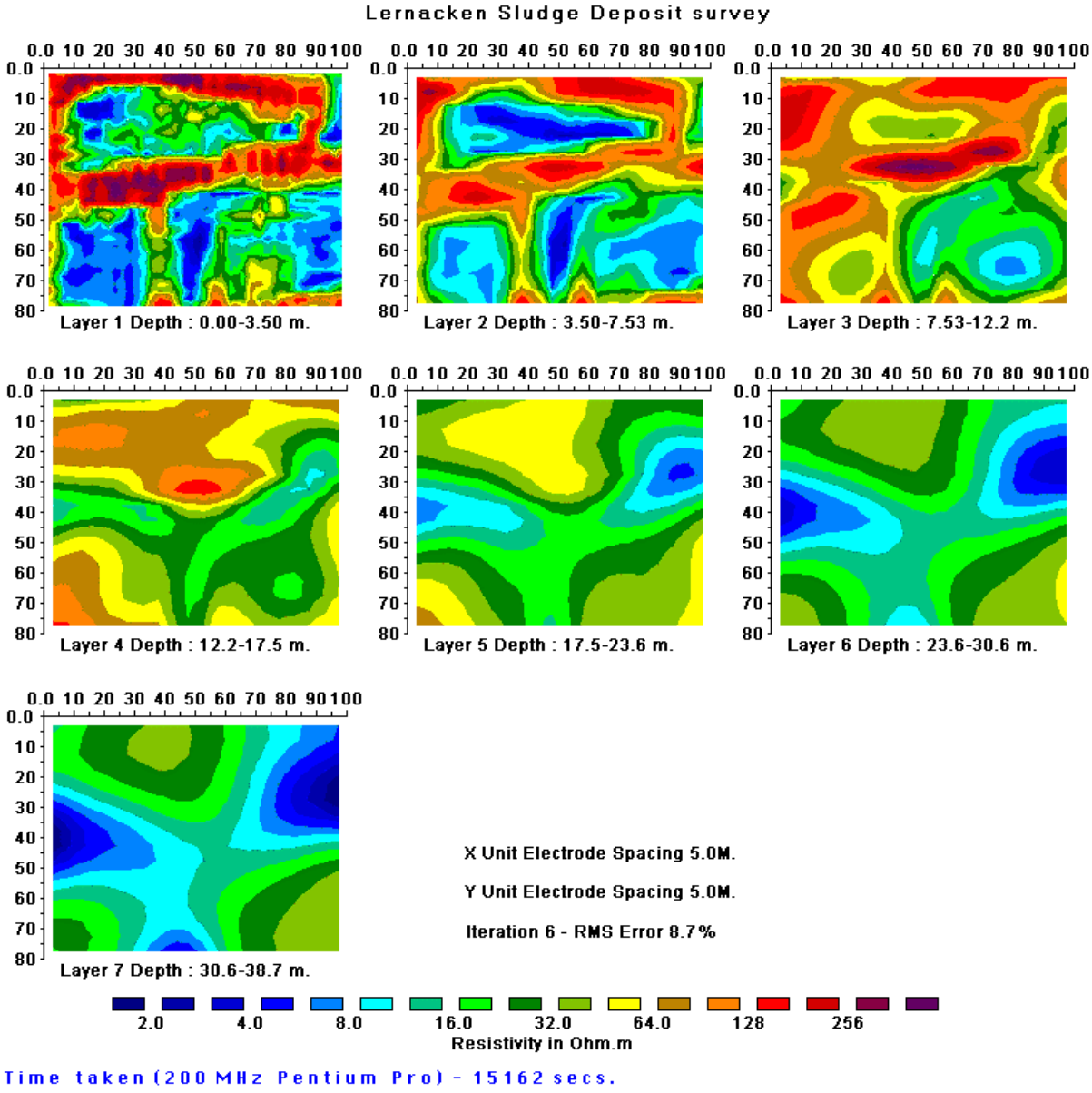

Figure 37. The 3-D model obtained from the inversion of the Lernacken Sludge deposit survey data set displayed as horizontal slices through the earth.

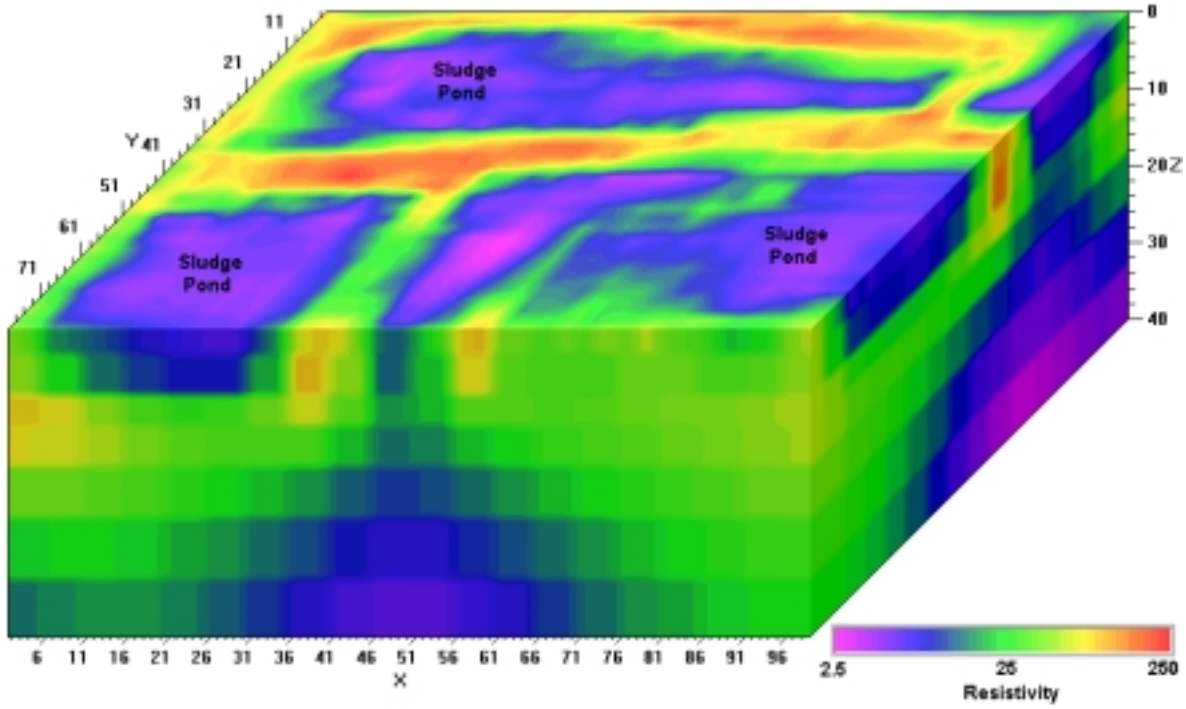

Figure 38. The 3-D model obtained from the inversion of the Lernacken Sludge deposit survey data set displayed with the Slicer/Dicer program. A vertical exaggeration factor of 2 is used in the display to highlight the sludge ponds. Note that the colour contour intervals are arranged in a logarithmic manner with respect to the resistivity.

Acknowledgments

Dr. Torleif Dahlin of Lund University in Sweden kindly provided the Odarslov Dyke and Lernacken data sets. The Grundfor data set was provided by Dr. Niels B. Christensen of the University of Aarhus in Denmark and Dr. Torleif Dahlin. The Rathcroghan data set was kindly provided by Dr. Kevin Barton and Dr. Colin Brown from data collected by the Applied Geophysics Unit of University College Galway, Ireland. Mr. Mats Lagmansson of Advanced Geosciences Inc. kindly provided the Sting Cave, the Fisher Island marine survey and the 3-D septic tank survey data sets. Many thanks to Richard Cromwell and Rory Retzlaff of Golder Assoc. (Seattle) for the survey example to map holes in a clay layer. Dr. Andrew Binley of Lancaster University kindly provided the interesting cross-borehole data set. The Bauchi data set was provided by Dr. Ian Acworth of the University of New South Wales, Australia. The Redas river survey data set was kindly provided by Jef Bucknix of Sage Engineering, Belgium. Finally, a special acknowledgment to Ron Barker of the School of Earth Sciences, University of Birmingham for the Tar Works and the 3-D Birmingham survey data sets. Slicer/Dicer is a registered trademark of Visualogic Inc.

References

Acworth, R.I., 1981. The evaluation of groundwater resouces in the crystalline basement of Northen Nigeria. Ph.D. thesis, Univ. of Birmingham.

Acworth, R.I., 1999. The electrical image method compared with resistivity sounding and electromagnetic profiling for investigation in areas of complex geology - A case study from ground-water investigation in a fractured rock environment. Submitted for publication (in review).

Barker R.D., 1992. A simple algorithm for electrical imaging of the subsurface. First Break **10**, 53-62.

Barker R.D., 1996. The application of electrical tomography in groundwater contamination studies. *EAGE 58th Conference and Technical Exhibition Extended Abstracts*, P082.

Barker, R. and Moore, J., 1998. The application of time-lapse electrical tomography in groundwater studies. The Leading Edge, **17**, 1454-1458.

Bernstone, C. and Dahlin, T., 1999. Assessment of two automated electrical resistivity data acquisition systems for landfill location surveys : Two case histories. Journal of Environmental and Engineering Geophysics, **4**, 113-122.

Carpenter, E.W. and Habberjam, G.M., 1956. A tri-potential method of resistivity prospecting. Geophysical Prospecting, **29**, 128-143.

Claerbout, J.F. and Muir, F., 1973. Robust modeling with erratic data. Geophysics, **38**, 826-844.

Christensen N.B. and Sorensen K.I., 1994. Integrated use of electromagnetic methods for hydrogeological investigations. Proceedings of the Symposium on the Application of Geophysics to Engineering and Environmental Problems, March 1994, Boston, Massachusetts, 163-176.

Dahlin T., 1996. 2D resistivity surveying for environmental and engineering applications. First Break, **14**, 275-284.

Dahlin, T. and Bernstone, C., 1997. A roll-along technique for 3D resistivity data acquisition with multi-electrode arrays, Procs. SAGEEP'97 (Symposium on the Application of Geophysics to Engineering and Environmental Problems), Reno, Nevada, March 23-26 1997, vol 2, 927-935.

Dahlin, T. and Loke, M.H., 1997. Quasi-3D resistivity imaging-mapping of three dimensional structures using two dimensional DC resistivity techniques. Proceedings of the 3rd Meeting of the Environmental and Engineering Geophysical Society. 143-146.

Dahlin,T. and Loke, M.H., 1998. Resolution of 2D Wenner resistivity imaging as assessed by numerical modelling, Journal of Applied Geophysics, **38**, 237-249.

Daniels F. and Alberty R.A., 1966. Physical Chemistry. John Wiley and Sons, Inc.

deGroot-Hedlin, C. and Constable, S., 1990. Occam's inversion to generate smooth, two-dimensional models form magnetotelluric data. Geophysics, **55**, 1613-1624.

Dey A. and Morrison H.F. 1979a. Resistivity modelling for arbitrary shaped two-dimensional structures. Geophysical Prospecting **27**, 1020-1036.

Dey A. and Morrison H.F., 1979b. Resistivity modeling for arbitrarily shaped three-dimensional shaped structures. Geophysics **44**, 753-780.

Edwards L.S., 1977. A modified pseudosection for resistivity and induced-polarization. Geophysics, 42, 1020-1036.

Ellis, R.G. and Oldenburg, D.W., 1994. The pole-pole 3-D DC-resistivity inverse problem : a conjugate gradient approach. Geophys. J. Int., **119**, 187-194.

Fox, R.C., Hohmann, G.W., Killpack,T.J. and Rijo, L., 1980, Topographic effects in resistivity and induced polarization surveys. Geophysics, **45**, 75-93.

Griffiths, D.H. and Turnbull, J., 1985. A multi-electrode array for resistivity surveying. First

Break **3** (No. 7), 16-20.

Griffiths D.H., Turnbull J. and Olayinka A.I. 1990, Two-dimensional resistivity mapping with a computer- controlled array. First Break **8**, 121-129.

Griffiths D.H. and Barker R.D.,1993. Two-dimensional resistivity imaging and modelling in areas of complex geology. Journal of Applied Geophysics, **29**, 211-226.

Johansson, S. and Dahlin, T., 1996. Seepage monitoring in an earth embankment dam by repeated resistivity measurements. European Journal of Engineering and Geophysics, **1**, 229-247.

Keller G.V. and Frischknecht F.C.,1966. Electrical methods in geophysical prospecting. Pergamon Press Inc., Oxford.

Koefoed O.,1979. Geosounding Principles 1 : Resistivity sounding measurements. Elsevier Science Publishing Company, Amsterdam.

Lagmansson, M., 1998. Marine resistivity survey. Advanced Geosciences Inc. web site (www.agiusa.com).

Li Y. and Oldenburg D.W. 1992. Approximate inverse mappings in DC resistivity problems. Geophysical Journal International **109**, 343-362.

Loke, M.H., 1994. The inversion of two-dimensional resistivity data. Unpubl. PhD thesis, Un. Of Birmingham.

Loke, M.H., 1999. Time-lapse resistivity imaging inversion. Proceedings of the 5th Meeting of the Environmental and Engineering Geophysical Society European Section, Em1.

Loke M.H. and Barker R.D.,1996a. Rapid least-squares inversion of apparent resistivity pseudosections using a quasi-Newton method. Geophysical Prospecting, **44**, 131-152.

Loke M.H. and Barker R.D.,1996b. Practical techniques for 3D resistivity surveys and data inversion. Geophysical Prospecting, **44**, 499-523.

Pazdirek, O. and Blaha, V., 1996. Examples of resistivity imaging using ME-100 resistivity field acquisition system. EAGE 58th Conference and Technical Exhibition Extended Abstracts, Amsterdam.

Panissod, C., Dabas, M., Hesse, A., Jolivet, A., Tabbagh, J. and Tabbagh, A., 1998. Recent developments in shallow depth electrical and electrostatic prospecting using mobile arrays. Geophysics, **65**, 1542-1550.

Sasaki, Y. 1992. Resolution of resistivity tomography inferred from numerical simulation. Geophysical Prospecting, **40**, 453-464.

Silvester P.P. and Ferrari R.L., 1990. Finite elements for electrical engineers (2nd. ed.). Cambridge University Press.

Slater, L., Binley, A.M., Zaidman, M.D. and West, L.J., 1997, Investigation of vadose zone flow mechanisms in unsaturated chalk using cross-borehole ERT. Proceedings of the EEGS European Section 3rd Meeting, Aarhus, Denmark, 17-20.

Spiegel, R.J., Sturdivant, V.R. and Owen, T.E., 1980, Modeling resistivity anomalies from localized voids under irregular terrain. Geophysics, **45**, 1164-1183.

Tong, L. and Yang, C., 1990, Incorporation of topography into two-dimensional resistivity inversion. Geophysics, **55**, 354-361.

Waddell, J. and Barton, K, 1995, Seeing beneath Rathcroghan. Archaeology Ireland, Vol. 9, No. 1, 38-41.

Witherly, K.E. and Vyselaar, J, 1990. A geophysical case history of the Poplar Lake Copper-Molybdenum deposit, Houston Area, British Columbia. in Fink, J.B., McAlister, E.O., Sternberg, B.K., Wieduwilt, W.G. and Ward, S.H. (Eds), 1990, Induced polarization : Applications and case histories : Investigations in Geophysics No. 4, Soc. Expl. Geophys.

Appendix A
Data format for dipole-dipole, pole-dipole and Wenner-Schlumberger arrays.

The dipole-dipole, pole-dipole and Wenner-Schlumberger arrays involve an additional parameter in the RES2DINV data format. For these arrays, the "**a**" spacing is defined as the distance between the P1 and P2 potential electrodes (Figure 39). The second parameter is related to the distance between the C1 and P1 electrodes. By convention, the distance between the C1 and P1 electrodes for the dipole-dipole array is given as "**na**", where "**n**" is the ratio of the C1-P1 distance to the P1-P2 distance. The "**n**" factor is frequently an integer, but non-integer values can also be used with the RES2DINV program. The data file DIPOLEN5.DAT distributed with the RES2DINV program package is an example with non-integer values for the "**n**" factor for some of the readings. Using this data file as a guide, the format for the dipole-dipole array is given below. The upper part of the file together with comments is as follows :-

DIPOLEN5.DAT file	*Comments*
Blocks Model	*Header with title*
1.00	*Smallest or unit electrode spacing*
3	*Array type (3 for dipole-dipole, 6 for pole-dipole, 7 for W-S)*
1749	*Number of data points*
1	*1 to indicate center of electrode array is given as x-location*
0	*0 to indicate no IP*
1.50 1.00 1.0 9.92	*The x-location, "a" spacing, "n" factor, apparent resistivity value*
2.50 1.00 1.0 9.89	*Same format for each data point*
3.50 1.00 1.0 9.85	
.	
.	
2.50 2.00 0.5000 9.89	*Example with non-integer "n" value*
3.50 2.00 0.5000 9.78	*Note that "n" is 0.5 and "a" is twice the unit electrode spacing*
.	
.	
3.50 2.00 1.5000 9.88	*Another example with non-integer "n"*
4.50 2.00 1.5000 14.54	*which is equals to 1.5 in this case*
.	
.	
5.00 3.00 1.3333 7.96	Note "n" is 4/3, and "a" is 3 times the unit electrode spacing
6.00 3.00 1.3333 11.06	
.	
.	
37.00 3.00 6.0000 10.96	*Last two data points*
38.00 3.00 6.0000 10.87	
0	*Followed by a few 0's*
0	
0	
0	

The same data format is used for the pole-dipole and the Wenner-Schlumberger arrays with the "**a**" and "**n**" factors as defined in Figure 39. For these arrays, the "n" factor is usually an integer value, but fractional values can also be accepted by the RES2DINV program. The DIPOLEN5.DAT file, in the set of data files provided with the RES2DINV program, is an example dipole-dipole array data set with fractional values of the "**n**" factor.

For the "normal" or "forward" pole-dipole array, it is assumed that the C1 current electrode is to the left of the P1 potential electrode (Figure 39b), i.e. the x-location of the C1

electrode is less than the x-location of the P1 electrode. When the C1 electrode is to the right of the P1 electrode, it is referred to as the "reverse" pole-dipole array. To distinguish it from the "forward" pole-dipole arrangement, a negative value is used for the "**n**" factor in the RES2DINV data format. The data file PDIPREV.DAT is an example with both the forward and reverse pole-dipole measurements.

For both the "forward" and "reverse" pole-dipole arrays, the x-location for the center of the array is defined as the mid-point between the C1 and P2 electrode (i.e. the location of the P1 electrode is not used in the determination of the array center).

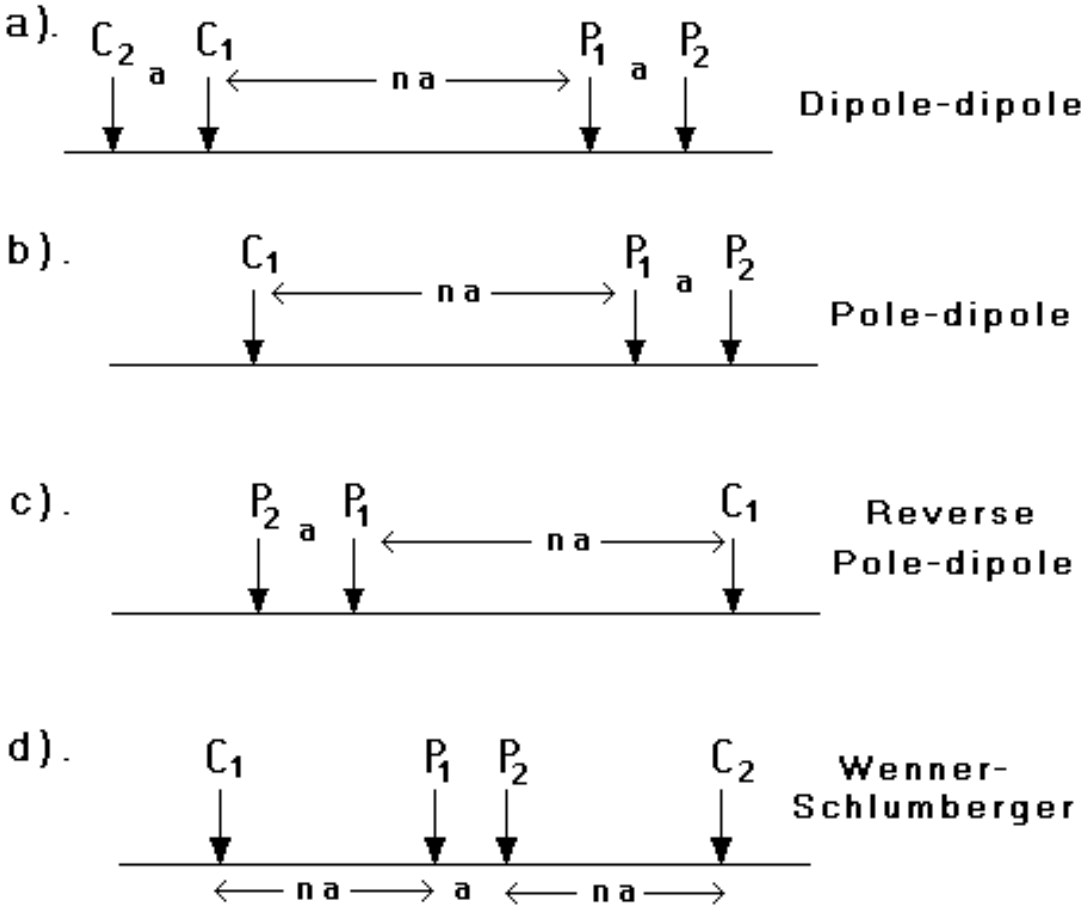

Figure 39. Arrangement of the electrodes for the dipole-dipole, pole-dipole and Wenner-Schlumberger arrays, together with the definition of the "**a**" spacing and the "**n**" factor for each array.

Appendix B
Topographic modelling

In surveys over areas with significant changes in the elevation of the ground surface, the effect of the topography must be taken into account when carrying out an inversion of the data set. It is now generally recognised that the traditional method of using the "correction factors" for a homogeneous earth model (Fox et al. 1980) does not give sufficiently accurate results if there are large resistivity variations near the surface (Tong and Yang 1990). Instead of trying to "correct" for the effect of the topography on the measurements, the preferred method now is to incorporate the topography into the inversion model. The RES2DINV program has 4 different methods that can be used to incorporate the topography into the inversion model. One method that uses the finite-difference method, and three based on the finite-element method. Figure 40 shows the inversion models for the Rathcroghan Mound (Waddell and Barton 1995) data set (Figure 40a) using the different topography modelling methods. In this particular inversion, the robust inversion method (section 2.6.2) was used to sharpen the edges of the high resistivity burial chamber near the centre of the line. This data set has a moderate amount of topography.

The first method the Schwartz-Christoffel transformation, which is a semi-analytical approach, that maps a 2-D region with an undulating surface into a rectangular mesh (Spiegel et al. 1980). The main advantage of this technique is that the faster finite-difference method can be used to calculate the apparent resistivity values for the inversion model. The inversion result is shown in Figure 40b.

The remaining three methods are similar in that they use a distorted finite-element mesh. In all these methods, the surface nodes of the mesh are shifted up or down so that they match the actual topography. In this case, the topography becomes part of the mesh and is automatically incorporated into the inversion model. The difference between these three methods is the way the subsurface nodes are shifted. The simplest approach, used by the first finite-element method, is to shift all the subsurface nodes by the same amount as the surface node along the same vertical mesh line. This is probably acceptable for cases with a small to moderate topographic variation (Figure 40c).

In the second finite-element approach, the amount the subsurface nodes are shifted is reduced in an exponential manner with depth (Figure 40d) such that at a sufficiently great depth the nodes are not shifted. This comes from the expectation that the effect of the topography is reduced or damped with depth. This produces a more pleasing section than the first finite-element method in that every kink in the surface topography is not reproduced in all the layers. For data sets where the topography has moderate curvature, this is probably a good and simple method (Figure 40d). One possible disadvantage of this method is that it sometimes produces a model with unusually thick layers below sections where the topography curves upwards. Thus in Figure 40d, the model is probably slightly too thick near the middle of the line above the burial chamber.

In the third finite-element method, the Schwartz-Christoffel transformation method is used to calculate the amount to shift the subsurface nodes. Since this method takes into account the curvature of the surface topography it can, for certain cases, avoid some of the pitfalls of the second finite-element method and produces a more "natural" looking model section (Figure 40e). For this data set, this method avoids the bulge near the middle of the line produced by the second finite-element method with a damped distorted mesh. However, in the middle part of the line, the model produced by this method is slightly thicker that that produced by the first finite-element method with a uniform distorted mesh.

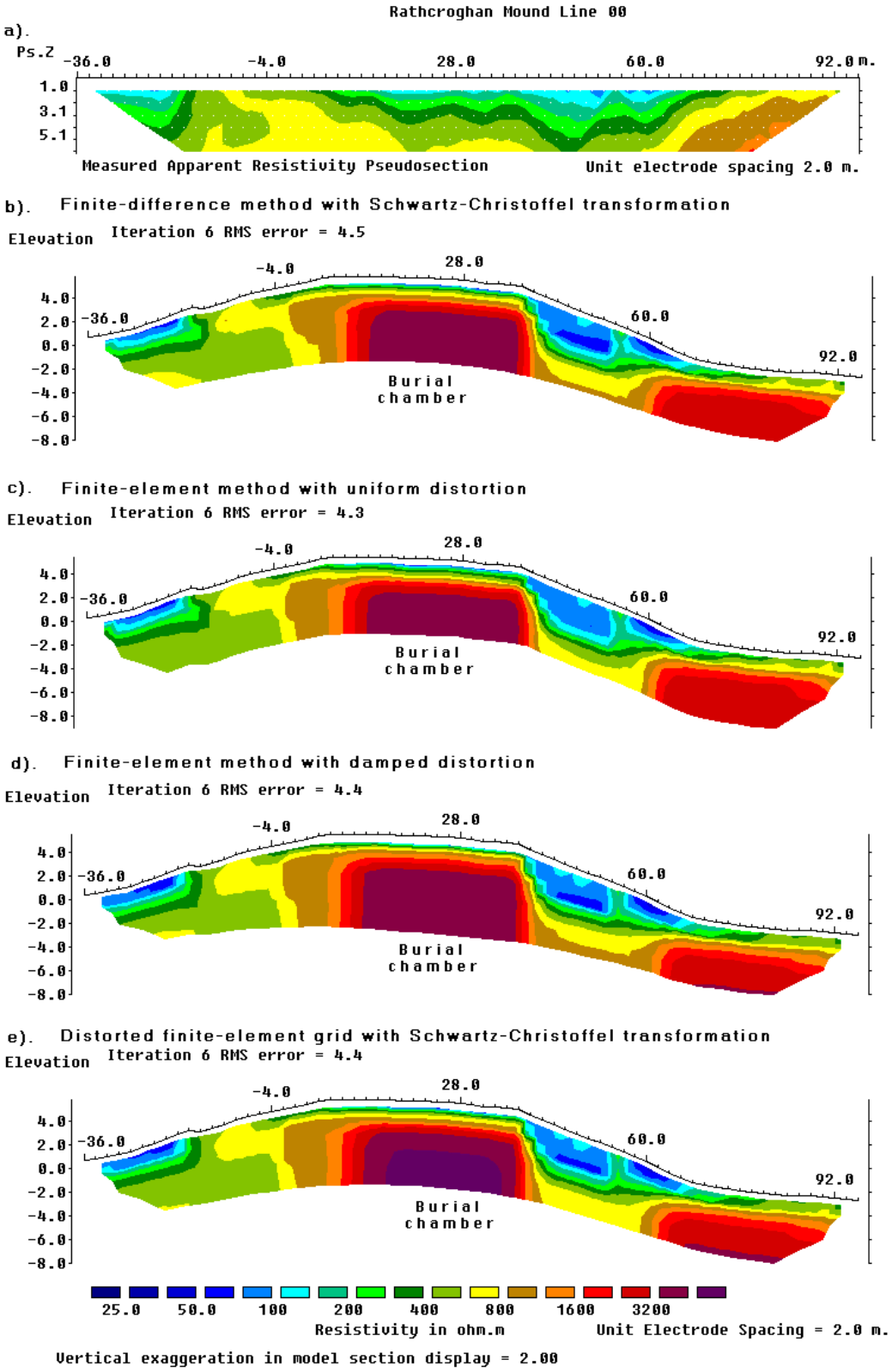

Figure 40. Inversion models for the Rathcroghan Mound data set. (a) Measured apparent resistivity data set. Models obtained using (a) the Schwartz-Christoffel transformation method using a finite-difference mesh (b) finite-element method with uniform distortion (c) finite-element method with damped distortion (d) finite-element method with the distortion calculated using Schwartz-Christoffel transformation for the topography modelling.

Appendix C
Inversion method

All inversion methods essentially try to find model for the subsurface whose response agrees with the measured data. In the cell-based method used by the RES2DINV and RES3DINV programs, the model parameters are the resistivity values of the model blocks, while the data is the measured apparent resistivity values. It is well known that for the same data set, there is a wide range of models whose calculated apparent resistivity values agree with the measured values to the same degree. Besides trying to minimise the difference between the measured and calculated apparent resistivity values, the inversion method also attempts to reduce other quantities that will produce certain desired characteristics in the resulting model. The additional constrains also help to stabilise the inversion process. The RES2DINV (and RES3DINV) program uses an iterative method whereby starting from an initial model, the program tries to find an improved model whose calculated apparent resistivity values are closer to the measured values. One well known iterative inversion method is the smoothness-constrained method (deGroot-Hedlin and Constable, 1990) that has the following mathematical form.

$$(\mathbf{J^T J} + u\mathbf{F})\mathbf{d} = \mathbf{J^T g} - u\mathbf{F r} \qquad \text{(C.1)}$$

where **F** = a smoothing matrix
J = the Jacobian matrix of partial derivatives
r = a vector containing the logarithm of the model resistivity values
u = the damping factor
d = model perturbation vector
g = the discrepancy vector

The discrepancy vector, **g**, contains the difference between the calculated and measured apparent resistivity values. The magnitude of this vector is frequently given as a RMS (root-mean-squared) value. This is the quantity that the inversion method seeks to reduce in an attempt to find a better model after each iteration. The model perturbation vector, **d**, is the change in the model resistivity values calculated using the above equation which normally results in an "improved" model. The above equation tries to minimise a combination of two quantities, the difference between the calculated and measured apparent resistivity values as well as the roughness (i.e. the reciprocal of the model smoothness) of the model resistivity values. The damping factor, *u*, controls the weight given to the model smoothness in the inversion process. The larger the damping factor, the smoother will be the model but the apparent resistivity RMS error will probably be larger.

The basic smoothness-constrained method as given in equation C.1 can be modified in several ways that might give better results in some cases. The elements of the smoothing matrix **F** can be modified such that vertical (or horizontal) changes in the model resistivity values are emphasised in the resulting model. In the above equation, all data points are given the same weight. In some cases, especially for very noisy data with a small number of bad datum points with unusually high or low apparent resistivity values, the effect of the bad points on the inversion results can be reduced by using a data weighting matrix.

Equation C.1 also tries to minimise the *square* of the spatial changes, or roughness, of the model resistivity values. This tends to produce a model with a smooth variation of resistivity values. This approach is acceptable if the actual subsurface resistivity varies in a smooth and gradational manner. In some cases, the subsurface geology consists of a number

of regions that are internally almost homogeneous but with sharp boundaries between different regions. For such cases, an inversion formulation that minimises the *absolute* changes in the model resistivity values can sometimes give significantly better results.

Appendix D
Statistical data filtering

One common problem in 2D and 3D surveys is in removing bad data points from a data set so that they will not influence the inversion result. For a 2D data set with a small number of data points, the bad data points can be removed manually as described in section 2.6.2. However, manually picking out the bad data points becomes impractical if there are a large number of bad data points, particularly if the data set contains more than a thousand data points. Furthermore, it is not practical to manually eliminate the bad data points for 3D data sets. One method that has been used for 3D surveys using the pole-pole array is by fitting a mathematical function to the potential measurements measured with a common current electrode. The data points where the potential values deviate significantly from the mathematical function (Ellis and Oldenburg 1994) that is used to simulate the potential variation are then removed from the data set. This method takes very little computer time and should be used where possible. However the success of this method depends on a reasonable coverage of measurements around the current electrode, such as in Figure 30a. In many surveys, the number of measurements made is much less than the ideal case, such as in Figure 30b with measurements only in certain directions. Furthermore some arrays, such as the pole-dipole and dipole-dipole arrays, might not show a sufficiently smooth variation of the potential values. In such cases, it might be difficult to find a sufficiently accurate and versatile mathematical function to fit the data.

RES2DINV and RES3DINV provides a general technique to remove the bad data points with minimal input from the user, and can be used for practically any array and any distribution of the data points. The main disadvantage of the method is the much larger amount of computer time needed. In this method, a preliminary inversion of the data set is first carried with all the data points. In this preliminary inversion, it is advisable to use the "Robust data inversion" option (section 2.6.2) to reduce the effect of the bad data points. Since this is just a trial inversion, it is probably only necessary to run the inversion to 3 or at most 4 iterations to reduce the computer time needed. After carrying out the trial inversion, switch to the 'Display' window in RES2DINV or RES3DINV, and read in the INV file containing the inversion results if necessary. After that, select the 'RMS error statistics' option that displays the distribution of the percentage difference between the logarithms of the measured and calculated apparent resistivity values. The error distribution is shown in the form of a bar chart, such as in Figure 41. Normally, the highest bar is the one with the smallest errors, and the heights of the bar should decrease gradually with increasing error values. The bad data points, caused by problems such as poor ground contact at a small number of electrodes, should have significantly higher errors than the "good" data points.

Figure 41 shows the error distribution bar chart for the data set shown in Figure 14 in section 2.6.2 that has a few bad data points. In the bar chart, almost all the data points have errors of 20 percent or less. The bad data points show up data points with errors of 60 percent and above, which can be easily removed from the data set by moving the green cursor line to the left of the 60% error bar. In this way the 5 bad data points are removed from this data set. For some data sets, the error distribution might show a more complicated pattern. As a general rule, data points with errors of 100 percent and above can usually be removed.

This method of using the results from a trial inversion to remove bad data points essentially uses the calculated apparent resistivity values for the trial model as the fitting function. The

calculated apparent resistivity values should be the most "natural" fitting function for the measured apparent resistivity data set. It provides a more accurate fitting function then any artificial mathematical formula that attempts to simulate the apparent resistivity variation from a field survey.

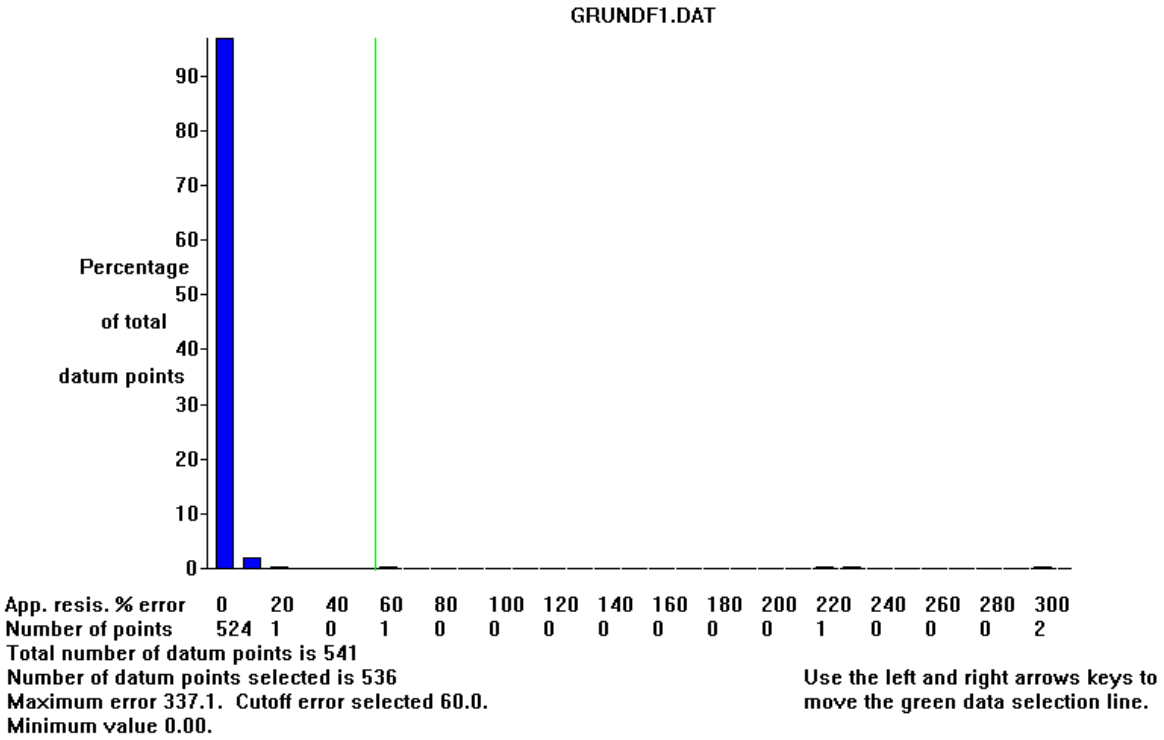

Figure 41. Error distribution bar chart from a trial inversion of the Grundfor Line 1 data set with 5 bad data points.